ECN-128

ECN

ECN-128

FEBRUARY 1983

FINAL REPORT ON THE REAL-80 EXERCISE

BY
W.L. ZIJP
É.M. ZSOLNAY**
H.J. NOLTHENIUS
E.J. SZONDI**
G.C.H.M. VERHAAG
D.E. CULLEN*
C. ERTEK*

* INTERNATIONAL ATOMIC ENERGY AGENCY
** NUCLEAR REACTOR OF THE TECHNICAL UNIVERSITY BUDAPEST

INDC (NED)-7
BME-TR-RES-6/82

Netherlands Energy Research Foundation

Netherlands Energy Research Foundation ECN

P.O. Box 1

1755 ZG Petten (NH)

The Netherlands

Telephone (0)2246 - 6262

Telex 57211

INDC(NED)-7
BME-TR-RES-6/82
ECN-128

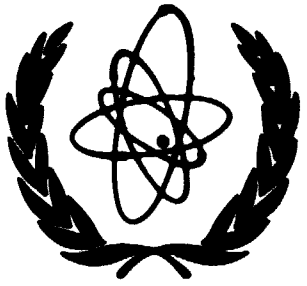

International Atomic Energy Agency

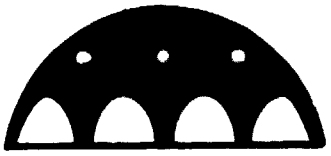

Nuclear Reactor of the Technical University Budapest

ECN

Netherlands Energy Research Foundation ECN

Final report on the REAL-80 exercise

W.L. Zijp; É.M. Zsolnay; H.J. Nolthenius;
E.J. Szondi; G.C.H.M. Verhaag; D.E. Cullen; C. Ertek.

February 1983

FINAL REPORT ON THE REAL-80 EXERCISE

W.L. Zijp[1], É.M. Zsolnay[2], H.J. Nolthenius[1], E J. Szondi[2],
G.C.H.M. Verhaag[1], D.E. Cullen[3], C. Ertek[3].

[1] Netherlands Energy Research Foundation ECN, Petten.
[2] Nuclear Reactor of the Technical University, Budapest.
[3] International Atomic Energy Agency, Vienna.

Part of the work described in this report has been carried out under contract to the European Commission and has been financed by the J.R.C. budget.

Petten, 16 December, 1982

ABSTRACT

The aim of the interlaboratory REAL-80 exercise, organized by the IAEA, was to determine the state-of-the-art in 1981 of the capabilities of laboratories to adjust neutron spectrum information on the basis of a set of experimental activation rates, and to subsequently predict the number of displacements in steel, together with its uncertainty.
The input information distributed on magnetic tapes to participating laboratories comprised values, variances and covariances for a set of input fluence rates, for a set of activation and damage cross-section data, and for a set of experimentally measured reaction rates. The exercise dealt with two clearly different spectra: the thermal ORR spectrum with 19 reaction rates, and the fast YAYOI spectrum with 12 reaction rates. Cross-section data were supplied both in a 620 groups structure and in a 100 groups structure. From 30 laboratories which were asked to participate, 13 laboratories contributed 33 solutions for ORR, and 35 solutions for YAYOI.
The spectral shapes of the solution spectra showed considerable spread, both for the ORR and the YAYOI spectrum. When the series of predicted activation rates in nickel and the predicted displacement rates in steel derived for all solutions is considered, one cannot observe significant differences due to the adjustment algorithm used. The largest deviations seems to be due to effects related to group structure and/or changes in the input data.
When comparing the predicted activation rate in nickel with its available measured value, we observe that the predicted value (averaged over all solutions) is lower than the measured value: 1 per cent lower for ORR and 7 per cent lower for YAYOI.
For the predicted displacement rate in steel we observed a coefficient of variation of 2,2 per cent for the ORR spectrum and 2,8 per cent for the YAYOI spectrum, if all of the participant responses are considered.

KEYWORDS

NEUTRON SPECTRA
SPECTRA UNFOLDING
CROSS SECTIONS
ACTIVATION DETECTORS
TRHESHOLD DETECTORS
NEUTRON FLUENCE
DAMAGING NEUTRON FLUENCE
STEELS
NEUTRON METROLOGY
PHYSICAL RADIATION EFFECTS
COMPARATIVE EVALUATIONS
NEUTRON DOSIMETRY

CONTENTS

LIST OF SYMBOLS FREQUENTLY USED

α_i^c = calculated reaction rate for i-th reaction (based on input values for group cross-sections and (input or output) values for group fluence rates);

α_i^m = measured reaction rate for i-th reaction;

$\underline{A}^c$ = vector of n calculated reaction rates α_i^c;

$\underline{A}^m$ = vector of n measured reaction rates α_i^m;

f = spectrum normalization factor;

m = number of energy groups;

n = number of experimental reaction rates;

r = rank of correlation matrix;

$\underline{r}_{ij}$ = correlation coefficient;

$\bar{r}_{ij}$ = average correlation coefficient;

$\underline{\underline{R}}$ = correlation matrix;

R_{dpa} = displacement rate per atom of iron;

R_{Ni} = activation rate per atom of nickel;

s_i = standard deviation of the difference between α_i^m and $f \cdot \alpha_i^c$;

S = sum of squares of deviations;

$\underline{S}$ = vector of n x m cross-section values σ_{ij}

$\underline{\underline{V}}(A^c)$ = covariance matrix for $\underline{A}^c$;

$\underline{\underline{V}}(A^m)$ = covariance matrix for $\underline{A}^m$;

w_i = statistical weighting factor for the i-th reaction rate;

$\underline{\underline{W}}$ = weighting matrix;

σ_{ij} = cross-section for reaction i and group j

ϕ_j = fluence rate for group j.

$\underline{\phi}$ = vector of m group fluence rates ϕ_j

0. EXECUTIVE SUMMARY

How well can laboratories predict displacement rates based on neutron spectrum adjustment?

Answered by the international interlaboratory exercise REAL-80.

Aim

The aim of the international interlaboratory REAL-80 exercise, organized and analyzed under the auspices of the IAEA, was to determine the state-of-the-art in 1981 of the capabilities of laboratories to adjust neutron spectrum information, based on a set of experimental reaction rates, and to subsequently predict the number of displacements in steel, as well as the uncertainty of this prediction.
The exercise, suggested at the third ASTM-Euratom Symposium on Reactor Dosimetry (Ispra, 1-5 October 1979), was planned to answer the following main questions:

1. What is the quality of the neutron spectrum derived by different existing unfolding/adjustment procedures?
2. What is the quality of an integral damage parameter, such as the number of displacement per atom (commonly called dpa), derived using the adjusted spectrum?
3. What is the quality of a predicted activation rate?

Since the time schedule for the preparatory phase was rather tight, it was decided mid 1980 to restrict the exercise in a first phase to only two neutron spectra, for which information could be made available.
The first spectrum, referred to as ORR, was that for the fuel region in the Oak Ridge Research Reactor, a high fluence rate materials testing reactor. It is a typical thermal reactor neutron spectrum with a predominant 1/E component in the intermediate energy range.
The second spectrum, referred to as YAYOI, is a typical fast reactor neutron spectrum. It refers to the central region of the Japanese YAYOI reactor, a 2 kW air-cooled fast neutron source reactor with a relatively hard neutron spectrum.

Input data

The IAEA prepared in 1980 the input data and distributed them to the participants in February 1981. The input spectra used in the exercise were based on multigroup reactor physics calculations. For the ORR spectrum there were 19 experimental reaction rates available, and for the YAYOI spectrum 12 experimental reaction rates (see table 6). Fig. 1 shows the two spectra together with the energy response regions for these reactions. The cross-section data needed for the exercise were provided both in a 620 and 100 groups structures, and were mainly based on the ENDF/B-V dosimetry file. The cross-section data in the 100 groups structure were also available in a modified form to account for the effects of self-shielding and the presence of cadmium covers. Variance and covariance information both for the input spectra and for the cross-section files and also for the reaction rates had been supplied (in a 100 groups structure, where applicable). The variances of the group fluence rates and of the group cross-sections were best available estimates. The correlation coefficients of the input group fluence rates were generated using a Gaussian function with a full width at half maximum (FWHM) of 2,5 groups (within a 100 groups structure), superimposed on a small flat contribution. The correlation coefficients for the group cross-sections were also defined by means of a Gaussian function, with a FWHM of 10 groups (again for a 100 groups structure). Therefore the input correlation matrices for fluence rates and cross-sections have an artificial nature.
The input displacement cross-section data used, originating from the ASTM standard procedure, refers to a model for displacements in iron, under the assumption that this model is an adequate approximation for displacements in ferritic steel.

Task

The uncertainties in the calculated reaction rates, based on input data only, are shown in table 11. It is noted that the uncertainties in the calculated reaction rates due to cross-section uncertainties are in general larger than those of the measured reaction rates.
The input neutron spectrum, the input group cross-sections and the

input reaction rates with their uncertainties in the form of covariance matrices were completely specified and distributed to the participants on magnetic tape.

The participating laboratories were asked to perform the following actions:

- Adjust (unfold) the two reactor neutron spectra for the ORR and the YAYOI reactor and make statements, if possible, on the uncertainties and the correlations for group fluence rates;
- Calculate the activation rate in nickel and also the standard deviation in this value, using the cross-section data supplied for $^{58}Ni(n,p)^{58}Co$;
- Calculate the displacement rate in iron and also the standard deviation in this value using the damage cross-section data supplied; - Submit to the IAEA the requested data in a prescribed format, preferably within two months after receipt of the the input data tape.

Response

From 30 laboratories which were asked to participate, 13 laboratories (listed in table 1) contributed 33 solutions for ORR, and 35 solutions for YAYOI. The solutions were obtained by means of 12 different spectrum adjustment codes (see table 3). Many of these codes are documented in the literature ([9]...[20]).

More information on the merits of several adjustment codes is available in a symposium paper published in the proceedings of the fourth ASTM-Euratom Symposium 1982 [21].

Only six of the adjustment codes (STAY'SL, NEUPAC, LSL, SENSAK, ITER-3 and SANDBP) could provide information on the correlation between output group fluence rates of the neutron spectrum.

All REAL-80 solutions received by the IAEA from the participating laboratories were forwarded to the analyzing laboratories in Budapest and Petten, where a joint team of "evaluators" analyzed the data received from the "participants". The evaluation of the contributed solutions comprised a variety of actions, such as:

- screening and treatment of numerical data supplied by the participants;
- conversion of data from different group structures to common group

structures;
- development of utility programs, especially for plotting tasks;
- development of new programs to study the propagation of uncertainties, the effects of spectrum normalization and the effects of group structure;
- calculation of the spectrum characteristics and their uncertainties;
- analysis of correlation matrices, using methods of factor analysis.

Categories of solutions

The complete set of output spectra is shown in fig. 18. Appreciable differences are present in the shape of the output spectra. Due to the many differences in the procedures used by the participants it was not reasonable to perform a direct comparison of output spectra and predicted reaction rates for the whole set of contributed solutions. A rather simple division of the output data into three categories was used to present results. These categories are solutions presented in
- a 100 groups structure;
- a 620 groups structure;
- other structures (284, 152 and 40 points; 50, 20 and 10 groups).

To facilitate the comparison of numerical output data, most output data are presented here in a relative way, i.e. normalized to the corresponding values valid for the input information.

To facilitate a quick comparison of the spread in the output spectra, all spectra were converted to a 12 groups structure, where each group covers a full decade on the energy scale. The modification ratios (ie $\phi_{out}(E)/\phi_{in}(E)$) and their standard deviations are shown in figs. 16 and 17. The spread in the 12 groups output fluence rate values is smallest (2 to 20 per cent) for the category of 100 groups solutions, larger (2 to 55 per cent) for the category of 620 groups solutions, and extremely large for the other groups structures (as large as 100 per cent). These large standard deviations are related to the fact that the few groups structure and the 12 decades structure are both coarse structures, and in general have no common group boundaries.
In general any two solution spectra which have clearly different few

groups structures (say less than 50) will show appreciable differences, if they are converted in a common rough group structure (eg a 12 decade structure). Therefore some caution is necessary when the results of the category "other structures" are considered.
With respect to the propagation of spectrum uncertainties (and their correlations) from input data to output data it turned out that the following two categories of codes could be distinguished:
- codes using generalized least squares (like STAY'SL, NEUPAC, etc.);
- other codes (like SAND-II).

The energy dependent pattern in the uncertainty for the input spectra and for the typical output spectra for these two solution categories are shown in fig. 15. The generalized least squares type solutions reduce the spectrum uncertainties in those energy ranges where there is appreciable detector response. In contrast the SAND-II type solution produces an appreciable and varying low value for the uncertainty over the whole energy range; it is to be noted that here the SAND-II type solution did not use the input spectrum uncertainties.

The spectrum normalization factor

Surprisingly it was found that the spectrum normalization factor plays an important role in the neutron spectrum adjustment, since it may introduce a dominating constant factor which in turn influences the energy dependent modification ratio. The various adjustment codes apply some different definitions for the normalization factor.
Minimization of the least squares expression

$$S = \sum_{i=1}^{n} w_i \, (\alpha_i^m - f \cdot \alpha_i^c)^2$$

leads to the general expression

$$f = \sum_{i=1}^{n} w_i \cdot \alpha_i^m \cdot \alpha_i^c \; / \; \sum_{i=1}^{n} w_i \cdot \alpha_i^c \cdot \alpha_i^c .$$

Various choices for the external weighting factors w_i are used in the

existing adjustment codes. They lead (see appendix 1) to the following four expressions

weight	normalization factor
$w_i = 1$	$f_1 = \Sigma\, \alpha_i^c \cdot \alpha_i^m \;/\; \Sigma\, \alpha_i^c \cdot \alpha_i^m$
$w_i = 1/(\alpha_i^c)^2$	$f_2 = (\Sigma\, \alpha_i^m/\alpha_i^c)/n$
$w_i = 1/(\alpha_i^m)^2$	$f_3 = (\Sigma\, \alpha_i^c/\alpha_i^m) \;/\; \Sigma\, \alpha_i^c/\alpha_i^m)$
$w_i = 1/(\alpha_i^c)$	$f_4 = \Sigma\, \alpha_i^m/\Sigma\, \alpha_i^c$

The generalized least squares principle leads to the expression

$$f_o = [(\underline{A}^c)^T \cdot \underline{\underline{W}} \cdot \underline{A}^c]^{-1} \cdot [(\underline{A}^c)^T \cdot \underline{\underline{W}} \cdot \underline{A}^m]$$

where

$$\underline{\underline{W}} = [\underline{\underline{V}}(A^c) + \underline{\underline{V}}(A^m)]^{-1}.$$

The normalization factors for the spectra (which were already roughly normalized at the input) were for YAYOI in the range between 0,99 and 1,32 (see table 9). The influence of the normalization factor on the energy dependent modification ratio $\phi_{out}(E)/\phi_{in}(E)$ for YAYOI, as calculated with a least squares type of code, is shown in fig. 19.
The factors f_1, f_4 and f_0 give similar patterns, while the factors f_2 and f_3 give patterns similar to those that result when no renormalization is used.
For all codes considered the normalization factor f is important since its magnitude will largely influence the energy dependent modification (ie the ratio $\phi_{out}(E)/\phi_{in}(E)$). The definition formula for f is especially important for those codes which cannot take into account the uncertainties of the input data set (eg the uncertainties of the experimental reaction rates). For these codes it may occur that the data (sub)set for one reaction which has relatively large uncertainties

becomes predominant in the determination of the solution spectrum. In principle only the newly defined normalization factor f_o is correct. Whether other normalization factors used in actual practice are good approximations to f_o is dependent on the structure of the weighting matrix $\underline{\underline{W}}$, and therefore, in general, dependent on the input data set. The conclusion is that the actual expression for defining the normalization factor is more important than previously assumed.

Criteria for fit

The following parameters were considered as measure for the closeness-of-fit between measured and calculated reaction rates.

$$DEV = \left\{ \sum_{i=1}^{n} \left[(\alpha_i^m - f \cdot \alpha_i^c)/\alpha_i^m \right]^2 / (n-1) \right\}^{1/2}$$

$$ARD = \left\{ \sum_{i=1}^{n} \left[(\alpha_i^m - f \cdot \alpha_i^c)/s_i \right]^2 / n \right\}^{1/2}$$

$$CHISQ = (\underline{A}^m - f \cdot \underline{A}^c)^T \cdot \underline{\underline{W}} \cdot (\underline{A}^m - f \cdot \underline{A}^c)$$

These three parameters show however the same trend (see fig. 23). This implies that - at least for the two data sets of ORR and YAYOI - there is no remarkable influence of input variances and correlations on the investigated fit parameters. The ARD parameter has the largest range, and therefore seems to be here the most sensitive parameter by which to judge the fit. An important conclusion is that there is no clear functional relation between the magnitude of a fit parameter, and the values of the predicted reaction rates R_{Ni} and R_{dpa}. This statement is supported by the following conclusive observations:

- Least squares adjustments can have ARD values much lower than the expectation value 1, occurring under ideal conditions;
- In these cases the plots of the modification ratio show large peaks (adjacent to deep valleys) in regions with appreciable response of the detector set, so that a levelling-off occurs in adjacent groups;
- Such structure will often not have any effect on the value of the

predicted reaction rates.

Analysis of the solution spectra leads to the conclusion that frequently an ARD value much less than unity is obtained. This is related to unrealistic structure occurring in the output spectrum. Therefore some caution is necessary when the fit parameter is used as convergence criterion in cases where the adjustment algorithm requires iteration.

Effect of coarse groups structure

When an energy group structure was used with less than 40 or 50 groups in the energy range of 10^{-10} to 20 MeV, the result was a spectrum shape without characteristic details. It is to be noted, that peculiarities are introduced by the procedures for converting one group structure into another one (see fig. 2g, 2h, 3g, 3h, 8a, 8c and 11d).
Nevertheless the integral parameters like R_{Ni} and R_{dpa} showed in most cases a good agreement with the results based on fine group calculations, provided that the coarse group calculations used appropriately weighted cross-section values.
If the input spectrum resulting from reactor physics calculation is available in a group structure which is inadequate to describe appreciable fluence rate gradients in the actual spectrum (see table 8), then no good adjustment can be achieved by any adjustment algorithm.

Effect of input covariances on uncertainties in integral quantities

This effect has been studied for the input data sets for ORR and YAYOI by means of separate calculations, in which the non-diagonal variance-covariance matrices were replaced by diagonal variance matrices. Both for the ORR and YAYOI spectra the correlations between the group fluence rates play a more important role than the correlations between the group cross-sections (see table 21).

Output correlation matrices

About one third of the solutions contained correlation matrices.
The correlation matrices of all these output spectra irrespective of

their merits were compared to that of the input spectra in various ways:

- by using perspective plots of the matrices;
- by considering some characteristic parameters like the rank of the matrix (r) and the average correlation coefficient ($\overline{r_{ij}}$);
- by investigating the rotated factor loadings (a well known procedure in the factor analysis technique).

One can distinguish two different types of methods for calculating correlation matrices:

1. The deterministic method, as used in the generalized least squares types of codes (like STAY'SL);
2. The stochastic method, using Monte Carlo variations of a SAND-II type of code (like SANDBP).

This is illustrated in figs. 28-36.

The perspective plots of the correlation matrices of the STAY'SL type show practically no corrrelations far from the main diagonal, and they reflect the main characteristics of the input spectrum correlation matrix. The SANDBP code however shows very strong correlations, even in the resonance energy region. The deterministic codes gave a decrease of $\overline{r_{ij}}$ relative to the input information. (while the stochastic method gives under the chosen circumstances an increase of $\overline{r_{ij}}$). The deterministic codes gave an increase of the rank r, indicating a narrowing of the band matrix. This means that these codes have loosened the correlations between the group fluence rates. The stochastic codes on the other hand yield a very low rank of the output correlation matrix; this indicates the presence of strong correlations.

Factor analysis of correlation matrices

Using the technique of factor analysis, it is found (see fig. 37) that the 100x100 group input correlation matrices can be reproduced reasonably by 20 to 30 factor loading vectors. For structure studies we considered the so-called rotated factor loading vectors, obtained according to Kaisers varimax criterion ([25], [26], [27]).

The output correlation matrices could be described with 35 to 40 factor loading vectors in case of deterministic codes, and with 6 to 7 factor loading vectors in case of stochastic codes (if we consider a 95 per cent contribution to the sum of the eigen values of the correlation matrix).
A study has been made to determine how well the first 20 rotated factor loading vectors, which roughly characterize the applied input correlation matrices, are reproduced (replicated) as one of the first 20 rotated factor loading vectors which characterize the participants output correlation matrices. Such replication occurred frequently (9 times for ORR, and 12 or 13 times for YAYOI, see table 26).
When examining these results one should realize that the input correlation matrix with its narrow band structure was artificially generated and may not represent the actual physical situation. Therefore one should use some caution when trying to generalize these findings.

Integral spectrum data

Although the spectrum shapes of the output spectra show considerable spread (see fig. 18), both for the thermal ORR spectrum and for the fast YAYOI spectrum, it was found that the integral spectrum data, such as $\phi(E>1MeV)$ and $\phi(E>0,1MeV)$ and ϕ_{tot} show much less variation (less than about 5 per cent) (see table 17).

Predicted reaction rates

When the series of predicted activation rates per nickel atom (R_{Ni}) and of predicted displacements rates per iron atom (R_{dpa}) is considered for all solutions, one cannot observe significant differences which can be unambiguously ascribed to the adjustment algorithm used.
The largest deviations from the average value seem to be due to effects originating from group structure and/or deviations from the input data (see table 18).

The spread in the predicted values of R_{Ni} and R_{dpa} derived from the sets of responses were less than the uncertainties quoted by some participants (see tables 17 and 19). If all of the participant re-

sponses are considered for the predicted values of R_{dpa}, the result is a coefficient of variation of 2,2 per cent for the ORR spectrum, and 2,8 per cent for the YAYOI spectrum (see table 17).

If the responses are considered for the predicted value for R_{Ni} the result is a coefficient of variation of 1,7 per cent for the ORR and of 7,1 per cent for the YAYOI spectrum (see table 17). If only the more homogeneous category of 100 groups solution spectra is considered, then the coefficient of variation of the R_{Ni} values becomes 1,4 per cent for the ORR spectrum, and 4,6 per cent for the YAYOI spectrum (see data in table 17). Since measured values for R_{Ni} were available both for ORR and YAYOI it was possible to compare the values predicted by the participants with its actual value.

For R_{dpa} such a simple comparison is not possible. More over one should realize that the validity of the displacement model was a basic assumption in the REAL-80 exercise. Although this model may be criticized, there is at present no practical alternative damage model available for engineering purposes.

When comparing the predicted value of R_{Ni} with its available measured value, we observe that the predicted value (averaged over all solutions) is lower than the measured value: 1 per cent lower for the ORR spectrum, and 7 per cent lower for the YAYOI spectrum (see table 18). Generally speaking, the participants data agree with the measured value for R_{Ni}. However, individual participants data showed deviations from the measured value which are between +4 and -4 per cent for ORR, and between -1 and -23 per cent for YAYOI (see table 18).

Main conclusions

With regard to the aim of the REAL-80 exercise, to determine the quality of adjusted spectra and derived integral values, we can draw the following general conclusions:

1. The neutron spectra, derived with various adjustment codes, can differ clearly in their shape.
2. The integral damage parameters, like the number of displacements per iron atom, R_{dpa}, derived with various adjustment codes, agree within a few per cent with each other. The spread in the values is cer-

tainly not larger than the uncertainties derived by the participants for the individual values.

3. For the two spectrum cases considered (ORR and YAYOI), the adjustment procedures have resulted in a considerable decrease in the uncertainties of the neutron spectrum and of the neutron spectrum characteristics. For the activation rate per nickel atom, R_{Ni}, the final uncertainty is a factor 2 to 3 smaller than the uncertainty derived from the input data. For R_{dpa} this improvement factor is about 1,5.
4. Values for the predicted reaction rates of R_{Ni}, as given by the participants agree with each other to within a few per cent. The spread in the values is again not larger than the uncertainties derived by the participants. However, the average of all participants values of R_{Ni} is clearly smaller than the available measured value.

Further observations

One should realize that the input correlation matrices - both for the neutron spectrum and the cross sections - have artificially been created by means of Gaussian functions for the sole purpose of the excercise. For this reason no physical interpretation of these matrices is possible. Similarly care has to be taken in the physical interpretation of the covariance information obtained from artificial input data.
More realistic results of spectrum adjustment procedures can only be expected, if more realistic covariance matrices for the input data, and especially for the input spectrum, become available.
Then one can also investigate whether some conlcusions from this exercise with respect to propagated uncertainties and correlations have a more general character.

Future prospects

The REAL-80 exercise has been extremely useful in allowing the status of adjustment procedures for calculating integral reaction rates to be determined as of 1980/1981.
However the first round of this exercise did not fully investigate all

aspects of adjustment, and the authors feel that there is much to be gained by organizing yet another round of this project: tentatively the next round of this exercise has been designated as REAL-84, and it will be organized in the near future by the IAEA.

Any scientist who is interested in participating is encouraged to contact the Nuclear Data Section of the IAEA.

1. INTRODUCTION

1.1. Background

In the concluding session of the third ASTM-Euratom Symposium on Reactor Dosimetry (held at Ispra, 1-5th October, 1979) the suggestion to organize a follow-up of the previous international activities [29] on the intercomparison of unfolding codes was enthusiastically supported. It was felt that such a new study should pay particular attention to the uncertainty of integral parameters (displacement rates and activation rates), derived from neutron fluence rate spectrum information (based on experimental activation rates) by an adjustment procedure. The IAEA was invited to organize the exercise and to schedule it for completion within a very tight time schedule. The IAEA Laboratory Seibersdorf, and in a later stage the IAEA Nuclear Data Section took responsibility for the organization of the exercise. After preparatory work in various laboratories, participants started work in February 1981 when the IAEA distributed magnetic tapes with input data required in the exercise, together with an information sheet ([1] and [2]). This information was sent to some 30 prospective participants all over the world.

The first results of the intercomparison based on solutions received before 15th August 1981, were reported at the IAEA Advisory Group Meeting on Nuclear Data for Radiation Damage Assessment and Related Safety Aspects (held in Vienna, 12-16th October, 1981) [3]. A second report [4] was presented at the 4th ASTM-Euratom Symposium on Reactor Dosimetry (held in Gaithersburg, MD, 22-26th March, 1982). An interim report [5] with more details was distributed among the participating laboratories in July, 1982.

The present report is an extended and updated version of the previous reports; it serves as a final report on this project and includes the most important characteristics of 68 solutions received from 13 participating laboratories (see table 1).

1.2. Project name

The exercise received the code name REAL-80 (Reaction Rate Estimates, Evaluated by Adjustment Analysis in Leading Laboratories).

1.3. Aim

The aim of the REAL-80 exercise was to arrive at a realistic value for the uncertainty in integral radiation damage parameters (like the displacement rate), when such a value is derived by means of existing adjustment procedures. The conditions had to be well defined and well chosen with respect to input values (comprising values and covariances for the fluence rates, activation and damage cross-section data, and experimental activation rates). For instance, the exercise was set up to give answers to questions like:

1. What is the quality of the neutron spectrum derived by different existing unfolding/adjustment procedures?
2. What is the quality of an integral damage parameter, like the number of displacements per atom (dpa), derived with aid of the adjusted spectrum?
3. What is the quality of a predicted activation rate?

The exercise was to be performed within a period of two years, so that the results would be available for discussion at the 4th ASTM-Euratom Symposium (held at Gaithersburg, MD, 22-26th March, 1982). It was emphasized that the outcome of the exercise reflects the state-of-the-art in 1981 of the capabilities of laboratories, in deriving values and uncertainties for the predicted number of displacements. All participating laboratories were asked to use their own existing practices.

1.4. Organization

The REAL-80 exercise was organized by the IAEA in Vienna, originally under the responsibility of the IAEA Seibersdorf Laboratory (responsible officer Dr. C. Ertek), later on under the responsibility of the IAEA Nuclear Data Section (responsible officers Dr. J.J. Schmidt and Dr. D.E. Cullen); W.L. Zijp (ECN, Petten) acted as consultant.
The analysis of the numerical results of this exercise has been performed (upon request by the IAEA Nuclear Data Section) by a joint team from the Budapest Technical University and the Petten research center.

For reasons of convenience, the term "evaluators" is used in this report to denote this joint team, and the term "participants" to denote the individual laboratories participating in the exercise.

1.5. Contents of the first phase of REAL-80

Since the time schedule for the preparatory phase was too tight to allow the required covariance information for the cross-section data and for the envisaged series of reactor neutron spectra to be prepared, it was decided in mid-1980 to start with a first phase, dealing with only two neutron spectra, for which detailed information would be available in time. Input information for the ORR spectrum, comprising 19 reaction rates (12 reaction rates without cover and 7 reaction rates inside a cadmium cover) was kindly supplied by Dr. L.R. Greenwood (ANL).
Input information for the YAYOI spectrum, comprising 12 reaction rates was kindly supplied by Dr. M. Nagazawa (University of Tokyo), supplemented with information from Dr. Greenwood.

The participating laboratories were asked to perform the following actions:

- Adjust (unfold) the two reactor neutron spectra for the ORR and the YAYOI reactor and make statements, if possible, on the uncertainties and the correlations for group fluence rates.
- Calculate the activation rate in nickel, using the cross-section data supplied for $^{58}Ni(n,p)^{58}Co$, and also the standard deviation in this value.
- Calculate the damage rate in iron, using the damage cross-section data supplied, and also the standard deviation in this value.
- Submit to the IAEA the requested data on magnetic tape in a prescribed format [6], preferably within two months after receipt of the IAEA tape with the input data.

2. INFORMATION ON THE INPUT DATA SETS

2.1. Input data

The input neutron spectrum, the input group cross-sections and the input reaction rates with their uncertainties in the form of covariance matrices were completely specified by numerical values on the magnetic tape and in the accompanying information sheets, distributed to participating laboratories.
One input set was derived for the Oak Ridge Research Reactor, a high fluence rate materials testing reactor, on which the R-2 (Studsvik, Sweden) and the HFR (Petten, the Netherlands) are modelled. The ORR spectrum is a typical thermal spectrum with a predominant 1/E component in the intermediate energy range.
The other set was derived for the central region (inside the vertical penetrating 2 cm diameter gloryhole) of the YAYOI reactor. YAYOI is a 2 kW air-cooled fast neutron source reactor with a relatively hard neutron specrum; the core fuel consists of 28 kg 93 per cent enriched metal uranium. For the YAYOI spectrum 12 reaction rates were available, and 19 reaction rates for the ORR set.
The input neutron spectrum for the ORR was calculated with a transport theory code. The thermal component of the spectrum was derived with an extrapolation procedure. The transport calculation was performed using a 100 groups cross-section library mainly based on the ENDF/B-V file.
The input spectrum for the YAYOI reactor was calculated with the one-dimensional ANISN code, with 39 groups; in this calculation the cross-section library ENDF/B-III was applied.
Based upon the model used in these transport calculation the calculated neutron spectra are expected to be of adequate quality for use in the REAL-80 exercise.

The reactor physics codes did not directly yield the covariance matrices which some adjustment codes require as part of the input; Dr. L.R. Greenwood developed variance-covariance matrices which were suitable for the REAL-80 exercise. The variances of the group fluence rates were reasonable guesses. Greenwood tested these data with the aid of a few extra adjustment runs; in the latter runs the variances were increased.

Dr. Greenwood stated that for these runs the same output should be obtained as for the "reasonable guess variances".
The correlation matrix of the input spectrum was generated by using a Gaussian function with a full width at half maximum (FWHM) of 2,5 groups (within a 100 groups structure) superimposed on a small flat contribution.
The correlation matrices for the ORR and the YAYOI input neutron spectrum were about equal. From a physics point of view this seems liable to criticism, but the time schedule of REAL-80 made it necessary to adopt some pattern in order to proceed without appreciable delay (within the schedule for this project there was not sufficient time to improve this input spectrum correlation information).

The input data set supplied for this exercise included the input neutron spectrum as well as a set of group cross-section data in a 100 groups structure. A scheme of this group structure is shown at the bottom of fig. 1. The primary source of the input cross-section data was the first version of the ENDF/B-V dosimetry file. The input data set also contained neutron self-shielding factors for the activation detectors of interest in this exercise, as well as modified group cross-sections (with modifications to take into account the effect of neutron self-shielding and the presence of cadmium covers) in a 100 groups structure. The calculation of the neutron self-shielding factors was originally performed with a very detailed multi-group cross-section library. The results of this procedure were afterwards condensed to the 100 groups structure.
The input data set for this exercise also contained a cross-section set with a 620 groups structure of the SAND-II type, covering the range from 10^{-10} to 18 MeV; neutron self-shielding and cadmium cover corrections were however not supplied for this 620 groups structure.
The variances available in the ENDF/B-V dosimetry file are given in a rather coarse energy structure. They are converted to the 100 groups structure so that the same energy dependent structure remained.
The correlation coefficients for the 100 groups cross-sections which were required to compose the variance-covariance matrix were not derived from the ENDF/B-V dosimetry file, but were rather calculated with a Gaussian function (FWHM = 10 groups) in a manner similar to that

described above for the input spectrum.
The cross-correlation between the different 100 group cross-section sets was defined to be 1 per cent.
No correlation data were available for the 620 groups structure cross-section set.
The correlation matrix for the input reaction rates was supplied in the input of the data set. This matrix for the ORR was flat and not based on physical considerations. The energy dependent responses of the activation and fission detectors in this exercise are shown in fig. 1.
In order to characterize the adjusted neutron spectrum two extra energy dependent cross-section data sets were supplied; these were the damage cross-section of iron(steel) and the activation cross-section of the reaction $^{58}Ni(n,p)$. The uncertainty for the two damage cross-sections was 15% for all groups in the 100 groups structure (Remark: For the YAYOI spectrum, however, non-constant cross-section uncertainties for the Ni reaction were present; some participants might have used these uncertainties). The self-correlation was defined also as a Gaussian with a FWHM of 10 groups.

2.2. Quality of input data

From the description given above it should be clear that the input data comprise information with two different qualities:
- good quality physical information (reaction rates, cross-sections, calculated input neutron spectra);
- so called "extra" data for which the quality cannot be easily judged (eg variances and covariances).

The influence of this extra information (especially the variances and the correlations of the input spectra, the cross-section self-correlations and the correlations of the ORR reaction rates) on the various output data can not easily be estimated. Several adjustment codes require these extra data and the output of these codes is strongly dependent on it.
In the preparation of physical information in a format suitable for use in neutron spectrum adjustments, often conversions and extrapolations are required. Such was the case in this exercise. For instance, the

output of a reactor physics spectrum calculation run may not give accurate detailed information on the neutron fluence rate for the actual detector position in the thermal energy region. If this is the case the calculated information has to be supplemented with extra data. Similary, in most cases the calculated neutron spectrum and the measured reaction rates are not valid for the same reactor power level. For this reason the calculated spectrum has to be normalized in a suitable way.

The reactor physics codes often yield results in a rather coarse group structure (eg 39 groups for the YAYOI input spectrum).

Since the input spectrum required 100 groups, a conversion procedure was necessary. Several conversion procedures can be applied (preservation of shape, smoothing). The results will be influenced by the selected procedure.

Also some properties of the extra data should be considered.

It is clear that if the uncertainties in the input data of an adjustment procedure are selected in an arbitrary way, the output uncertainties may be physically meaningless.

The correlation matrix of the input spectrum will influence the output. In the derivation of this matrix the point values of the Gaussian function were considered, and not the values averaged over the corresponding energy groups. Different matrices will be obtained by these two methods, which will of course influence the results.

The chi-square value which can be calculated for an input data set of an adjustment run is dependent on the definition of the set. For the ORR input data set an unlikely small chi-square value was observed (see table 6), when a least squares adjustment procedure was applied.

This indicates too good a consistency of the input data. The unlikely good consistency is probably caused by the extra data, but of course, also other inconsistencies may be present in the good quality data. In view of the remarks above one should realize that the numerical output values (especially the uncertainties of the adjusted spectrum and the predicted reaction rates) may be somewhat unrealistic. Therefore it may not be concluded, for instance, that the uncertainties in the predicted displacement rate are representative of the present state of the art in adjustment.

However, the input data set as such (realistic or not) has served a

useful purpose in this exercise.
In the future the same input data set can be used also by laboratories which would like to test their abilities to adjust neutron spectra.

2.3. Choice between two cross-section sets

The participants had the freedom to use either the 620 groups or the 100 groups cross-section data. As stated before, only the latter contained corrections for self-shielding and the cadmium cover. Unfortunately, the information sheets were not clear enough on that point and this circumstance might have led to misunderstandings.
Furthermore, apart from these cross-sections, clear differences were observed between the two cross-section sets for some reactions.
This can be seen from table 2 where the effect of self-shielding and cadmium correction is also shown.

2.3.1. The 620 group cross-section data

During the preparatory phase of this project it was discovered that there were some non-negligible discrepancies between two sets of 620 groups cross-section data, derived from the ENDF/B-V dosimetry file by two different laboratories using quite different computer codes. After the exercise it turned out that some of the 620 group cross-section data sets used in the REAL-80 exercise were not completely correct. The results of the adjustment procedures will only be slightly influenced by this. Currently a new version of the modified ENDF/B-V dosimetry files in a 620 group form is available at the international data centers.

2.3.2. The displacement cross-section data

In the REAL-80 input data set two different sets of displacement cross-sections were given. The ASTM standard procedure E693-79 refers to the calculation of displacements in ferritic steel (iron) [7]. In this model it is assumed that the displacement cross-section for iron is an adequate approximation for ferritic steel. In the REAL-80 input data set these cross-section values were given in 100 and 620 groups structure, the latter one coded as ASTM-DISPL-STEEL.

In the Euratom Working Group on Reactor Dosimetry (EWGRD) values have been derived for the displacement cross-sections in stainless steel (with the following composition in mass percent: 74 per cent Fe, 18 per cent Cr and 8 per cent Ni) based on the data of M. Lott et al. [8]. These data (in 620 groups structure) have been coded as EUR-DISPL-STEEL in the REAL-80 exercise.

A quantitative comparison of these two displacements cross-section data sets shows appreciable differences between the ASTM standard and the Euratom practice, due to the different origins of the cross-section data sets and the different groups structures (in combination with conversion procedures for group values). The fission spectrum averaged cross-sections however differ by less than 2,5 per cent.

Due to practical reasons, all or nearly all participants used the ASTM displacement cross-section data.

3. DATA TREATMENT BY EVALUATORS

3.1. General

The IAEA forwarded all REAL-80 solutions received from participants on magnetic tape to the analyzing laboratories in Budapest and Petten. Software was developed for reading and sorting input data, for special calculations and for plotting tasks.
The evaluation of the participants data involved the following actions.

- Classification of information on the REAL-80 from the participants.
- Comparison of integral and uncertainty data supplied by the participants.
- Comparison and characterization of the energy dependent neutron spectrum data.
- Recalculation and comparison of integral and uncertainty data.
- Investigation of the effect of various normalization procedures.
- Calculation of various values which are a measure of the fit between measured and calculated reaction rates.
- Study of the output correlation matrices with the aid of factor analysis.

A part of the calculations performed by the evaluators used a 640 groups structure of the SAND II type, covering the energy range between 10^{-10} and 20 MeV. For a definition of group boundaries see [30].
In these calculations the output spectra and variances were converted to this 640 groups structure preserving the shape. Also the cross-section libraries were converted to this structure. Due to this approach no information was lost.

3.2. Treatment of data sets

The computerized treatment of the solution data sets gave a number of problems. The main problems were:

- transcription errors;
- deviations from the output format (format, units, etc.);
- incompleteness of output data;

- obvious mistakes in numerical data.

Much attention had to be paid to adaptions and corrections of the output data sets.
During the evaluation of the output data sets of the participants, it turned out that the output data sets did not contain all of the information about the actual input data applied in the adjustment of the participants. This missing information could refer to the omission of data (eg variance, covariance reaction rates, etc.) or to the special treatment procedure of the input data (eg conversion from group structure, conversion to point representations, self-shielding corrections).
Additional correspondence with the participants was required to obtain this information. From the experiences of data treatment and evaluation it became clear, that a more stringent description of the format is necessary, when the second phase of the exercise is started.

3.3. The plots

The output spectra of the participants have been plotted using the 640 groups structure.
Two types of spectrum plots are given for each output spectrum:
- one type of plot showing the fluence rate per unit energy as function of energy;
- a second type of plots showing the fluence rate per unit lethargy as function of the neutron energy.

In each type of plot the fluence rate is presented as a histogram (constant within each group).
In the case that the original group structure had energy values which are not the same as values of the 640 group structure, peaks can be generated in the plot of the fluence rate per unit lethargy when it is derived from the fluence rate per unit energy. These peaks do not indicate errors in the data.
In the spectrum plots the variances (if available) are plotted at distances of one standard deviation in positive and negative direction.
The data in the plots of the ratio of output and input spectrum are

given in the 100 groups structure. This 100 groups spectrum was obtained by averaging all the ratios for the groups of the 640 groups structure belonging to one group of the 100 groups structure.
This procedure was followed also, if the spectrum of the participant was presented in point values or in more than 100 groups.
Better plots can be obtained if a conversion of the input spectrum is made to the same group structure as used for the output spectrum. This was done for a few solutions in which the energy boundaries coincide with energy boundaries of the input spectrum. This procedure leads naturally, in case of coarser output spectrum structure, to loss of information of the input spectrum, and due to this the comparison of this plot with the other plots becomes more complicated. Both types of plots are presented here (see figures 8c, 8d, 9c and 9d).
Also plots were prepared of the significance of the modificaton. The "significance" is defined as the difference of the corresponding output and input spectrum values divided by the standard deviation belonging to the output spectrum.
The significance was plotted in the 100 groups structure.
The output correlation matrices supplied by the participants have also been plotted; the three dimensional information was transformed to a perspective plot. On these plots the axis subdivision is the group number and not the logarithmic energy value. The lowest energy value is at the left side of the plots.
Other plots are presented of characteristic values and of the results of the factor analysis.

3.4. The calculations

A number of characteristic values, group fluence rates (with group widths equal to energy decades) and reaction rates were calculated for output data of the participants. In these calculations all pertinent cross-section data were used in the 640 groups form. This leads to incorrect results in the cases where the output spectrum of the participant consists of less than 100 groups. Some examples of other group structure spectra are shown in fig. 2 and 3.
For this reason also some calculations have been performed with cross-section libraries of 10, 20 and 50 groups.
The group cross-section values in these libraries were calculated using

the input spectrum as weighting function for the 100 groups cross-sections in order to obtain "weighted cross-sections".
Much attention has been paid to judge the fit between the measured reaction rates and the calculated reaction rates for the output spectrum. For this purpose special calculations were made. These calculations were used to define DEV, ARD and CHISQ (see further 4.5).
The normalization of the input spectrum effects the modification obtained in an adjustment procedure.
The effect of various normalization procedures have been investigated (see for details appendix 1).

A program was written to perform the factor analysis of the output correlation matrices (see for details appendix 3).
The original (large) correlation matrices were split up into a set of vectors without information loss. These characteristic vectors (called factor loading vectors) were then compared and analyzed for the output set received from participants.
The calculated rotated factor loading vectors, (defined in appendix 3) were plotted.
With another small program the approximation matrix resulting from a number of rotated factor loading vectors could be calculated.
This gave the possibility to study the influence of certain factors.

3.5. The presentation

During the evaluation of the neutron spectrum data it became clear that it was not reasonable to perform a direct comparison of all output spectra at the same time. This is due to differences in the procedures used by the participants. These differences are due to alterations made by participants in the input data (eg deletion of reaction rates; use of 620 or 100 groups cross-section libraries; deletion of uncertainty information; differences in conversion procedure for cross-section or input spectrum data from one group structure to another; difference in neutron self-shielding; use of other cross-section data; use of other input spectra).
A rather simple division of the output data in three categories gives in our opinion the best survey of results. These categories are

solutions presented in:

- a 100 groups structure;
- a 620 groups structure;
- another structure.

All relevant tables with results are presented using this classification. Most numerical output data in this report are given relative (ie as a ratio) to the corresponding data for the input set (eg in most cases input neutron spectrum); this approach facilitates quick comparison.

4. REVIEW OF RESPONSES AND ADJUSTMENT CONDITIONS

The names of participating laboratories are listed in table 1. In the tables of this report, only the IAEA code will be used to identify each solution. In the next sections various aspects will be discussed.

4.1. Number of solutions

A total of 68 solutions from 13 laboratories were received and considered. Groupings and information on the solutions are listed in tables 3 and 4. The exercise allowed the participants to prepare more than one solution for the same problem. As a result, in some cases several solutions were given, either with more than one adjustment code, or with the same code under different conditions (eg using different number of reaction rates, more than one group structure, different convergence criteria, etc.).

4.2. Adjustment codes

The solutions were obtained by means of 12 different spectrum adjustment codes (see table 3). A relatively large number of solutions are based on adjustment codes of SAND-II type. Four distinct version of this code have been identified: SAND-II, SANDBP, SANDMX2 and SANDPET. Only a few laboratories have prepared solutions with more than one code. Results with NEUPAC and ITER-3 seem to be very similar to the ones of STAY'SL. For many adjustment codes literature references are readily available ([9]...[20]). However for a few codes no references were known.

In some cases the participants used their own version of a published code (eg STAY'SL or SAND-II) under the same code name, without clear indication of the modifications introduced. Such practices are confusing and should be avoided. Since various aspects of adjustment procedures have recently been published in the proceedings of the fourth ASTM-EURATOM symposium 1982 [21], these aspects will not be repeated here.

4.3. Number of energy groups

The number of energy groups used in the adjustment procedure was 100 in more than half of the cases, while only 15 per cent of the results was presented in 620 groups. This situation is probably due to the advice given by the IAEA to the participants to use the 100 groups data set because the 620 groups cross-section data were not accompanied by self-shielding and cadmium cover information.

4.4. Special group structures

Sometimes solutions were based on a groups structure other than the 620 and 100 groups of the input specification. In these cases the conversion procedure (with interpolation and extrapolation schemes) was not always specified by the participants. This means that the input data for these special groups structures are not uniquely defined. This implies that systematic effects and deviations might have been introduced by the participants choice of a new groups structure. In cases where solutions with coarse groups structures (50, 40, 20 and 10 groups) were used, it was observed that the shape of the neutron spectrum deviated from that of other solutions (see fig. 4 and 5, or 10 and 11), but in the integral data supplied by the corresponding participants only slight differences could be found.
To show the effect of the different energy groups structures extra calculations were performed in a number of cases using the participants groups structures. See further section 5.2.1.

4.5. Criteria for fit

The parameters of fit defined below are measures of the closeness-of-fit between measured and calculated reaction rates.
The criteria of fit used in the various adjustment codes are not the same. For that reason a comparison of the adjustment results on the point of fit or convergence is not so easy.
The evaluators calculated the results with aid of three different expressions which characterize the fit.
These expressions are defined as follows:
DEV - "standard deviation";

ARD - average relative deviation;

CHISQ - "chi-square", which is a logical generalization of the ARD parameter.

The results of these three relations are mainly determined by a summation of the squares of the differences of measured and calculated reaction rates for a specified set of reactions.
The main difference of the three relations is the weighting of the contribution of each reaction. The following formulas describe the relations:

$$DEV = \left\{ \sum_{i=1}^{n} \left[(\alpha_i^m - f.\alpha_i^c)/\alpha_i^m \right]^2/(n-1) \right\}^{1/2}$$

$$ARD = \left\{ \sum_{i=1}^{n} \left[(\alpha_i^m - f.\alpha_i^c)/s_i \right]^2/n \right\}^{1/2}$$

$$CHISQ = (\underline{A}^m - f.\underline{A}^c)^T . \underline{\underline{W}} . (\underline{A}^m - f.\underline{A}^c)$$

where:

n = number of input reaction rates;

α_i^m = measured (input) reaction rates;

α_i^c = calculated reaction rate for the solution (output)spectrum;

f = normalization factor;

s_i = estimated uncertainty of the difference between α_i^m and $f.\alpha_i^c$;

$\underline{A}^m$ = vector of n measured reaction rates (α_i^m);

$\underline{A}^c$ = vector of n calculated reaction rates (α_i^c);

$\underline{\underline{W}}$ = weighting matrix, defined as the inverse of the covariance-matrix, which depends on the input data set.

Various calculations have been performed to obtain values for the goodness-of-fit. For the ARD calculations the values of s_i did comprise the uncertainties of the measured reaction rates, and of the calculated reaction rates in so far as dependent on cross-section

uncertainties.

These calculations comprise a) results with calculated reaction rates by the evaluators, b) results with reaction rates from the participants and c) also reaction rates calculated by the evaluators for special group structures.

In the calculated results for the parameters the evaluators often observed that the output spectra are not normalized in the same way. This may be due to the application of different sets of reaction rates in the input of the adjustment procedure, but also properties of the adjustment code itself may be important in this respect. For this reason it was decided to perform a simple normalization before the calculation of the DEV and ARD parameters. No extra normalization has been done for the CHISQ calculations. For the sake of comparison of the fit parameters all parameters had to be calculated with the same definition of the normalization factor f. The normalization factor used by the evaluators is the value which is required to make (for the complete reaction rate set) the average ratio of calculated reaction rates based on the output spectra and the corresponding measured values equal to one. Thus the averaging is performed over 19 reactions for the ORR and over 12 reactions for the YAYOI. A further discussion on the normalization factor is given in section 5.2.2 and in appendix 1.

Fit parameters have been derived for more sets of calculated reaction rates. One set was obtained by the evaluators with aid of the given 100 groups cross-section library and the output spectra of the participants. A second set consisted of the values supplied by the participants. In a few cases, where one reaction rate was missing in the output of the participant, the output was supplemented with a calculated reaction rate (100 groups) by the evaluators for the reaction of interest. In the case that more than one reaction rate was missing in the output set of the participant, no fit parameters were calculated.

It should be noted that in the calculation of the ARD and CHISQ uncertainty data are required. The standard deviation s_i required for the ARD calculation is determined as the combination of the uncertainty in the measured reaction rate and the uncertainty in the calculated reaction rate due to the cross section uncertainties.

In the CHISQ calculation the weighting matrix is based on the variance

plus-covariance information as supplied in the input data set.

4.6. Correlation data

Only six of the adjustment codes used by the participating laboratories (ie STAY'SL, NEUPAC, LSL, SENSAK, IITER-3 and SANDBP) provided information on the correlation between the output group fluence rates of the neutron spectrum. Information was not always supplied by participants on the calculational procedure for the covariance data (or the related correlation matrices). The correlation information supplied by participants originated sometimes from a generalized least squares procedure, and sometimes from a procedure using Monte Carlo variations of cross-sections and reaction rates in a code based on the SAND-II principle.

5. ANALYSIS OF OUTPUT DATA

5.1. Comparison of adjusted spectra

5.1.1. The plots

Fig. 1 illustrates the 30, 60 and 90 per cent energy ranges for the ORR and YAYOI spectrum respectively.

A series of plots have been made for each output spectrum. Each participant received a full set with the evaluators plots and numerical data corresponding to his submitted solutions. In this report only a small number of these plots is included, which still will show some properties of the various spectra. Figs. 2 and 3 show the effect of using various groups structures for the ORR or YAYOI respectively. Fig. 4 through 9 present results for the ORR spectrum and figs. 10 through 14 present results for the YAYOI spectrum. In a number of plots a ratio is given with respect to the input neutron spectrum. The ratio plots for output spectra with less than 100 groups show a typical staircase structure. This is due to a continuous change of the group fluence rate values in the input spectrum in a coarse group of the output spectrum.

This "staircase" structure masks the ratio which would be obtained in the case that the input spectrum would be reduced also to the coarse group structure.

The disadvantage of reduction of the input spectrum is the loss of information (see 5.2.1.).

This report contains two similar series of plots for the ORR and YAYOI spectra. The first plots of this two series (fig. 4 and 5, and fig. 10 and 11) show the input neutron spectrum and some output neutron spectra in different groups structures. The output spectra were calculated with different adjustment codes.

In the first figures of the series the neutron fluence rate per unit energy is plotted with a fluence rate scale comprising 25 decades. These plots show all output information. The second series of plots shows the main part of the neutron spectrum on a scale with 3 decades for the fluence rate per unit lethargy.

Ratios of the output fluence rate to the corresponding input fluence

rate are shown in fig. 6 ... 8 and fig. 12 and 13.
These ratios $\phi_{out}(E)/\phi_{in}(E)$ show the energy dependent modifications of the input spectrum and are called here modification ratios. The results show that practically all the modification ratios were different. The series of these modification ratios included here comprise results for different energy groups structures and different adjustment codes. The last plot of the two series (fig. 9 and fig. 14) shows the "significance" of the spectrum adjustment. The significance value for a certain group is defined as the difference of output and input spectrum divided by the uncertainty value given for the same group of the output spectrum. In fig. 15 the spectrum uncertainties are shown. For comparison purposes, the uncertainties of the input spectra are also plotted in this figure.

5.1.2. The decade structure

The program that produced the plots also converted the output spectrum to a decade structure. This decade structure was used to determine the spread of the fluence rate values in the various decade groups. In a previous report [5] the spread of all solutions for the ORR and the YAYOI spectra in the decade structure was calculated. This has not been repeated here. The main reason is that it is not possible to convert "the other group structures" in a correct way to the decade structure, which is too coarse for that purpose (see 5.2.1.).
The spread in the decade group values for the output spectra of the 100 groups category was calculated for all solutions, except for one clear discrepant solution. Furthermore, the pecularity of RFSP not to give the first and last group value was not taken into account in the spread calculations. Results for the two extreme decade groups of these solutions were neglected in the calculation of the spread. Within any given decade all solutions were different; even the generalized least squares adjustment codes did not yield identical results. The group fluence rates in the decade group structure are given in table 5 and in the figures 16 and 17.
The spread in the solutions presented in 100 groups for the ORR (17 solutions) is lower than 4 per cent, except in group 6 (10^{-5}....10^{-4} MeV) and 7 (10^{-4}....10^{-3} MeV) where standard deviations

of about 11 and 16 per cent are found.
When the various decade values of the solutions are compared, it turns out that the generalized least squares codes give a modification ratio which is much smaller than one (about 0,7) in decade group 6, and a modification ratio which is larger than one (about 1,5) in decade group 7.
This type of modification is only present for the generalized least squares codes. The modification results of the other codes are in the decade groups much flatter than for the generalized least squares codes.
In the corresponding values for YAYOI also differences between the generalized least squares codes and other codes can be found. The spread in the solutions above group 8 (ie for $E>10^{-2}$ MeV) is smaller than about 7 per cent if all solutions (neglecting one discrepant solution) are considered (21 solutions). Below this energy the generalized least squares codes introduce small modifications (less than 8 per cent) while other codes gives modification between 10 and 40 per cent.

For the 620 groups solutions the spread is rather large. The number of solutions is low (6 for the ORR and 4 for the YAYOI). In the solutions differences can be expected due to various reasons:
- Failure to use neutron self-shielding correction by one participant.
- The use of different cross-section libraries.
- The deletion of some reactions in the adjustment (where in most cases different reactions were deleted).

For this reason no conclusion could be reached from the 620 groups results.

The average values for the other group structures presented in table 5 show an irregular pattern with a large spread in values.
This spread is caused mainly by the rather arbitrarily chosen decade groups structure used by the evaluators. For a number of solutions this structure is too fine. For a good comparison of spectrum shapes a structure which is coarse compared to the structures of the output spectra is needed (see 5.2.1.).

No calculations with such a structure have been performed during this analysis.

5.1.3. Discussion of modifications

The results presented in the fluence rate plots show that appreciable differences are present in the shape of the output spectra (figure 18).

In figures 5 and 11 the structure, especially in the resonance region for a code of the SAND II type, is pronounced. Also the distortion, which may occur due to a coarse groups structure, can be seen from these plots. The plots of the modification ratio (ie $\phi_{out}(E)/\phi_{in}(E)$) give more details for the differences of the series of output spectra.

In figs. 6 and 7 and figs. 12 and 13 the difference in the modification observed for various adjustment programs can be seen. Noteworthy is the fact that programs of the same type yield different output spectra. The programs of the SAND-II type give much structure in the resonance region and a rather smooth modification in the fast region. The CRYSTAL-BALL program produces very smooth modifications. The results obtained using generalized least squares adjustment procedures all have a typical modification in the resonance region of ORR which is not found using other adjustment codes.

The RFSP programs applied in REAL-80 did not give output for the first and last group. The SAND-II type programs also introduce modifications in the energy range 10^{-10}.....10^{-3} MeV of the YAYOI spectrum; the other adjustment codes do not give modifications in this energy range.

In fig. 8 modification patterns are shown for output spectra with a groups structure different from the 100 or 620 groups structures used in the input data description.

In this figure the "staircase" effect is clearly visible. This effect is also seen for the LOUHI78 code, where point values and a specific interpolation were presented so that a continuous spectrum representation became available. In the comparison of the modifications of GERDMO-2 with the other results one should consider that GERDMO-2 used a different input spectrum in the adjustment than that used by the other codes.

When we examine the significance of the spectrum adjustment (defined at the end of section 5.1.1. and shown in fig. 9 and 14) we observe that in most cases these adjustments are small or of the same order as the output uncertainty, but that in a few cases larger values are clearly present. This is the case for "staircase" plots, but also a few adjustment codes show unexpected results. For reason of comparison a 20 group significance plot is also presented for an input spectrum in 20 groups (see fig. 9c, 9d and 14b). From the decade groups calculations it was observed that the generalized least squares codes give in some energy ranges a typical modification which is different from that by the other adjustment codes. For example, as mentioned in 5.1.2. generalized least squares codes produce modifications in the energy region between $10^{-5}...10^{-3}$ MeV for the ORR spectrum (see fig. 6), and below 10^{-2} MeV for the YAYOI spectrum (see fig. 12).
Table 6 lists the contributions of the individual reactions to the chi-square and the ARD parameter, as calculated in a typical STAY'SL run. This table also gives total chi-square value as measure of the consistency of the input data set.

5.2. Adjustment conditions

5.2.1. Coarse group structure

In addition to the data treatment procedures for all solutions (mentioned in section 3.1) the evaluators performed special calculations to consider the effects of coarse groups structures, as used by some participants.
In these calculations the starting spectrum was the input spectrum of the REAL-80 exercise. This spectrum was converted to 50, 20 and 10 groups structures, which were applied by participants in the REAL-80 exercise, and had the advantage that the energy boundaries of these coarse groups were also present as energy boundaries in the 100 groups input spectrum. The conversion of this input spectrum was performed in such a way that the group fluence rate in the coarse group was equal to the sum of group fluence rates in the corresponding fine groups. The resulting spectrum shapes are shown in fig. 2 and fig. 3 for ORR and YAYOI respectively. These spectra were also converted to a decade group

structure using the same conversion principle (with a linear subdivision of group fluence rates, when the original group boundaries did not coincide with the new boundaries). The results of the various representations of the two input spectra in the decade structure are shown in table 7; in this table all decade values for the two converted input spectra are presented relative to the values derived for the 100 groups structure. These results show that relative values larger than 10 can be present. The actual deviation depends on the spectrum shape and the selection of the boundaries of the groups structure with respect to the decade groups structure. From these results it is clear that the comparison of decade groups is not useful for spectra with different group structures which contain less than 100 groups.

The coarse group spectra were also expanded to the 640 groups structure with conservation of spectrum shape and spectrum normalization. With these expanded spectra the reaction rates were calculated using the 640 groups representation of the 100 groups cross section data set. These calculated reaction rates were compared with the calculated reaction rates valid for the original 100 groups spectrum. In case this approach was used to calculate reaction rates using a few groups spectrum and a cross-section data set in the same few groups structure, weighted with the 100 groups spectrum, then of course identical reaction rates as for the 100 groups calculations were obtained. Table 8 shows the results for the case that the REAL-80 input cross-section data in 100 groups were used without weighting. The results show that important deviations (larger than 10 per cent) can be found even for the 50 groups structure. For the 10 groups structure ratios larger than 4 are present. From these results listed in table 8 it is clear that calculation of reaction rates with unweighted cross section values for spectra with less than 100 groups leads to significant errors. On the other side these data show also what may occur if a coarse group input spectrum resulting from reactor physics calculations is converted to a spectrum with a finer group structure which is required by available adjustment codes. If the input spectrum is not available in a fine groups structure, then the calculation of correct reaction rates requires the use use of weighted coarse group cross-section data. In this case only the coarse group input spectrum is available as weighting function; such

weighting function to derive weighted cross-section values is not adequate, if the actual spectrum contains appreciable gradients in one or several energy groups.
An inadequate input spectrum representation will yield inaccurate calculated reaction rates, which may deviate too much (say more than 30 per cent) from the measured reaction rates; such a large discrepancy is not a good starting point for any adjustment algorithm. The conclusion is as follows: Good spectrum adjustment results can only be obtained if the input spectrum resulting from reactor physics calculations is available in a group structure which allows an adequate representation of the shape of the actual spectrum to be determined.

5.2.2. Effect of the spectrum normalization

The neutron spectrum normalization procedures used by the different adjustment codes perform a preliminary fitting to the input data, and as a result they affect the neutron spectrum adjustment. Thus, in principle, the neutron spectrum normalization is part of the adjustment procedure itself.
Some general expressions used for the neutron spectrum normalization factor are derived and discussed in appendix 1. In those cases where, - together with the usual input data -, also the input covariance information is available, the generalized least squares procedure can be applied to determine the best value for this parameter (see App. 2).
In the REAL-80 exercise the input neutron spectra (for the ORR and YAYOI reactor) were given in a normalized form, together with the chosen normalization factors. These data were then used by the participants in their neutron spectrum adjustment; in some cases the participants used an additional (re)normalization.
The effect of the neutron spectrum normalization on the adjustment procedure has been studied in some detail. Table 9 shows some characteristic results, obtained for the YAYOI reactor spectrum by means of an extended version of the STAY'SL code.
The normalization formulas used here correspond to those listed in Appendix 1. The data in table 9 show that the resulting normalization factors for the various procedures are in the range between 0,99 and 1,32. Consequently, the energy dependent modifications performed by the

adjustment procedure on the input spectrum will also show different patterns (see the plots for YAYOI in figs. 19 and 20), resulting in different solutions for the same input data (see also CHISQ parameter in table 9).

The role of the neutron spectrum normalization can be especially important in those cases where the adjustment code of interest can not take into account the uncertainties of the input data during its adjustment procedure and where the differences in these uncertainties are important.

In this case, in the absence of appropriate weighting factors, the normalization will actually determine which reaction rates play an important role and therefore determine the neutron spectrum modifications.

The influence of the normalization on the consistency of the renormalized input data is shown by the χ^2-values, listed in table 9. From these data one can understand the spread observed in the chi-square values and in the shape of the generalized least squares solutions supplied by the different participants.

5.2.3. Effect of the input correlation matrix on the solutions

Runs were performed using the STAY'SL code to examine the influence of the input covariance information on the results of the neutron spectrum adjustment. Three different cases were considered by the evaluators to study the effect of the pattern of the input neutron spectrum correlation matrix:

a. A matrix with a Gaussian function for the correlation as used in the REAL-80 input data set (see section 2.1.).
b. A pure diagonal matrix (see Appendix 3).
c. A matrix with strong correlations (an artifical correlation matrix generated with everywhere positive elements between 0,99 and 1; see figure 21).

The corresponding variances and all the other input parameters were used in the form defined by the REAL-80 input data set. The results for the YAYOI neutron spectrum are shown in figure 22, and table 10. Different solutions for the three cases were obtained. The most signifi-

cant modifications on the input spectrum were observed for the Gaussian shape and diagonal correlation matrices. Only very slight changes in the input spectrum were possible if it is assumed that there is a strong correlation between the different group fluence rate values. The use of a diagonal matrix supposes that no correlation is present in the input neutron spectrum. Consequently, the adjustment procedure has more "freedom" to perform spectrum modifications, and so more structure can appear in the solution spectrum (see figure 22).

For the determination of the uncertainties in the integral spectrum characteristics one needs the covariance matrices for the corresponding cross section data (see Appendix 4). The output correlations of the generalized least squares codes are based on the corresponding input data. This means that the input covariance information will essentially determine the variances and the correlation matrix of the output spectrum (see section 6.2). The effect of the covariance information on the uncertainties of the different integral parameters is discussed in section 5.4.3. Based on what is said there the results obtained for the uncertainties in table 10 can be understood.
The uncertainty values of R_{Ni} and R_{dpa} involve contributions due to the neutron spectrum and cross-section uncertainties. These data are also presented for the different solutions in table 10.

During the evaluation of participants data an improved set of uncertainties of measured reaction rates for the ORR neutron spectrum became available (table 11). No significant deviation was found in the results of the neutron spectrum adjustment performed with this new data set.

5.2.4. The fit parameters

In section 4.5 the fit parameters are defined. The numerical results are given in table 12. The values indicated with suffix 1 are calculated by the evaluators. In these calculations the reaction sets described in the input of the exercise were applied (19 reactions and 12 reactions for the ORR and YAYOI respectively) in combination with the 100 groups REAL-80 cross-section values and the output spectrum of the participant. Due to this approach the values for the fit parameters

can be compared directly. The fit values indicated with suffix 2 are calculated for those cases where the reaction rates calculated by the participants and by the evaluators were not the same. In this case the reaction rates given by the participants were used. If not all reaction rates were used by the participants, the missing reaction rate was obtained from the evaluators calculations in order to obtain comparable fit values. In the case that the evaluators and participants data agreed, or that more than one reaction was missing no extra calculations have been performed. The fit parameters with suffix 3 were calculated with special cross-section libraries. The library of interest is indicated in table 12. All DEV and ARD calculations are preceded by a normalization procedure of the output spectrum. The normalization results are listed also in table 12 under the columm heading $\overline{\alpha_m/\alpha_c}$. The results of the evaluators calculations demonstrate that the YAYOI normalization differs in a number of cases from the value 1. This has to do with the different reaction sets which were in a number of cases used by the participants. Two deviations were present (eg the inclusion of the reaction NI58P and the deletion of the reaction TI47P); the consequence is that the output spectra are normalized in different ways. This effects directly the calculated reaction rates for the output spectrum. In the case that the spread of the R_{Ni} value for all "100 groups" participants results is calculated (see table 13) without the extra normalization, a standard deviation of 4,6 per cent is found. If the normalization shown in table 12 is used the spread becomes 3,8 per cent. For the R_{dpa} the spread was 2,4 per cent and after correction it was 1,8 per cent. This indicates that the normalization is an important part of the adjustment.

The actual fit parameters DEV, ARD and $\sqrt{CHISQ}$ presented in fig. 23 show all more or less the same pattern. In the plots the successive points for the various solutions have been connected in order to facilitate the comparison of the behaviour of the fit parameters. For YAYOI the $\sqrt{CHISQ}$ eye-guide does not show some extremes which are present in the two other eye-guide lines. This is related to the fact that the CHISQ 1 values were derived for output spectra, not renormalized by the evaluators.

The range in magnitude of the fit parameters observed for the output

spectra is the largest for the ARD, followed by the DEV. Due to the large differences observed for the ARD values the ARD parameter seems to be the most sensitive parameter by which to judge the convergence, but it has to be stated that the rather large differences in ARD values do not seem to effect the calculated reaction rates R_{Ni} and R_{dpa}. The range at the ARD values is larger for ORR than for the YAYOI solutions. Nevertheless, the spread in the calculated reaction rates for nickel and for the displacements is smaller for ORR than for YAYOI (see table 13).

An advantage of using of the "average relative deviation" (ARD) as a fit parameter is that a value of the order of one can be expected. In that case the deviation of the measured and calculated reaction rate and the uncertainty of this deviation are about equal.

Table 12 shows that the values of the ARD are roughly equal to 0.6 for ORR and to 0.9 for YAYOI. If the 100 groups data are considered the spread in this value is about 50 per cent for ORR, and less than 10 per cent for YAYOI (in the latter calculation one outlier was removed). This indicates that solutions with a wide range of ARD values seems to give reasonable calculated reaction rates for nickel activation and atom displacements. For this reason it can be concluded that the parameters which were applied here to determine the fit are not optimal ones. Nevertheless, they are the best ones available at present.

In table 11 uncertainties are presented for all reaction rates. A suitable combination of the contributing terms determines the uncertainty values for s_i, which are required for the determination of the ARD-parameter.

Analysis of the solution spectra leads to the conclusion that frequently an ARD value much less than unity is obtained; this is related to unrealistic structure occurring in the output spectrum. Therefore some caution is necessary when the fit parameter is used as convergence criterion in cases where the adjustment algorithm requires iteration.

5.3. Characteristic spectrum data

The participants calculated integral spectrum characteristics, the nickel activation rate, and the displacement rate in steel (see table 13). For the calculation of displacement rates both participants and

evaluators used the 100 groups displacement cross section set based on the ASTM standard practice [7]. The results show that the spread in these data is small (less than 3 per cent). Only the nickel activiation rate of YAYOI shows a large spread of 5 per cent and more. These results for the activation rates and the displacement rates are plotted in figures 24a, 25a, 26a and 27a.

The large spread in the nickel activation rates is due to appreciable differences in the energy dependent modification ratic in the high energy region of the YAYOI spectrum. This large spread in this energy region can also be seen in the results for group fluence rates in the decade structure presented in table 5. The reason for this effect is not clear. Of course differences are present in the input; some participants used the NI58P reaction or left out the reaction TI47P. But there seems to be other reasons, but these could not yet be identified.

The evaluators also calculated the same spectrum characteristics as the participants, plus a few additional characteristics. The results of the calculations for the nickel activation rate and the displacement rate in steel are presented in figures 24b, 25b, 26b and 27b. These data and the other data are listed also in tables 14 and 15. In the comparison of these data one should consider that the data for the groups "620" and "other groups structures" is less reliable or even unreliable, as mentioned in section 3.3, 4.4 and 5.2.1

The definitions of the physical quantities listed in table 15 are given in table 16. A few of these quantities are used to obtain data for the comparison of the low energy side of the neutron spectra.

An interesting parameter is the normalized Damage-to-Activation Ratio (DAR). The normalization of the DAR is performed in such a way that the fission neutron spectrum yields a DAR value equal to 1. The displacement rate obtained for steel relative to the activation rates for the reactions $^{58}Ni(n,p)$ and $^{54}Fe(n,p)$ can be considered. The numerical values are listed in table 15. If only the category of 100 groups spectra is considered and after removal of one outlier the average DAR value is 1,02 for ORR, with a spread of 1,2 per cent, and 1,12 for YAYOI, with a spread of 3,3 per cent.

The spread in the values is low in comparison with the spread in reaction rates. This indicates that normalization problems may be expected

for the output spectra. This is not surprising, since the effect of the normalization cancels in the definition of DAR.
In table 14 some data for integral quantities are shown, calculated with cross section values in a special groups structure, as used by the participant. These libraries contained the input spectrum weighted group cross-sections in the groups structure of the participants.
Based on the output spectrum it is possible to compare for the reaction $^{58}Ni(n,p)$ the calculated reaction rates with the measured reaction rates. This comparison also gives an idea of the quality of the adjustments. In fig. 24 and 26 these values are shown. These figures show that a good result is obtained for the ORR; for the YAYOI however the calculated reaction rates are clearly lower than the measured ones. This indicates an inconsistency. In table 17 and 18 a summary is presented for some characteristic data.

5.4. Uncertainties in output data

5.4.1. Uncertainties supplied by the participants

The uncertainty data in integral parameters as supplied by the participants are listed in table 19. Relative values regarding the input neutron spectrum are given. Large discrepancies are present in the uncertainty data predicted by the various adjustment codes. Some SAND-type solutions supply extremely small uncertainty values. This is partly due to the fact that the contribution of the input neutron spectrum uncertainties was not taken into account in the calculation of the uncertainties of R_{Ni} and R_{dpa}.
No agreement is found even in the uncertainty data obtained by the same type of adjustment codes (generalized least squares).

The subdivision of the results into three categories of output spectra (based on the neutron energy groups structure) may not be fully justified in this case since for calculations of the output spectra and correlation data various amounts of the given input covariance information were used. Similarly, various amounts of the output covariance data were taken into account for determination of the uncertainties in R_{Ni} and R_{dpa}.

These are the main reasons for the large differences found in the uncertainty data of integral spectrum parameters.

5.4.2. Uncertainties calculated from the output information of the participants

A second set of uncertainty data was calculated by the evaluators from the output neutron spectra and covariance information supplied by the participants. Two different uncertainty values were determined for each solution spectrum:

- The uncertainty based upon all the output covariance information given by the participants (the case "with correlations").
- The uncertainty based upon only the output variances (the case "without correlations").

Results for the 100 groups solutions are give in table 20. From these table we derive the following observations:

- Rather good agreement with the participants data (table 19) was obtained in the case of the uncertainties for the integral spectrum data.
- No agreement with the participants data was found in the uncertainty values for R_{Ni} and R_{dpa}.
- A relative small spread (compared with the participants data) is present in the uncertainties of R_{Ni} and R_{dpa} in table 20. This is due to the contribution of the corresponding cross section uncertainties, which are the same for all solution spectra.
- Nearly identical results for the generalized least squares type adjustment codes were obtained.
- The uncertainties derived from diagonal covariance matrices are significantly lower than the corresponding values obtained for all output covariance information (see 5.4.3.).
- The SANDBP results give extremely low uncertainty values for ϕ_{tot}, $\phi(E>1\ MeV)$ and $\phi(E>0,1\ MeV)$. This is due to the structure of their output spectrum correlation matrices (see 5.4.3. and figures 28 and 29).

5.4.3. Effect of covariance information on the uncertainties

As shown in appendix 4 the uncertainty of the integral neutron fluence rates are determined by the covariance data of the neutron spectrum of interest. Assuming constant values for the variances (and for the energy group widths) let us investigate the effect of the structure of the actual correlation matrix on the uncertainties of integral spectrum characteristic .

Generally one can write (see appendix 4):

$$S = \sum_k \phi_k$$

$$s^2 = \mathrm{var}(S) = \sum_k \sum_l \mathrm{cov}(\phi_k, \phi_l)$$

Some special cases will be considered.

a. For a diagonal matrix the above expression becomes simply

$$s_1^2 = \sum_k \mathrm{var}(\phi_k)$$

b. A matrix with elements calculated with a Gaussian function (like the input correlation matrices for the REAL-80 exercise). This type of matrix yields a variance s_2^2. In this case all matrix elements are > 0. Consequently the relation $s_2^2 > s_1^2$ is obtained.

c. A band matrix. (The correlation matrices of the STAY'SL type solutions in the REAL-80 exercise are examples of this type). The variance for this output matrix is denoted by s_3^2. Depending on the ratio of the number of positive and negative matrix elements both the relations $s_3^2 > s_1^2$ and $s_3^2 < s_1^2$ are possible.

d. The matrix $\underline{\underline{E}}$ which has all matrix elements equal to unity is the extreme of the strong correlations. Then

$$s_4^2 = \sum_k \sum_l \sqrt{\mathrm{var}(\phi_k) \cdot \mathrm{var}(\phi_l)}$$

This is the maximum value for the variance in the integral value under consideration.

e. Strong correlations are present if all the elements of the correlation matrix have absolute values near unity. Depending on the sign and value of the matrix elements both the relations $s_5^2 > s_1^2$ and $s_5^2 < s_1^2$ may occur.
To determine which sign holds for the difference $(s_1^2-s_3^2)$ and also for $(s_1^2-s_5^2)$ one needs the complete uncertainty information instead of only the correlation matrices.

To support the considerations made above some calculations for the ORR and YAYOI input spectra were performed. Alternatively diagonal and Gaussian shape band correlation matrices for the input neutron spectrum and cross sections were used. The input variances were always the same as defined by the REAL-80 exercise. The uncertainties obtained in this way for the integral spectrum characteristics are given in table 21. In that table the first two lines both for the ORR and YAYOI spectrum present the values for s_2^2 and s_1^2 respectively. The results are in agreement with the statement written under b).
If the correlation matrices both for the input fluence rates and the cross-sections for σ_{Ni} and σ_{dpa} have a diagonal structure, then the calculated uncertainties in the integral spectrum characteristics R_{Ni} and R_{dpa} are appreciably smaller than for the case of correlation matrices with a Gaussian shape. Furthermore for diagonal matrices the variances of the group fluence rates are more important than the variances of the group cross-sections with respect to their influence on $s(R_{Ni})$ and $s(R_{dpa})$.

6. ANALYSIS OF OUTPUT CORRELATION MATRICES

The influence of the neutron spectrum covariance information on the neutron spectrum adjustment was investigated earlier (see points 5.2.3., 5.4.3.). In this chapter correlation matrices accompanying the solution neutron spectra will be considered.

6.1. General considerations

The covariance information for the output spectra was made available by the participants in the form of correlation matrices, in most cases with 100 x 100 elements (exceptions: SENSAK with 40 x 40 and LSL with 20 x 20 matrix elements).
The comparison of such a large amount of data is not a simple matter. For this reason the following approach was taken.

- Perspective plots have been used for their general characterization.
- A numerical characterization has been applied after considerable data reduction.

The method of factor analysis (see eg [25], [26] and [27] and App. 3) have been used for the statistical analysis of the correlation matrices, as well as for the necessary data reduction.
The correlation matrices of the 100 groups solutions have been analyzed in the same way, but some problems arose in the processing of the 40 groups and 20 groups cases. This was due to the following reasons:

a. correlation matrices of coarse structure (eg 20 groups) cannot be derived from the correlation matrices of finer groups structure without loss of information, while on the other hand;
b. no appropriate algorithm is presently available for the extension of the coarse groups structure to 100 groups (eg what type of interpolation formula should be used?).

Therefore, detailed intercomparison will be given only for the 100 groups solutions. The results of SENSAK and LSL were also analysed but their direct intercomparison to the 100 groups data will not always be possible (see section 6.3.3.).
The usual grouping of the reactor neutron spectrum (as fast or fission,

intermediate or slowing down and thermal neutron energy regions) will be used in presentation of the results, as - due to neutron and reactor physics processes - strong correlations may be present in a reactor spectrum within these energy regions and correlations may occur between the different energy regions as well.

6.2. Overall characterization

About one third of the REAL-80 solutions contained correlation matrices (see table 22). The analysis of the adjustment codes in question showed there was a fundamental difference between the algorithms used to calculate the correlation matrices. On can distinguish two different types of methods:

1. The deterministic method (STAY'SL [9], NEUPAC [10], SENSAK [11], LSL [12], ITER-3 [13]);
2. the stochastic method (SANDBP [14]).

A general characterization of the correlation matrices is given by presenting them in perspective plots (figures 28...36). These plots show that the pattern of the correlation matrices based on deterministic calculations by a STAY'SL type generalized least squares approach, and those based on the stochastic model of Monte Carlo variations using the SAND-II approach, are remarkably different.

The perspective plots of the correlation matrices for the STAY'SL-type output spectra show practically no correlations for energy groups far from each other. The structures shown in these plots reflect the main characteristics of the input spectrum correlation matrix.

On the other hand, the program SANDBP gives solutions with very strong correlations in the resonance energy region. This effect is especially striking in case of the YAYOI spectrum, where the 90 per cent response regions of the detectors in the set always lie above an energy of 0,1 MeV (see figure 1 and 29).

The Y46BC and Y47BC solutions differ from each other only in the 5-points smoothing applied in the latter case. The perspective plots in fig. 29 and 36 show that the smoothing procedure had the effect that more and larger surfaces appeared, especially in the slowing down region, without modification of the general pattern of the matrix.

Since the smoothing resulted in a modification only of correlations characteristic of the detector set, its application did not influence the overall solution.
Similar patterns were however obtained for the adjustment codes STAY'SL (fig. 32 and 33), SENSAK (fig. 34), LSL (fig. 35) and ITER-3, which indicates a close similarity in the general performance of these programs.
Finally, one should realize, that the input correlation matrices (both for the neutron spectrum and the cross-sections) have artificially been created by means of Gaussian functions for the sole purpose of the exercise (see section 2.1.). For this reason no physical interpretation of these matrices was possible. Similarly, care has to be taken in the physical interpretation of the covariance information obtained from these artificial input data.

6.3. Numerical characterization

6.3.1. The average correlation coefficients and the variances of matrix element values

These values (defined in appendix 3) are shown in table 23 for the various correlation matrices.

The input correlation matrix was defined both for the ORR and YAYOI neutron spectrum in the form of band-matrices having elements determined by a Gaussian superimposed on a small background of 0,4 per cent. This means that its elements are practically different from zero, only in the vicinity of the main diagonal. The largest value for the average correlation coefficient, $\bar{r}_{ij}$ was obtained for both spectra in the thermal neutron energy region, due to the limited number of energy groups present. Only a very weak correlation was found in the slowing down part of the spectrum, where many more energy groups are present (see table 23). The variances are obtained in accordance with the definition of the input spectrum correlation matrix. Very slight differences between the ORR and YAYOI input correlation matrices supplied to the participants were detected by this parameter.
Probably these differences are due to some rounding procedure during

the preparation of the three digit values for the input data set.

The correlation matrices for the solution neutron spectra show a completely different character depending whether they were derived in a deterministic way with a STAY'SL-type code or in a stochastic way by Monte Carlo variations.

The deterministic codes in most cases decrease the value of $\bar{r}_{ij}$ relative to the input information. The largest modification in the correlations were introduced by these codes in the thermal and fission neutron energy regions in case of the ORR neutron spectrum. For the YAYOI spectrum the correlations were significantly modified in the fission energy region, where the main response of the detector set is present.

The results of the adjustment codes SENSAK and LSL (see solutions 043JA, Y44JA and 031HA, Y25HA) can be considered only as formal ones in the thermal neutron energy region, since they contain here only 1 or 2 energy groups. Furthermore, the SENSAK gives only positive correlations through the entire spectrum, which is a surprising result compared with the other generalized least squares solutions.

The STAY'SL-type codes give nearly identical results for the variances of all matrix elements. Practically no modification in the correlation data relative to the input information was detected by the $\overline{r_{ij}}$ parameter in the intermediate neutron energy region of the ORR spectrum. Only slight modifications in the corresponding values can be observed also in case of the YAYOI neutron spectrum (see also the corresponding perspective plots).

In contrast to the situation presented above, the results obtained with the Monte Carlo model show strong correlations in all the three energy regions of the spectra (see table 23 for the solutions 045BC, 055BC and Y47BC, Y56BC). In case of 045BC the reaction FE58GCd was deleted from the adjustment procedure. Consequently, the comparison of the results for 045BC and 055BC shows the effect of this detector on the correlations. Similar considerations hold for the YAYOI solutions coded by 046BC and Y56BC with respect to the reaction TI47P. Furthermore, in the solution Y47BC 5-points smoothing with the SAND-procedure was applied.

The results show that this smoothing procedure introduces significant modifications with respect of correlations only in the slowing down part of the spectrum. This observation is in agreement with the well-known property of the SAND-type codes being susceptible to reflect the structure of the detector cross sections in the solution neutron spectrum.

6.3.2. The rank of the correlation matrix

A main characteristic of a matrix is its rank. The rank of the correlation matrices in question can be found by looking at the number of non-zero eigenvalues. Information on this effective rank (see appendix 3) is presented in table 24.

Input information. As already mentioned above, the input correlation matrices were given in form of Gaussian type band matrices of high rank; the effective rank is about 40 to 50 both for the ORR and YAYOI spectra. This implies that too many group fluence rates can be modified independently from each other in the neutron spectrum adjustment procedure, which from a physics point of view is doubtful. Nevertheless, one should not forget that this input information was artificially generated.

STAY'SL, NEUPAC and ITER-3 solutions. These adjustment codes - due to their similar algorithm and identical energy groups structure - give comparable results.

All of them increase the rank of the solution correlation matrix with respect to the input (table 24). The following values for the rank r were obtained:

r = 52 ... 54 for ORR, and

r = 45 ... 49 for YAYOI.

Although the input spectrum correlation matrix was unrealistic in itself, these codes have 'loosened' the solution spectrum correlations relative to the input. The higher rank indicates a 'narrower' band matrix, and the forced small correlations may underestimate the uncertainty propagations (see section 5.4.3.).

Stochastic model solutions. If the number of actually existing correlations is quite high, then the correlation matrix will have a very low rank. This fact is observed for the SANDBP case, where the following rank values were obtained:

r = 7 ... 8 for ORR, and

r = 5 ... 6 for YAYOI.

The low rank indicates the presence of strong correlations (in cases of input spectra of this type there are many constraints for the solution spectrum, so that the code can not yield too strong modifications. See also section 5.2.3.).

6.3.3. Analysis of the factor matrices

In the factor analysis the correlation matrices to be investigated are replaced by the product of 'factor loading matrices' being created from the factor loading vectors (for more details and definitions see appendix 3). For characterization of the 'goodness' of this approximation the average communalities are used. It follows from the derivation of the approximating matrix that the sum of the communality values in its main diagonal agrees with the sum of eigenvalues taken into account for the original correlation matrix. That means that the average communality is equal to the corresponding cumulative percentage of eigenvalues (table 25). By properly selecting the number of the factor loading vectors a value near 1 can be obtained for the communalities, that is to say no unjustified loss of information will result from this transformation. In our calculations a value of 80 per cent for the average communalities was accepted. Based on the data in table 24 one may conclude that about 20 factor loading vectors have to be taken into account both for the ORR and YAYOI neutron spectra.

In fig. 37 the output spectrum correlation matrix for the solution Y53AA is compared, with the corresponding approximating matrices generated by 28 and 20 factor loading vectors, respectively. The plots show that by taking only the 20 most dominant eigenvectors instead of the complete set an acceptable approximation for the correlation matrix can be obtained.

Input information. The average communalities for the input spectrum

correlation matrices and for the solutions in question are shown in table 25.

The rotated factor loading vectors (see appendix 3) calculated for the YAYOI input spectrum correlation matrix and for the solution Y53AA are shown in figure 38. The values for the corresponding rotated factor loadings are plotted as a function of the neutron energy. The rotated factor loading curves can be reflected through the horizontal axis, ie only the shape and not the algebraic sign of the curves are here of importance.

The factors no. 2, 6, 10 and partly no. 8 refer to the fission energy region (energy groups 70 - 100).

The $r_{1,1}...r_{8,8}$ submatrix represents the correlations in the thermal energy region. According to the rotated factor loading curve no. 3 the strongest correlation in this region must be present at the neutron energies $10^{-8}...10^{-7}$ MeV, correspondingly to the most probable energy value of the thermal neutrons. Nevertheless - due to the mathematics derivation - two additional factor loading vectors which are not interpretable from a physics point of view (no. 9 and 14) are also present. Similar considerations for the slowing down part of the spectrum and for the ORR input spectrum correlation matrix can be made.

STAY'SL, NEUPAC and ITER-3 solutions. Table 26 compares the rotated factor loading vectors obtained for the correlation matrices of the input spectrum and their replication in the spectra. A graphical comparison is given in figure 38.

The data show that the STAY'SL-type adjustment codes only slightly change the input correlation information. In energy regions not or poorly covered by the response of the detector set the output spectrum correlation matrix reflects the input information. These energy regions are: for ORR spectrum E = 360 keV ... 1 MeV and E > 14 MeV; for YAYOI spectrum E < 15 keV, E = 360 keV ... 1,8 MeV and E > 14 MeV (see fig. 1). Factor loading vectors not present in table 26 were created by the adjustment procedure of the codes in question.

In case of the ORR solutions 12...15 of the investigated 20 rotated factor loading vectors were approximately identical. For the YAYOI solutions with the same type of code 18-20 rotated factor loading vectors were approximately the same. This fact also indicates a close

similarity in the performance of these adjustment codes.
With respect to the correlation matrices for the cross-sections we remark that these in the REAL-80 exercise were approximated by a band matrix which is "broader" than the one for the input spectrum (see section 2.1.). Since the band width of the cross-section correlation matrix comprised roughly one third of the number of energy groups, it seemed not practical to study the propagation of cross-section correlation into the complete output correlation matrix. Moreover these cross-section correlations are not expected to lead to any new statement (their effect must occur in the corresponding response regions, in case of partial coincidence of the response ranges of the detectors the superposition of their effect will be present). Such a study seems reasonable if realistic information on cross-section correlations could be used. The first data sets of this type have found use just at time the REAL-80 project was evaluated [22], [23].

Characterization of SANDBP solutions. As can be seen from table 24 it was possible to arrive at a cumulative percentage of eigenvalues of 95 per cent via 6 to 7 factors in case of the more complicated ORR spectrum, and via 4 to 5 factors in case of the simpler YAYOI spectrum. This surprisingly low value as compared with that obtained earlier shows that the number of actually existing effects exceeds the number of factors found.
In other words: since the rank of the correlation matrix is low, each mathematical factor represents more physical effects. This can also be recognized by the corresponding rotated factor loading curves (figures 39 and 40).
The rotated factor loading vector no. 1 of ORR indicates an effect in the fission energy region (in energy groups 81...90) and at the same time a considerable fluctuation in the slowing down region (in energy groups 10...45) in accordance with the cross-sections of the detectors. The rotated factor loading vector no. 2 indicates two considerable effects in opposite directions in energy groups 82...90 and 91...100 of the fission energy region. A comparison of the rotated factor loading curves and the cross-sections showed that factor no. 1 of ORR contained the total effect of the reaction C059G as well as a partial superimposed effect of the reaction cross sections U238G, U238GCd and SC45G.

The effects detected by rotated factor loading vector no. 2 are due to the reactions SC45G, FE54P and NI60P.
Similar considerations can be made for the YAYOI correlation matrix in connection with the reactions W186G and AU197G.

SENSAK and LSL solutions. The rotated factor loadings of the SENSAK and LSL solutions cannot be compared with the 100 groups input information and 100 groups solutions due to the other energy groups structure.
In case of the SENSAK solution some rotated factor loadings have a pattern which corresponds to the overall pattern of extremes in a cross-section curve; but further identification is not possible since the input data are unknown.
The thermal neutron energy region consists of one or two energy groups for the LSL and SENSAK code respectively, so that this region cannot be investigated from point of view of correlations.

6.4. Discussion

Only six of the adjustment codes used by the participating laboratories (ie STAY'SL, NEUPAC, SENSAK, LSL, ITER-3 and SANDBP) provided information on the correlation between the output group fluence rates of the neutron spectrum. Information was not always supplied on the calculation procedure for the covariance data (or the related correlation matrices). The information originated sometimes from the properties of the least squares principle (deterministic model) and sometimes from Monte Carlo variations applied in accordance with the input standard deviations (stochastic process).
The patterns of the correlation matrices based on deterministic calculations and those based on the stochastic model were significantly different.
In case of deterministic adjustment codes most of the factor loadings of the input spectrum correlation matrix can be identified also in the solution matrix. The output correlation matrix will be determined by these factor loadings in the energy regions where the response of the detector set used in the adjustment procedure is poor.
The input spectrum and cross-section correlation matrices were artificially generated. Consequently they have only mathematical meaning and

cannot describe the real physical correlations present in a reactor neutron spectrum and in the cross-section functions, respectively. As the correlation matrices of the adjusted neutron spectra are used in the calculation procedure of uncertainty values for different spectrum characteristics, the replication of the main characteristics of the input correlation matrices will lead in these cases to unrealistic results.

The first data sets of the physically acceptable correlation matrices for cross-section data are already available (eg [22], [23]), but more realistic correlation matrices for input spectra based on physics calculations are hardly or not available.

The correlation matrices of stochastic-type solutions differ strongly from the pattern described above. Correlations in the neutron spectrum originating from reactor physics processes can be observed in these matrices. The pattern of the cross-section curves of the detector set can also be identified in the energy dependent factor loading values. This effect has a more pronounced character here than in cases of the deterministic-type solutions.

Intercomparison of correlation matrices having different group numbers will not be possible before adequate information and suitable mathematical apparatus has become available. Nevertheless, the statements referring to the role of input correlation matrices in case of the 100 groups STAY'SL-type solutions are valid also for the results of codes like SENSAK and LSL, which were applied with far less than 100 groups. Considering the information on the ranks of the correlation matrices of some 27 solutions, we may conclude that at least 40 to 50 energy groups are required for the generation of interpretable correlation matrices. On the other hand, the matrices are increasingly difficult to treat numerically when their size increases. Therefore it is not practical to have more than 100 groups.

A fundamental problem is the high rank of the output correlation matrices of codes using a deterministic model. The rank of these matrices is higher than the rank of the correlation matrix for the input spectrum. This means that these generalized least squares codes have loosened the correlations between the group fluence rate values. The rank of correlation matrices obtained by the use of stochastic algorithms is low and in a number of cases the physical reasons for the detected

correlations are identifiable. However, it is possible that their rank is lower than would be realistic. Each factor in this case represents more effects.

7. GENERAL OBSERVATIONS

7.1 Consideration of input data

7.1.1. Quantity and quality

For the preparation of a complete set of input data, the organizers used numerical data of various nature (experimental reaction rate data; evaluated cross-section data; reactor physics based spectrum data; experimental, evaluated and estimated uncertainty data; experimental and artificial correlation data). One should realize that in principle the quality of the results obtained with an adjustment procedure, is dependent on the amount and quality of the input information actually used. Therefore full consideration should be given to the quality of the input data set.

7.1.2. Different groups structures

Sometimes solutions were based on a groups structure different from the 620 or 100 groups for which input data were provided for REAL-80. In these cases the conversion procedure (with interpolation and extrapolation schemes) were not specified by the participants; the input data for these special groups structures may not have unambiguous values. This implies that systematic effects and deviations might have been introduced by the participants choice of an own groups structure.

7.1.3. Self-shielding effect

The differences between the solution spectra obtained with the 100 groups and the 620 groups cross-section libraries respectively, can be due to the different physics information present in these two libraries. Furthermore the absence of prescribed self-shielding information may also have had some influence. In cases where the participants directly used the 620 groups cross-section data, they had to calculate the neutron self-shielding factors themselves; one participant did not consider this effect at all.

7.1.4. Two damage models

Furthermore the 620 groups cross-section library contained for steel two different displacement cross-section evaluations originating from ASTM and from EURATOM. A rough quantitative comparison of the two cross-section curves showed appreciable local differences. However the fission spectrum-averaged cross-sections differ by less than 2,5 per cent. If different cross-section sets were used, these could have influenced the results for and R_{dpa}. However, all or nearly all participants used the 100 groups ASTM displacement cross-section set.

7.1.5. Two group structures (integral)

The participants had much freedom in selecting the cross-section data for the prediction of the activation rate in nickel (R_{Ni} and the displacement rate in steel (R_{dpa}). The supplied input data set comprised 100 groups and 620 groups versions of the relevant cross-sections.

7.2. Comparison of output data

7.2.1. Deviations from input

Most participants did not use the same input information in their adjustment procedure. For example:

- the complete set of input data was not always used;
- sometimes numerical data were used which differ from those in the supplied data set (eg another cross-section file, another input spectrum etc).

This effect hampers a good simultaneous comparison of all solutions. It turned out that the solutions could not well be classified according to their adjustment principle, due to these many different conditions for the input.

In the present situation one of the best criteria to make a classification for the solutions is based on the number of energy groups applied in the adjustment (620 groups, 100 groups, other structures). It should be realized that even with this classification the solutions within one category are not always directly comparable (presence of "apples" and "oranges").

7.2.2 Few groups

During the calculations for the evaluation of the solutions, some difficulties were encountered in the interpretation of neutron spectra presented in a groups structure with less than 100 groups. To obtain correct results for the relevant reaction rates in these cases extra calculations should have been made by the evaluators making use of appropriately weighted few groups cross-section data. This approach was not followed, since the 100 groups structure was taken as reference, and reduction to fewer groups gives rise to loss of information with respect to the reference structure. Consequently the evaluation procedure resulted in some differences between evaluators data and participants data in the relevant groups structures. This background explains the "staircase pattern" of some plots showing the modification ratio $\phi_{out}(E)/\phi_{in}(E)$.

7.2.3. Interaction

The exercise involved the handling of a large amount of numerical data. During the course of time some contacts between organizers and participants were helpful. In a few cases these contacts have led to modifications in solutions already submitted.

7.2.4. Participants uncertainties (integral)

In the uncertainty estimates for each integral parameter as supplied by the participants, a large spread is present (see table 19). Even for the generalized least squares codes appreciable differences were found.

7.2.5. Evaluators uncertainties (integral)

The uncertainty values as calculated by the evaluators from the participants output data show however better agreement.
Important differences in the uncertainties were only obtained for the predicted reaction rates for activation in nickel (R_{Ni}) and for displacements in steel (R_{dpa})

7.2.6. Role of output spectrum covariances

The uncertainty value of integral spectrum characteristics is

determined primarily by the correlation matrices for the solution spectrum and the cross-sections involved. The modifications of the corresponding variances of this spectrum play only a secondary role (see table 10).

7.2.7. Increase of matrix rank

For the generalized least squares codes the output correlation matrix has a higher rank than the input spectrum correlation matrix. This means that these codes have loosened the correlations between the group fluence rate values.

8. CONCLUSIONS

8.1. General aspects

8.1.1. Consistency input data

With respect to the interpretation of the results for the ORR spectrum, one should bear in mind that the whole set of input data was not optimal with respect to the consistency of the data.

8.1.2. Uniqueness of solutions

There were no two solutions (not even from the generalized least squares codes like STAY'SL) which give identical output data.

8.1.3. Spectrum shapes

The spectral shapes of the output spectra show considerable spread, both for the thermal ORR spectrum and for the fast YAYOI spectrum (see fig. 18). The integral spectrum parameters, such as ϕ(E>1 MeV), ϕ(E> 0,1 MeV), and ϕ_{tot}, show much less variation (see tables 13 and 14).

8.2.4. Role of titanium reaction

For the adjustment of the YAYOI spectrum many participants deleted the ^{47}Ti(n,p) reaction. It is noted that the influence of the deletion of this reaction is not the same for the predicted activation rate in nickel and for the predicted displacement rate in steel. It is therefore concluded that deletion of the ^{47}Ti(n,p) reaction leads to an appreciable change in the output spectrum of YAYOI.

8.2. Adjustment parameters

8.2.1. Differences in fit

The Average Relative Deviation (ARD) parameter was considered as a general and simple characteristic of the solution spectrum expressing the fit between measured and calculated reaction rates. It was found that the values for this parameter were not the same for all solutions; this fact in itself will already result in some differences in the integral and spectrum-averaged data.

8.2.2. Criteria for fit

The various criteria considered by the evaluators to judge the fit between input and output reaction rates seem to show the same trend (see fig. 23).
This implies that - at least for the input data sets for ORR and YAYOI -there is no remarkable influence of input variances and correlations on the investigated fit parameters. Of the parameters considered (DEV, ARD, CHISQ) the ARD-parameter has the largest range, and therefore seems to be the most sensitive parameter to judge the fit.
Some caution is necessary when the fit parameter is used as convergence criterion in cases where the adjustment algorithm requires iteration.

8.2.3. Insufficiency of fit parameters

An important conclusion is that there is no clear functional relation between the magnitude of a fitting parameter, and the values of predicted reaction rates (ie activation rate in nickel; displacement rate in iron). It is noted that these reactions have a smooth cross-section shape, and a main response in the keV and MeV energy range, in contrast to responses for (n, γ) reactions. This statement is supported by the following conclusive observations:

- Least squares adjustments can have ARD-values much lower than the value of 1, which is the expectation value which occurs if all uncertainties are of random nature and follow the same multivariate normal distribution.
- In these cases the plots of the modification ratios show large peaks (adjacent to deep valleys) in regions with appreciable response of the detector set. (Remark: which activation reaction contributes most to this response may be dependent on its statistical weight; ie determined by the input uncertainties of the reaction rate value);
- Such structure will often not have any effect on the value of the predicted reaction rates.

8.2.4. Normalization factor

The spectrum normalization factor plays an important role in the neutron spectrum adjustment, since it may introduce a dominating constant

modification factor.

Furthermore the normalization factor may determine the energy dependent modification ratios (ie $\phi_{out}(E)/\phi_{in}(E)$ especially in those cases (see section 5.2.2.) where

a. the adjustment code cannot take into account the uncertainties of the input data, and

b. these relative uncertainties are not of the same order of magnitude.

Therefore the actual definition of the normalization factor (see appendix 1) is more important than previously realized.

8.2.5. Few groups

When an energy groups structure is used with less than 40 to 50 groups in the energy range of 10^{-10} to 20 MeV, the result is a spectrum shape without characteristic details.

It is to be noted that pecularities are introduced by the procedures of converting one group structure in to another one (see figures 2g, 2h, 3g, 3h, 8a, 8c, 11d).

Nevertheless, the integral parameters (such as R_{Ni}, R_{dpa}, etc) showed in most cases a good agreement with the results based on a fine group structure, if appropriately weighted cross-section values are used in the spectrum adjustment, when this is performed with a coarse groups structure.

8.2.6. Correlation matrix pattern

The pattern of the correlation matrix for the output spectrum derived in a deterministic way with a STAY'SL type code is clearly not the same as the pattern of the correlation matrix derived in a stochastic way by means of the SAND-II algorithm with Monte Carlo variations of the input reaction rates and the input cross-sections, without making strict assumptions for the covariance matrix of the input spectrum.

8.3. Predicted reaction rates

8.3.1. Influence of algorithm

When we consider the series of predicted activation rates per nickel atom and predicted displacement rates per iron atom for all solutions, one cannot observe significant differences due to the adjustment algorithm used. The largest deviations from the average value seem to be

due to effects originating from groups structure and/or deviation from the given input data.

8.3.2. Nickel in YAYOI

For the YAYOI spectrum the predicted displacement rates in steel show more agreement than the predicted activation rates in nickel. This may suggest that one has to be very careful in deriving calculated displacement rates from the experimental response from only one (nickel) threshold activation detector and supplementary spectrum information.

8.3.3. Size of spread

The coefficients of variation for the activation rates in nickel and the displacement rates in steel derived from the sets of responses were less than the largest uncertainties quoted by some participants.

8.3.4. Spread in R_{dpa}.

For the predicted displacement rate in steel we observed a coefficient of variation of 2,2 per cent for the ORR spectrum and 2,8 per cent for the YAYOI spectrum, if all of the participant responses are considered. (see data in table 17).

8.3.5. Spread in R_{Ni}.

With respect to the predicted activation rate in nickel we arrived, when taking into account all responses as supplied by the participants, at a coefficient of variation of 1,7 per cent for the ORR spectrum and of 7,1 per cent for the YAYOI spectrum. If only the category of 100 groups solution spectra is considered, then these values become 1,4 per cent for the ORR spectrum, and 4,6 per cent for the YAYOI spectrum (see data in table 17).

8.3.6. Check for Ni reaction

When comparing the predicted activation rate in nickel with its available measured value, we observe that the predicted value (averaged over all solutions) is lower than the measured value: 1 per cent lower for

ORR, and 7 per cent lower for YAYOI (see data in table 18, fig. 24 and 26).

8.4. Main conclusions

8.4.1. Answer to the problem

With regard to the aim of the REAL-80 excercise to determine the quality of adjusted spectra and derived integral values (see section 1.3), we can make the following statement:

1. The neutron spectra, derived with various adjustment codes can differ clearly in their shape.
2. The integral damage parameters, like the number of displacements per iron atom (R_{dpa}) derived with various adjustment codes agree within a few per cent with each other. The spread in the values is certainly not larger than the uncertainties derived by the participants for the individual values.
3. For the two spectrum cases considered (ORR and YAYOI), the adjustment procedures have resulted in a considerable decrease of the uncertainties of the neutron spectrum and of the neutron spectrum characteristics. For R_{Ni} the final uncertainty was a factor 2 to 3 smaller than the uncertainty derived from the input data. For R_{dpa} this improvement factor is about 1.5 (see tables 19 and 20).
4. Values for the predicted activation rate in nickel (R_{Ni}), as given by the participants agree with each other to within a few per cent. The spread in the values is again not larger than the uncertainties derived by the participants. However the average of all participants values of R_{Ni} is somewhat smaller than the available measured value.

8.4.2. Check for Ni reaction

Generally speaking, the participants data agree with the measured value for R_{Ni}.

However, individual participants data showed deviations from the measured value, which are between +4 and -4 per cent for ORR and between -1 and -23 per cent for YAYOI.

8.4.3. Performance of codes

Although the spectrum shapes derived by various adjustment codes can show appreciable differences, it is concluded that many adjustment codes give good performances in predicting integral spectrum characteristics.

As stated already elsewhere [21], the adjustment codes using a generalized least squares algorithm are in principle the best; they should be preferred especially when better and more covariance information for input spectra and input cross-sections become available.

Clear recommendations should be made on procedures for converting fluence rates and cross-sections from one group structure to another.

Users of adjustment codes should realize better the role of the spectrum normalization factor.

8.4.3. Conditions for progress

More realistic results of spectrum adjustment procedures can only be expected, if more realistic covariance matrices for the input data, and especially for the input spectrum become available.

9. ACKNOWLEDGEMENT

The work of Dr. L. Greenwood from ORNL in the preparation of the input data set for this REAL-80 exercise is gratefully acknowledged. Without his timely and helpful assistance this exercise could not have been possible in its present time schedule.

10. REFERENCES

[1] Cullen, D.E.; "Summary of ORR and YAYOI data for the REAL-80 project, distributed 6 Feb. 1981".
Report IAEA-NDS-33
(International Atomic Energy Agency, Nuclear Data Section, Vienna, February 1981).

[2] Cullen, D.E.; Letter with some additional information "YAYOI and ORR calculations for REAL-80".
(International Atomic Energy Agency, Vienna, 26 February 1981).

[3] Zijp, W.L., Ertek, C., Zsolnay, É.M., Szondi, E.J., Nolthenius, H.J. and Cullen, D.E.: "First results of the REAL-80 excercise",
Report ECN-106, IAEA/RL/86, BME-TR-RES-5/81 (Energieonderzoek Centrum Nederland, Petten, October 1981).

[4] Zijp, W.L., Nolthenius, H.J., Zsolnay, É.M., Szondi, E.J., Verhaag, G.C.H.M., Cullen, D.E., Ertek, C.;
"Status report on the REAL-80 exercise".
Proceedings of the 4th ASTM-EURATOM Symposium on Reactor Dosimetry, Gaithersburg, Maryland, 22-26 March 1982.
Report NUREG/CP-0029 vol 2 (also CONF-820321/Vol2) p. 1089 (USA Nuclear Regulatory Commission Washington D.C. 1982).

[5] Zijp, W.L., Nolthenius, H.J., Zsolnay, É.M., Szondi, E.J., Verhaag, G.C.H.M., Cullen, D.E., Ertek, C.;
"Interim report on the REAL-80 exercise".
Report ECN-82-65, BME-TR-INT-1/82 (Energieonderzoek Centrum Nederland, Petten, May 1982).

[6] Ertek, C., Zijp, W.L.; "Information sheet for the REAL-80 project", dated 1980-12-08.
Distributed by IAEA in February 1981 among prospective participants.

[7] ASTM Standard practice for characterizing neutron exposures in ferritic steels in terms of displacements per atom (dpa).

[8] Lott M. et al.: "Sections efficaces de création de dommages", Nuclear Data in Science and Technology, Vol. I, p. 89, Report IAEA-SM-17C/65 (IAEA, Vienna, 1973)

[9] Perey, F.G.; "Least-squares doximetry unfolding: the program STAY'SL".
Report ORNL/TM-6062, ENDF-254.
(Oak Ridge National Laboratory, Oak Ridge, October 1977).

[10] Sasaki, M., Nakazawa, M.,;"NEUPAC Unfolding code for use with neutron spectra from activation data of dosimeter foils.
Report PSR-177.
(Oak Ridge National Laboratory, Radiation Shielding Information center, Oak Ridge, January 1981).

[11] McCracken, A.K.; "Few channel unfolding in shielding - The SENSAK code".
Proceedings of the third ASTM-EURATOM symposium and Reactor Dosimetry, Ispra, 1 to 5 October 1979).
Report: EUR 6813, Vol 2, p 732 (C.E.C.-JRC, Luxembourg,1980).

[12] Stallmann, F.W.;"LSL. A logarithmic least squares adjustment method". Proceedings of the 4th ASTM-EURATOM symposium on Reactor Dosimetry, Gaithersburg, 22-26 March 1982.
Report NUREG/CP-0029 vol 2 (also CONF-820321/Vol2) p 1123 (USA Nuclear Regulatory Commission, Washington D.C., 1982).

[13] Najzer, M., Glumac, B.; "Unfolding of REAL-80 sample problems by ITER-3 and STAY'SL codes".
Proceedings of the 4th ASTM-EURATOM symposium on Reactor Dosimetry, Gaithersburg, 22-26 March 1982.
Report NUREG/CP-0029 vol 2 (also CONF-820321/Vol2) p. 1171 (USA Nuclear Regulatory Commission, Washington D.C., 1982).

[14] Szondi, E.J., Zsolnay, É.M.; "SAND8P, an iterative neutron spectrum unfolding code".
Report BME-TR-RES-2/81.
(Nuclear Reactor of the Technical University, Budapest, March 1981).

[15] McElroy, W.N. et. al.: "A computer automated iterative method for neutron flux spectra determination by foil activation".
Vol I-IV. Report AFWL-TR-67-41 (1967).

[16] Berg, S.: "Modifications of SAND II".
Report BNWL-855 (1968).

[17] Oster, C.A.; McElroy, W.N.; Marr, J.M.: "A Monte Carlo program for SAND II error analysis".
Report HEDL-TME-73-20 (Hanford Engineering Development Laboratory, Washington, 1974).

[18] Kam, F.B.K.; Stallmann, F.W.: "Crystal Ball - a computer program for determining neutron spectra from activation measurements".
Report ORNL-TM-4601 (Oak Ridge National Laboratory, Tennessee, June 1974).

[19] Fischer, A.; Turi, L.: "The RFSP programme for unfolding neutron spectra from activation data".
Report INDC (HUN)-8/U (IAEA, Vienna, 1972).

[20] Routti, J.T.; Sandberg, J.V.: "General purpose unfolding program LOUHI78 with linear and nonlinear regularization".
Report TKK-F-A359 (Helsinky University of Technology, Helsinky, October 1978).

[21] Zijp, W.L.; Stallmann, F.W.: "Workshop on spectrum adjustment procedures", proceedings of the 4th ASTM-Euratom Symposium on Reactor Dosimetry, Gaithersburg, 22-26 March 1982.
Report NUREG/CP-0029 Vol II (also CONF 803021/Vol2) page 1221 (USA Nuclear Regulatory Commission, Washington D.C., 1982).

[22] Muir, D.W.; Mac Farlane, R.E.; Boicourt, R.M.: "Multigroup processing of ENDF/B dosimetry covariances".
Proc. 4th ASTM-Euratom symposium on Reactor Dosimetry, Gaithersburg, 22-26 March 1982.
Report NUREG/CP-0029 Vol2 (also CONF-820321, Vol 2) p 655 (USA Nuclear Regulatory Commission Washington D.C., 1982).

[23] Muir, D.W.; Ertek, C.; Cross, B.:"100 by 100 group relative covariance matrices of $^{46}Ti(n,p)$, $^{58}Ni(n,p)$, $^{58}Ni(n,2n)$, $^{47}Ti(n,np)$, $^{47}Ti(n,p)$, $^{48}Ti(n,np)$, $^{48}Ti(n,p)$".
Report IAEA/RL/83 (IAEA, Vienna, December 1980).

[24] Perey, F.K.: "Spectrum unfolding by the least squares method"
Proc. of an IAEA Technical Committee Meeting, Oak Ridge, 10-12 October 1977.
Report IAEA TECDOC-221, p 195 (IAEA, Vienna, 1979).

[25] Morrison D.F.: "Multivariate statistical methods", Second Edition (McGrawHill, New York, 1976).

[26] Jahn W. and Vahle H.: "Die Faktoranalyse und Ihre Anwendung", (Verlag die Wirtschaft, Berlin, 1968).

[27] Szondi, E.J.: "Application of factor analysis to neutron spectrum unfolding".
Report BME-TR-RES-2/82 (Nuclear Reactor of the Technical University, Budapest, March 1982).

[28] Kovács, M.; Zsolnay, É.M.; Szondi, E.J.: "Analysis of mathematical methods used in the multifoil activation neutron spectrometry".
Paper presented at the Visegrad symposium, 27 September-2 October 1982.
Report BME-TR-RES-4/82, (Nuclear Reactor of the Technical University, Budapest, October 1982).

[29] Fischer, A.; "International intercomparison of neutron spectra evaluation methods using activation detectors".
Report Jül-1196 (Kernforschungsanlage Jülich, Juni 1975).

[30] Zijp, W.L., Nolthenius, H.J., Rieffe, H.Ch.; "Cross section library DOSCROS81 (in a 640 group structure of the SAND II type".
Report ECN-111, (Energieonderzoek Centrum Nederland, Petten, December 1981).

Table 1. List of participating laboratories

REAL-80

PARTICIPATING LABORATORIES			CODES APPLIED
CZE	NRI	PRAGUE	SAND-II
GER	KFA	JÜLICH	SANDMX2
GER	PTB	BRAUNSCHWEIG	STAY'SL
HUN	BME	BUDAPEST	SANDBP, RFSP
JAP	TOKU	TOKYO	NEUPAC
NED	ECN	PETTEN	CRYSTAL BALL, RFSP-JÜL, STAY'SL, SANDPET
SF	HUT	HELSINKI	LOUHI78
UK	RRA	DERBY	SENSAK
UNO	IAEA	SEIBERSDORF	SAND-II
USA	ANL	ARGONNE, IL.	STAY'SL-TYPE
USA	GEVNC	PLEASANTON, CA.	GERDMO2
USA	ORNL	OAK RIDGE, TN.	WINDOWS, LSL
YUG	IJS	LJUBLJANA	ITER, STAY'SL

Table 2. Comparison of some important reaction rates calculated for the input spectrum

Part A: ORR

reaction	(R_{620}/R_{100})*
SC45G	1,034
SC45GCd	-
TI46P	1,000
TI48P	0,996
FE54P	0,993
MN55G	1,032
FE58G	1,013
FE58GCd	-
CO59G	1,002
CO59GCd	-
NI60P	0,982
AU197G	1,328
AU197GCd	-
AU1972N	0,987
U235F	1,334
U235FCd	-
NP237FCd	-
U238F	0,999
U238G	3,225
U238GCd	-

Part B: YAYOI

reaction	(R_{620}/R_{100})*	
NA23G	0,929	
MG24P	0,992	
AL27A	0,999	
AL27P	1,000	
SC45G	0,989	
TI46P	1,000	
TI47P	1,000	
TI48P	0,999	
FE54P	0,993	
MN55G	1,287	
FE56P	1,004	
FE58G	1,059	
NI58P	0,984	**
CO59A	1,003	
CO59G	1,009	
NI60P	0,983	
IN115N	0,999	
W186G	0,998	
AU197G	1,005	
AU1972N	0,994	
U235F	1,001	
U238F	0,999	
U238G	1,016	

* R_{620} = reaction rate calculated with 620 groups data.
R_{100} = reaction rate calculated with 100 groups data.
No self-shielding correction and Cd correction is used in R_{620}.

** It was the intention that this nickel reaction was not used in the adjustment, since it played a role in the check of the performance of adjustment procedures.

Table 3. Grouping of REAL-80 solutions.

Viewpoint	Number of solutions		Number of laboratories	
	ORR	YAYOI	ORR	YAYOI
Total number considered	33	35	12	13
- in 100 groups	18	22	7	8
- in 620 groups	6	4	3	3
- in other structure	9	9	4	4
- without uncertainties	15	14	2	3
- with uncertainties only for spectrum	4	4	1	1
- with uncertainties for spectrum and characteristics	14	17	9	9
- without correlations	20	21	4	5
- with correlation matrix for spectrum	12	13	7	7
- with correlations for spectrum and characteristics	1	1	1	1
- SAND-II, SANDBP, SANDPET, SANDMX2	11	12	4	5
- STAY'SL	7	6	4	4
- CRYSTAL BALL	1	1	1	1
- WINDOWS	2	2	1	1
- LOUHI-78	2	1	1	1
- NEUPAC	1	1	1	1
- LSL	3	4	1	1
- RFSP-JÜL	2	2	2	2
- SENSAK	1	1	1	1
- GERDMO2	1	1	1	1
- ITER-2	1	2	1	1
- ITER-3	1	2	1	1

Table 4. Information on the solutions

Part A: ORR

	IAEA code	no.	presentation neutron spectrum: number of groups or points	presentation neutron spectrum: form a)	presentation neutron spectrum: interp. data b)	g) st.dev.spec.	st.dev.char.	cor.matrix spectrum	remarks
ORR spectrum	000XX	0	100	GE	-	Y	-	Y	input spectrum
	001BB	1	620	PE	1	Y	Y	-	40 iterations, + uncertainty activities
	003EB	2	40	PE	2	Y	-	-	-
	005EB	3	40	PE	2	Y	-	-	smoothing
	006AB	4	100	GE	-	Y	Y	Y	-
	008FB	5	100	GU	-	Y	Y	Y	+ uncertainty activities
	018BD	6	621	PE	5	-	-	-	AU1972N deleted, 4 iterations, e)
	019BD	7	100	PE	5	-	-	-	AU1972N deleted, 12 iterations, f) } no integral
	020BD	8	621	PE	5	-	-	-	AU1972N deleted, 6 iterations, e) } data
	021BD	9	621	PE	5	-	-	-	AU1972N deleted, 6 iterations, e)
	023CA	10	100	GE	-	-	-	-	3 iterations
	031HA	11	20	GG	-	Y	Y	Y	+ uncertainty activities
	032HA	12	10	GG	-	-	-	-	-
	033HA	13	50	GG	-	-	-	-	-
	034GA	14	20	GG	-	-	-	-	AU1972N deleted, c)
	035GA	15	20	GG	-	-	-	-	AU1972N, U238G, U235F, FE58G deleted, c)
	036AC	16	100	GE	-	Y	Y	Y	+58NI(n,p)
	038AC	17	100	GE	-	Y	Y	Y	+58Ni(n,p)
	040IA	18	284	PE	2	-	-	-	AU1972N, U238G, and U238GCD deleted, d)
	043JA	19	40	GG	-	Y	Y	Y	-
	045BC	20	100	GE	-	Y	Y	Y	FE58GC deleted, iterations, + uncert.activities
	049DA	21	100	GE	-	-	-	-	-
	050AA	22	100	GG	-	Y	Y	Y	cov. mat. integral data
	051BA	23	100	GE	-	-	-	-	-
	055BC	24	100	GE	-	Y	Y	Y	+ uncertainty activities
	062BA	25	100	GE	-	Y	Y	-	Monte Carlo
	064BA	26	640	GE	-	-	-	-	-
	065BA	27	640	GE	-	-	-	-	U235F deleted

Table 4 (continued).

	IAEA code	no.	presentation neutron spectrum: number of groups or points	presentation neutron spectrum: form a)	presentation neutron spectrum: interp. data b)	st.dev.spec.	st.dev.char.	cor.matrix spectrum	remarks
ORR	067DA	28	100	GE	-	-	-	-	-
	069AC	29	100	GE	-	Y	-	Y	-
	071AC	30	100	GE	-	Y	-	Y	+58NI(n,p), no integral data
	074AD	31	100	GG	-	Y	Y	Y	
	075KB	32	100	GG	-	Y	Y	Y	
	076KA	33	100	GG	-	Y	-	-	

a) The form of the output spectrum data supplied by the participants is coded with two letters:
- PE = point values; fluence rate per unit energy;
- GE = group values; fluence rate per unit energy;
- GU = group values; fluence rate for unit lethargy;
- GG = group values; group fluence rate values.

b) Interpolation scheme:
1 denotes $\phi_E(E)$ is constant (constant-linear);
2 denotes $\phi_E(E)$ is linear in E (linear-linear);
5 denotes $\ln\phi_E(E)$ is linear in lnE (linear-log).

c) REAL-80 cross-section set not used.

d) Analytical input spectrum.

e) No self-shielding applied;

f) Relative output spectrum;

g) The letter Y indicates that these data are present.

Table 4 (continued)

Part B: YAYOI

	IAEA code	no.	presentation neutron spectrum: number of groups or points	presentation neutron spectrum: form a)	presentation neutron spectrum: interp. data b)	g) st.dev.spec.	st.dev.char.	cor. matrix spectrum	remarks
YAYOI spectrum	Y00XX	0	100	GE	-	Y	-	Y	input spectrum
	Y02BB	1	620	PE	1	Y	Y	-	40 iterations
	Y07AB	2	100	GE	-	Y	Y	Y	-
	Y10FB	3	100	GU	-	Y	Y	Y	NI58P used, + uncertainty activities
	Y22BD	4	100	PE	5	-	-	-	12 iterations, f)
	Y24CA	5	100	GE	-	-	-	-	4 iterations
	Y25HA	6	20	GG	-	Y	Y	Y	-
	Y26HA	7	20	GG	-	-	-	-	reduced weight for TI47P
	Y27HA	8	10	GG	-	-	-	-	-
	Y28HA	9	50	GG	-	-	-	-	-
	Y29GA	10	20	GG	-	-	-	-	W186G deleted, c)
	Y30GA	11	20	GG	-	-	-	-	W186G, TI47P deleted, c)
	Y37AC	12	100	GE	-	Y	Y	Y	NI58P used
	Y41IA	13	152	PE	2	-	-	-	TI47P and MN55G deleted, no reaction-rate calc., d)
	Y44JA	14	40	GG	-	Y	Y	Y	-
	Y46BC	15	100	GE	-	Y	Y	Y	TI47P deleted, 4 it., + uncert. act.
	Y47BC	16	100	GE	-	Y	Y	Y	TI47P deleted, 6 it., + uncert. act.
	Y48BC	17	620	GE	-	Y	Y	-	TI47P deleted, 2 it., + uncert. act.
	Y52DA	18	100	GE	-	-	-	-	-
	Y53AA	19	100	GG	-	Y	Y	Y	cov.mat. of integral data
	Y54BA	20	100	GE	-	-	-	-	-
	Y56BC	21	100	GE	-	Y	Y	Y	+ uncertainty activities, [illegible] rations
	Y57BC	22	620	GE	-	Y	Y	-	2. iterations, + uncertainty activities

Table 4 (continued)

	IAEA code	no.	presentation neutron spectrum			st.dev.spec.	st.dev.char.	cor. matrix spectrum	remarks
			number of groups or points	form a)	interp. data b)				
YAYOI	Y61EB	23	40	PE	2	Y	-	-	-
	Y63BA	24	100	GE	-	Y	Y	-	Monte Carlo, 1 iteration
	Y66BA	25	640	GE	-	-	-	-	-
	Y68DA	26	100	GE	-	-	-	-	-
	Y70AC	27	100	GE	-	Y	-	Y	-
	Y72BD	28	100	GG	-	-	-	-	NI58P used, no reaction rates are given
	Y73BD	29	100	GG	-	-	-	-	TI47P deleted, no reaction rates are given
	Y77AD	30	100	GG	-	Y	Y	Y	NI58P used
	Y78KB	31	100	GG	-	Y	Y	Y	NI58P used
	Y79KA	32	100	GG	-	Y	-	-	NI58P used
	Y80AD	33	100	GG	-	Y	Y	Y	NI58P used,TI47P deleted
	Y81KB	34	100	GG	-	Y	Y	Y	NI58P used,TI47P deleted
	Y82KA	35	100	GG	-	Y	-	-	NI58P used,TI47P deleted

a) The form of the output spectrum data supplied by the participants is coded with two letters:
- PE = point values; fluence rate per unit energy;
- GE = group values; fluence rate per unit energy;
- GU = group values; fluence rate per unit lethargy;
- GG = group values; group fluence rate values.

b) Interpolation scheme:
1 denotes $\phi_E(E)$ is constant (constant-linear);
2 denotes $\phi_E(E)$ is linear in E (linear-linear);
5 denotes $\phi_E(E)$ is linear in lnE (linear-log).

c) REAL-80 cross-section set not used.

d) Analytical input spectrum.

e) No self-shielding applied.

f) Relative output spectrum.

g) The letter Y indicates that the data are present.

Table 5 Group fluence rates in decade structure

Part A: ORR

Group no.	decade (in MeV)	ϕ_{in} absolute input value (in $m^{-2} \cdot s^{-1}$)	100 groups solutions		620 groups solutions		other groups structure	
			$\overline{\phi out/\phi in}$	st. dev. (in%)	$\overline{\phi out/\phi in}$	st. dev. (in%)	$\overline{\phi out/\phi in}$	st. dev. (in%)
1	10^{-10}...10^{-9}	3,45 x 10^{13}	1,04	2,9	3,59	58	5,82	80
2	10^{-9} ...10^{-8}	2,61 x 10^{15}	1,04	2,1	1,60	29	1,10	45
3	10^{-8} ...10^{-7}	3,60 x 10^{16}	1,05	1,3	0,95	19	0,76	41
4	10^{-7} ...10^{-6}	1,33 x 10^{16}	1,05	2,2	0,94	11	2,05	58
5	10^{-6} ...10^{-5}	1,31 x 10^{16}	1,03	2,8	0,91	9,5	0,86	19
6	10^{-5} ...10^{-4}	1,61 x 10^{16}	0,87	10,7	0,79	13	0,82	37
7	10^{-4} ...10^{-3}	7,87 x 10^{15}	1,21	15,9	0,78	41	1,45	17
8	10^{-3} ...10^{-2}	7,12 x 10^{15}	1,01	3,6	0,82	21	1,52	53
9	10^{-2} ...10^{-1}	1,59 x 10^{16}	1,02	3,5	0,96	11	1,40	75
10	10^{-1} ...10^{0}	4,32 x 10^{16}	1,01	2,1	1,01	3,5	1,09	33
11	10^{0} ...10^{1}	3,80 x 10^{16}	1,05	2,2	1,08	2,8	1,06	1,7
12	10^{1} ...18	6,88 x 10^{13}	1,05	3,2	1,07	15	1,48	51

Remark: $\overline{\phi out/\phi in}$ means average output value relative to the input value

Table 5 Continued

Part B: YAYOI

Group no.	decade (in MeV)	ϕ_{in} absolute input value (in $m^{-2}.s^{-1}$)	100 groups solutions		620 groups solutions		other groups structure	
			$\overline{\phi out/\phi in}$	st. dev (in%)	$\overline{\phi out/\phi in}$	st. dev. (in%)	$\overline{\phi out/\phi in}$	st. dev. (in%)
1	$10^{-10}...10^{-9}$	$2,57 \times 10^{-2}$	1,13	12	1,67	53	18,2	161
2	$10^{-9}...10^{-8}$	$1,11 \times 10^{1}$	1,12	10	1,15	30	4,40	152
3	$10^{-8}...10^{-7}$	$5,62 \times 10^{2}$	1,12	10	0,93	17	1,31	95
4	$10^{-7}...10^{-6}$	$4,28 \times 10^{4}$	1,15	11	0,98	15	1,15	106
5	$10^{-6}...10^{-5}$	$1,96 \times 10^{6}$	1,32	22	1,52	12	0,79	70
6	$10^{-5}...10^{-4}$	$6,84 \times 10^{7}$	1,18	14	1,50	55	1,11	105
7	$10^{-4}...10^{-3}$	$6,26 \times 10^{9}$	1,20	17	1,48	14	1,17	121
8	$10^{-3}...10^{-2}$	$9,22 \times 10^{11}$	2,21	13	1,42	4,5	1,33	76
9	$10^{-2}...10^{-1}$	$6,46 \times 10^{13}$	1,34	5,4	1,20	26	0,97	53
10	$10^{-1}...10^{0}$	$8,02 \times 10^{14}$	1,33	2,8	1,34	8,5	1,38	5,5
11	$10^{0}...10^{1}$	$7,46 \times 10^{14}$	1,18	2,3	1,19	2,0	1,19	9,0
12	$10^{1}...18$	$1,68 \times 10^{12}$	0,86	6,6	0,83	20	0,99	40

Remark: $\overline{\phi out/\phi in}$ means average output value relative to the input value

Table 6. Chi-square and ARD contribution (calculated in a typical STAY'SL run)

Part A: ORR

reaction	chi-square[1]) contribution	ARD [2]) contribution
SC45G	0,01	- 0,39
SC45GCd	0,00	- 0,03
TI46P	- 0,03	0,07
TI48P	- 0,33	0,23
FE54P	0,02	0,07
FE58G	1,02	0,57
FE58GCd	2,40	0,53
C059G	- 0,04	- 0,27
C059GCd	0,06	0,13
NI60P	0,70	- 0,49
AU197G	0,04	0,07
AU197GCd	0,00	- 0,04
AU1972N	1,01	- 0,48
U235F	- 0,13	- 0,12
U235FCd	0,36	- 0,28
NP237FCd	- 0,01	- 0,01
U238F	0,12	0,12
U238G	0,31	- 0,23
U238GCd	- 0,37	0,32

Part B: YAYOI

reaction	chi-square contribution	ARD [2]) contribution
NA23G	- 2,61	- 1,31
MG24P	0,04	- 0,07
AL27A	0,67	- 0,14
AL27P	0,01	0,41
TI47P	1,47	- 1,19
TI48P	1,04	- 0,72
MN55G	- 1,31	- 0,31
FE56P	- 0,23	0,33
C059A	- 0,37	0,29
IN115N	0,73	0,56
W186G	7,40	1,31
AU197G	9,06	1,34

$\chi^2_{ORR} = 5,14;\ n = 19$

$\omega^2_{ORR} = \frac{\chi^2}{n} = 0,27$

ARD = 0,29

$\chi^2_{YAYOI} = 15,9;\ n = 12$

$\omega^2_{YAYOI} = \frac{\chi^2}{n} = 1,32$

ARD = 0,81

1) The computation of χ^2 involves a double summation (see relation A2.24 in appendix 2). The values indicated with "chi-square contribution" are the terms contributing to the second summation. Since the $\underline{\underline{W}}$ matrix is non-diagonal χ^2 cannot be broken down into components which are uniquely associated with the separate reactions. A large value of the chi-square contribution for a certain reaction indicates some level of improbability of the input data for this reaction.

2) In the calculation of the Average Relative Deviation (defined in section 4.5.) f = 1 was used.

Table 7. Comparison of the group fluence rate values in the decade structure for various representations of the input spectrum.

Part A: ORR

group no.	energy region (in MeV)	group fluence rate 100 groups (in $m^{-2}.s^{-1}$)	relative values with respect to the 100 groups data		
			50 groups	20 groups	10 groups
1	$1,0\ 10^{-10}...1,0\ 10^{-9}$	$3,451\ 10^{+13}$	6,95	12,30	2,32
2	$1,0\ 10^{-9}...1,0\ 10^{-8}$	$2,610\ 10^{+15}$	0,92	1,63	0,31
3	$1,0\ 10^{-8}...1,0\ 10^{-7}$	$3,596\ 10^{+16}$	0,96	0,88	0,22
4	$1,0\ 10^{-7}...1,0\ 10^{-6}$	$1,325\ 10^{+16}$	1,08	1,04	3,05
5	$1,0\ 10^{-6}...1,0\ 10^{-5}$	$1,305\ 10^{+16}$	1,00	0,95	0,58
6	$1,0\ 10^{-5}...1,0\ 10^{-4}$	$1,611\ 10^{+16}$	0,99	0,98	1,15
7	$1,0\ 10^{-4}...1,0\ 10^{-3}$	$7,866\ 10^{+15}$	1,14	1,35	1,69
8	$1,0\ 10^{-3}...1,0\ 10^{-2}$	$7,115\ 10^{+15}$	0,99	1,03	1,09
9	$1,0\ 10^{-2}...1,0\ 10^{-1}$	$1,594\ 10^{+16}$	1,00	1,00	0,99
10	$1,0\ 10^{-1}...1,0\ 10^{+0}$	$4,319\ 10^{+16}$	1,00	1,01	1,01
11	$1,0\ 10^{+0}...1,0\ 10^{+1}$	$3,801\ 10^{+16}$	1,00	1,00	1,00
12	$1,0\ 10^{+1}...2,0\ 10^{+1}$	$6,877\ 10^{+13}$	1,00	1,00	1,00

Part B: YAYOI

group no.	energy region (in MeV)	group fluence rate 100 groups (in $m^{-2}.s^{-1}$)	relative values with respect to the 100 groups data		
			50 groups	20 groups	10 groups
1	$1,0\ 10^{-10}...1,0\ 10^{-9}$	$2,570\ 10^{-1}$	4,03	16,10	80,89
2	$1,0\ 10^{-9}...1,0\ 10^{-8}$	$1,113\ 10^{+1}$	0,93	3,72	18,68
3	$1,0\ 10^{-8}...1,0\ 10^{-7}$	$5,616\ 10^{+2}$	1,03	1,66	3,70
4	$1,0\ 10^{-7}...1,0\ 10^{-6}$	$4,281\ 10^{+4}$	1,09	2,54	3,20
5	$1,0\ 10^{-6}...1,0\ 10^{-5}$	$1,957\ 10^{+6}$	1,02	1,21	1,29
6	$1,0\ 10^{-5}...1,0\ 10^{-4}$	$6,835\ 10^{+7}$	1,10	1,45	3,99
7	$1,0\ 10^{-4}...1,0\ 10^{-3}$	$6,260\ 10^{+9}$	1,01	1,37	4,92
8	$1,0\ 10^{-3}...1,0\ 10^{-2}$	$9,217\ 10^{+11}$	1,04	1,41	2,45
9	$1,0\ 10^{-2}...1,0\ 10^{-1}$	$6,460\ 10^{+13}$	1,01	1,01	1,00
10	$1,0\ 10^{-1}...1,0\ 10^{+0}$	$8,015\ 10^{+14}$	0,99	0,99	1,00
11	$1,0\ 10^{+0}...1,0\ 10^{+1}$	$7,456\ 10^{+14}$	1,00	1,00	1,00
12	$1,0\ 10^{+1}...2,0\ 10^{+1}$	$1,681\ 10^{+12}$	1,00	1,00	1,00

Table 8. Effect of coarse group input spectrum representation on calculated reaction rates.

Calculated reaction rates using 100 groups cross-section data (without weighting with the 100 groups input spectrum) are compared to values obtained for the 100 groups input spectrum.

Part A: ORR

reaction	calculated for 100 groups	calculated reaction rates relative to the 100 group values		
		50 groups	20 groups	10 groups
SC45G	1,144 10^{-10}	1,01	1,04	0,51
SC45GCd	6,190 10^{-12}	1,00	0,99	1,12
TI46P	5,275 10^{-14}	1,03	1,20	1,92
TI48P	1,375 10^{-15}	1,07	1,62	4,32
FE54P	3,906 10^{-13}	1,01	1,11	1,38
FE58G	5,215 10^{-12}	1,02	1,05	0,58
FE58GCd	4,720 10^{-13}	1,03	0,98	1,61
CO59G	1,897 10^{-10}	1,05	1,17	0,54
CO59GCd	3,312 10^{-11}	1,20	1,64	0,81
NI60P	1,261 10^{-14}	1,05	1,43	3,35
AU197G	9,244 10^{-10}	1,09	0,82	0,65
AU197GCd	5,123 10^{-10}	1,15	0,63	0,78
AU1972N	1,522 10^{-14}	1,11	2,10	4,97
U235F	1,888 10^{-9}	0,99	0,98	0,55
U235FCd	1,524 10^{-10}	0,99	0,97	1,22
NP237FCd	8,188 10^{-12}	1,00	1,01	1,05
U238F	1,591 10^{-12}	1,00	1,03	1,20
U238G	6,205 10^{-11}	0,95	0,87	0,91
U238GCd	4,930 10^{-11}	0,93	0,82	1,01
NI58P	5,142 10^{-13}	1,01	1,09	1,35
IRONDAM	5,450 10^{-9}	1,00	1,02	1,11

Part B: YAYOI

reaction	calculated for 100 groups	calculated reaction rates relative to the 100 group values		
		50 groups	20 groups	10 groups
NA23G	6,803 10^{-17}	1,00	1,02	0,99
MG24P	1,664 10^{-16}	1,06	1,45	4,16
AL27A	7,807 10^{-17}	1,06	1,56	4,32
AL27P	3,838 10^{-16}	1,03	1,24	2,09
TI47P	2,068 10^{-15}	1,01	1,09	1,40
TI48P	3,005 10^{-17}	1,06	1,47	3,78
MN55G	6,732 10^{-16}	1,00	1,00	1,01
FE56P	1,026 10^{-16}	1,05	1,35	3,27
NI58P	9,632 10^{-15}	1,01	1,10	1,39
CO59A	1,585 10^{-17}	1,05	1,50	3,93
IN115N	1,829 10^{-14}	1,00	1,03	1,15
W186G	7,915 10^{-15}	1,00	0,99	0,96
AU197G	1,940 10^{-14}	1,00	1,00	0,97
IRONDAM	1,031 10^{-10}	1,00	1,02	1,12

All weighted cross-sections yielded the correct reaction rates.

Table 9. Effect of the normalization factor on the least-squares adjustments for YAYOI.
Note : the normalization feature of the adjustment procedure was not used in these calculations.

parameters	normalization factor[1])					
	with unit value f	f1	f2	f3	f4	opti-mized: f0
normalization factor	1,00	1,325	1,068	0,992	1,308	1,262
χ^2 for renormalized input data	15,646	8,002	12,816	16,041	8,126	8,583
CHISQ1 [2])	8,602	7,014	8,256	8,774	7,078	6,924
ϕ_{tot} [3])	1,233	1,296	1,248	1,232	1,293	1,285
ϕ_{tot} [4])	1,233	0,979	1,168	1,241	0,989	1,018
ϕ(E>1MeV) [3])	1,134	1,199	1,146	1,129	1,195	1,188
ϕ(E>0,1 MeV) [3])	1,229	1,295	1,242	1,223	1,292	1,284

Remarks:

1) The definitions for the various normalization factors are given in appendix 1.
2) CHISQ1 considers the consistency between measured and calculated output reaction rates, taking into account the input uncertainties, and considering a specified normalization factor.
3) These data are relative to the corresponding value of the unnormalized input spectrum.
4) These data are relative to the corresponding data of the renormalized input spectrum (different for each factor).

Table 10. Integral parameters and their uncertainties for the YAYOI solution spectrum obtained with different input neutron spectrum correlations.

All data are relative to the corresponding values for the input spectrum (listed in table 21), except the χ^2 value (no additional normalization was applied).

Input spectrum correlation matrix	χ^2	Φ_{tot}	$\Phi(E>1MeV)$	$\Phi(E>0,1MeV)$	R_{Ni}	R_{dpa}	standard deviation for								
							Φ_{tot}	$\Phi(E>1MeV)$	$\Phi(E>0,1MeV)$	R_{Ni}			R_{dpa}		
										total	due to Φ contr.	due to σ contr.	total	due to Φ contr.	due to σ contr.
strong correlation	68,17	1,038	1,030	1,037	0,972	1,031	0,170	0,119	0,164	0,316	0,112	1,004	0,611	0,145	0,999
Gaussian as used in input data set	15,65	1,233	1,134	1,229	0,947	1,126	0,443	0,635	0,504	0,424	0,320	0,993	0,695	0,447	0,993
diagonal	27,14	1,160	1,083	1,154	0,987	1,082	0,284	0,393	0,309	0,398	0,278	1,002	0,641	0,299	0,991

Table 11. Uncertainties in reaction rates
(in per cent).

Part A: ORR

reaction code	$s(\alpha_1^m)$	$s(\alpha_2^m)$	$s(\alpha_\sigma^c)$	$s(\alpha_{\phi inp}^c)$
SC45G	5	1,9	16,3	33,4
SC45GCd	5	2,1	23,8	30,6
TI46P	5	2,0	12,4	23,6
TI48P	5	2,0	11,2	24,9
FE54P	5	2,5	4,1	20,3
FE58G	5	2,7	6,6	32,1
FE58GCd	5	3,3	7,2	27,3
CO59G	5	2,1	15,0	29,8
CO59GCd	5	2,0	24,4	43,9
NI60P	5	2,5	11,3	25,7
AU197G	5	1,9	2,0	31,1
AU197GCd	5	2,0	3,1	48,2
AU1972N	5	2,6	15,5	30,8
U235F	5	2,5	0,4	32,9
U235FCd	5	2,4	2,1	27,4
NP237FCd	5	3,2	8,8	15,1
U238F	5	2,2	2,5	18,3
U238G	5	3,4	6,4	31,3
U238GCd	5	3,3	7,4	37,4
NI58P	5	2,2	8,7	19,6

Part B: YAYOI

reaction code	$s(\alpha_1^m)$	$s(\alpha_\sigma)$	$s(\alpha_{\phi inp})$
NA23G	4,1	7,5	18,5
MG24P	3,1	21,7	38,5
AL27A	2,9	3,4	37,8
AL27P	8,4	9,7	31,9
TI47P	11,5	10,5	25,4
TI48P	3,8	11,3	34,5
MN55G	2,8	7,2	16,5
FE56P	2,8	5,3	35,7
CO59A	2,4	6,8	35,9
IN115N	3,9	12,8	20,3
W186G	4,9	7,5	15,2
AU197G	3,8	6,7	16,8
NI58P	2,4	8,7	27,3

Uncertainties

$s(\alpha_1^m)$ REAL-80 value in experimental reaction rate.

$s(\alpha_2^m)$ Measured value in experimental reaction rate.

$s(\alpha_\sigma^c)$ Cross section contribution in calculated reaction rate.

$s(\alpha_{\phi inp}^c)$ Input neutron fluence rate contribution in calculated reaction rate.

Table 12 Fit parameters

Part A: ORR

	IAEA code	$\overline{a_m/a_c}$ 1	DEV 1	ARD 1	CHISQ 1	$\overline{a_m/a_c}$ 2	DEV 2	ARD 2	CHISQ 2	CHISQ 3	Remarks
100 groups	000XX	1,01	10,31	1,11	5,06						input spectrum
	006AB	0,999	3,44	0,29	1,49						
	008FB	0,990	4,03	0,44	1,73	1,00	3,39	0,29	1,5		
	019BD	1,19	6,12	0,60	5,34	1,01	4,79	0,39	13,5		
	023CA	1,01	9,72	1,00	4,91						
	036AC	1,00	4,87	0,51	2,27	1,00	3,15	0,32	1,48		
	038AC	1,00	3,52	0,35	1,61						
	045BC	1,01	8,17	0,83	4,50						
	049DA	1,01	8,34	0,84	4,36						
	050AA	0,999	3,65	0,31	1,57						
	051BA	0,995	6,73	0,74	3,17						
	055BC	0,993	8,59	0,83	3,65						
	062BA	0,991	7,29	0,82	3,62	1,00	6,75	0,74	3,25		
	067DA	1,01	9,05	0,97	4,98	1,01	9,41	1,01	5,02		
	069AC	0,999	3,71	0,32	1,59						
	071AC	0,999	3,70	0,32	1,59						
	074AD	1,00	3,08	0,28	1,42						
	075KB	1,00	3,43	0,34	1,68						
	076KA	1,00	3,35	0,32	1,59						
620 groups	001BB	0,973	15,3	1,59	3,20	1,00	3,24	0,37	2,36		
	018BD	1,13	14,2	1,55	8,33				75,1		
	020BD	1,11	13,2	1,54	5,12				42,9		
	021BD	1,11	13,1	1,53	5,12				43,0		
	064BA	1,01	10,4	1,05	4,46	1,00	5,70	0,89	22,7		
	065BA	1,03	8,99	0,88	4,59	1,00	5,41	0,55	2,54		
other groups structures	003EB	0,959	8,30	0,85	2,14	1,00	3,88	0,42	2,15		
	005EB	0,959	8,39	0,92	1,96	1,00	3,20	0,35	1,58		
	031HA	0,906	26,7	2,76	9,37	1,00	2,12	0,31	0,59	1,97	for CHISQ 3: weighted σ in 20, 10 and 50 groups were used
	032HA	0,682	82,9	7,27	117	1,00	4,07	0,53	1,30	4,02	
	033HA	0,966	6,53	0,73	2,17				0,38	1,88	
	034GA	0,898	50,5	4,89	41,7				44,5		
	035GA	0,960	54,2	5,13	23,6						no CHISQ 2 (only 15 reactions were used)
	040IA	1,10	9,73	0,93	3,05				2,93		
	043JA	1,14	21,3	2,50	6,39	1,00	2,06	0,24	0,71		

Suffix:

1 - Evaluators calculations 100 groups

2 - Participant data

3 - See remarks in final column

Table 12 (continued)

Part 3: YAYOI

	IAEA code	$\bar{\sigma}_m/\bar{\sigma}_c$ 1	DEV 1	ARD 1	CHISQ 1	$\bar{\sigma}_m/\bar{\sigma}_c$ 2	DEV 2	ARD 2	CHISQ 2	CHISQ 3	Remarks
100 groups	Y00XX	1,03	19,6	2,25	15,75					26,7	inputspectrum for CHISQ3
											σ in 620 grs. was used
	Y07AB	0,998	7,92	0,72	6,88				6,88		
	Y10FB	0,981	10,2	0,88	8,14	0,982	10,2	0,88	7,79		
	Y22BD	1,16	15,2	1,81	8,36	0,997	7,81	0,73	5,82		
	Y24CA	0,982	11,3	1,00	9,72				9,72		
	Y37AC	0,975	10,8	0,96	10,2	0,983	10,2	0,84	7,34		
	Y46BC	0,968	11,4	0,96	7,64				7,64		
	Y47BC	0,967	11,7	1,02	9,61				9,61		
	Y52DA	1,00	11,1	0,95	8,73				8,73		
	Y53AA	0,996	8,50	0,78	7,90				7,90		
	Y54BA	0,992	9,93	0,92	8,58				8,58		
	Y56BC	0,990	11,2	0,97	8,81				8,81	- -	
	Y63BA	0,998	10,0	0,94	8,58				8,62		
	Y68DA	0,986	12,6	1,11	10,3	1,01	13,6	1,18	11,5		
	Y70AC	0,984	10,4	0,91	9,16				9,16		
	Y72BD	0,967	11,3	0,93	6,84						no reaction rates were given
	Y73BD	0,970	10,7	0,88	6,36						no reaction rates were given
	Y77AD	0,975	10,8	0,90	7,22				7,22		
	Y78KB	0,977	10,4	0,87	6,95				6,95		
	Y79KA	0,974	10,4	0,87	6,84				6,84		
	Y80AD	0,972	11,6	0,96	7,60				7,60		
	Y81KB	0,969	11,5	0,95	7,25				7,25		
	Y82KA	0,968	11,4	0,94	7,16				7,16		
620 groups	Y02BB	1,10	13,2	1,62	4,25	1,00	5,13	0,47	2,69	36,6	for CHISQ3 σ in 620 grs. was used
	Y48EC	0,964	13,9	1,25	11,2				26,9	26,9	for CHISQ3 σ in 620 grs. was used
	Y57BC	0,989	13,1	1,22	11,1				26,1	26,1	for CHISQ3 σ in 620 grs. was used
											for CHISQ3 σ in 620 grs. was used
	Y66BA	0,996	7,86	0,78	6,76	0,992	9,56	1,04	16,2	22,2 +	other σ was used by participant
other groups structures	Y25HA	0,801	21,0	2,80	12,4	0,991	6,01	0,48	2,21	7,62	
	Y26HA	0,794	20,7	2,69	12,9	0,975	9,88	0,72	3,51		for CHISQ3 σ weighted with input
	Y27HA	0,410	63,0	8,26	102	0,990	7,17	0,57	3,17	9,62	spectrum was used in the corresponding
	Y28HA	0,973	8,70	0,82	7,07	0,994	4,70	0,37	1,36	6,88	group structures
	Y29GA	0,754	29,0	3,78	13,8						only 11 reaction rates were given
	Y30GA	0,705	30,3	3,78	25,2						only 10 reaction rates were given
	Y41IA	0,972	11,5	1,09	9,62						no reaction rates given
	Y44JA	1,09	8,10	0,73	8,37	0,994	6,22	0,49	2,56		
	Y61EB	1,03	19,6	2,25	6,24	1,00	7,10	0,69	5,57		

Suffix:

1 - Evaluators calculations 100 groups

2 - Participant data

3 - See remarks in final column

Table 13 Integral parameters as supplied by participants.
Reference values as given on the magnetic tape.

	Φ_{tot}	ϕ(E>1MeV)	ϕ(E>0,1MeV)	R_{Ni}	R_{dpa}	R^{m}_{Ni} [1]
ORR	1,932 x 10^{17}	3,808 x 10^{16}	8,127 x 10^{16}	5,142x10^{-13}	5,450 x10^{-9}	5,310x10^{-13}
YAYOI	1,614 x 10^{15}	7,473 x 10^{14}	1,548 x 10^{15}	9,632x10^{-15}	1,031 x10^{-10}	1,070x10^{-14}

Part A: ORR

	IAEA code	relative values for				
		Φ_{tot}	ϕ(E>1MeV)	ϕ(E>0,1MeV)	R_{Ni}	R_{dpa}
100 groups	006AB	1,03	1,06	1,01	1,03	1,04
	008FB	1,03	1,06	1,01	1,03	1,04
	019BD	-	-	-	-	-
	023CA	1,02	1,02	1,02	1,01	1,02
	036AC	1,02	1,06	1,01	1,02	1,04
	038AC	1,03	1,06	1,01	1,03	1,05
	045BC	1,00	1,07	1,01	1,03	1,04
	049DA	1,01	1,02	1,01	1,01	1,02
	050AA	1,04	1,06	1,04	1,03	1,05
	051BA	1,04	1,04	1,04	1,00	1,03
	055BC	1,01	1,05	1,02	1,04	1,04
	062BA	1,05	1,03	1,05	1,00	1,03
	067DA	1,00	1,01	1,00	0,990	1,00
	069AC	1,03	1,06	1,03	1,02	1,04
	071AC	-	-	-	-	-
	074AD	1,03	1,06	1,01	1,03	1,04
	075KB	1,04	1,06	1,03	1,01	1,05
	076KA	1,03	1,06	1,02	1,02	1,05
Aver.		1,03	1,05	1,02	1,02	1,04
St.d.%		1,4	1,8	1,4	1,4	1,3
620 groups	001BB	1,06	1,04	1,03	1,04	1,06
	018BD	1,01	1,06	1,04	1,07	1,13
	020BD	-	-	-	-	-
	021BD	-	-	-	-	-
	064BA	1,03	1,08	1,04	1,04	1,06
	065BA	1,00	1,07	1,04	1,02	1,05
Aver.		1,03	1,06	1,04	1,04	1,08
St.d.%		2,6	1,6	0,48	2,0	3,4
other groups structures	003EB	1,10	0,981	1,02	1,01	1,06
	005EB	1,01	0,992	0,896	1,03	1,01
	031HA	1,02	1,06	1,02	1,02	1,04
	032HA	1,04	1,08	1,03	1,00	1,04
	033HA	1,03	1,06	1,03	1,02	1,04
	034GA[2])	1,67	1,07	1,51	1,06	1,30
	035GA[2])	1,07	1,06	1,16	1,05	1,12
	040IA[3])	0,932	1,03	0,856	0,980	0,936
	043JA	1,01	1,02	1,00	0,990	1,02
Aver.		1 04	1,03	1,00	1,01	1,04
St.d.%		3,3	3,9	5,2	1,5	1,70
Total aver.		1,03	1,05	1,02	1,02	1,04
Total st.d%		2,1	2,5	2,8	1,7	2,2

1) Measured value for the reaction rate of NI58P.
2) Cross-section library not from REAL-80, not included in standard deviation calculation.
3) Analytical input spectrum, not included in standard deviation calculation.

Table 13 (continued)

Part B: YAY01

	IAEA code	relative values for				
		ϕ_{tot}	$\phi(E>1MeV)$	$\phi(E>0,1MeV)$	R_{Fe}	R_{dpa}
100 groups	Y07AB	1,27	1,18	1,26	0,933	1,16
	Y10FB	1,26	1,19	1,26	1,04	1,18
	Y22BD[4])	1,27	1,12	1,24	0,841	-
	Y24CA	1,26	1,19	1,27	1,06	1,19
	Y37AC	1,24	1,15	1,23	1,03	1,15
	Y46BC	1,29	1,21	1,28	1,09	1,21
	Y47BC	1,28	1,21	1,28	1,09	1,21
	Y52DA	1,23	1,22	1,23	1,03	1,17
	Y53AA	1,25	1,15	1,25	0,948	1,15
	Y54BA	1,24	1,13	1,23	1,00	1,15
	Y56BC	1,25	1,17	1,25	1,05	1,18
	Y63BA	1,25	1,13	1,24	0,994	1,14
	Y68DA	1,20	1,18	1,20	1,08	1,16
	Y70AC	1,24	1,15	1,23	1,04	1,15
	Y72BD	1,28	1,20	1,25	1,10	-
	Y73BD	1,28	1,20	1,26	1,08	-
	Y77AD	1,28	1,21	1,28	1,08	1,21
	Y78KB	1,28	1,18	1,27	1,06	1,20
	Y79KA	1,29	1,19	1,27	1,07	1,20
	Y80AD	1,28	1,21	1,28	1,10	1,22
	Y81KB	1,29	1,21	1,28	1,10	1,22
	Y82KA	1,30	1,21	1,28	1,10	1,22
Aver.		1,26	1,18	1,26	1,05	1,18
St.d.%		2,0	2,4	1,8	4,6	2,4
620 groups	Y02BB	1,34	1,22	1,32	0,870	1,18
	Y48BC	1,23	1,21	1,23	1,10	1,20
	Y57BC	1,20	1,17	1,20	1,05	1,16
	Y66BA	1,31	1,18	1,32	0,92	1,18
Aver.		1,27	1,20	1,27	0,99	1,18
St.d.%		5,2	2,0	4,9	11	1,4
other groups structures	Y25HA	1,28	1,20	1,28	0,998	1,18
	Y26HA	1,28	1,21	1,28	1,08	1,21
	Y27HA	1,24	1,10	1,23	1,03	1,15
	Y28HA	1,28	1,16	1,29	0,955	1,17
	Y29GA[2])	1,32	1,43	1,38	0,869	1,23
	Y30GA[2])	1,24	1,08	1,29	1,23	1,21
	Y41IA[3])	1,22	0,978	1,22	1,06	1,24
	Y44JA	1,16	1,05	1,15	0,852	1,06
	Y61EB	1,34	1,10	1,33	0,900	1,18
Aver.		1,26	1,14	1,26	0,97	1,16
St.d.%		4,7	5,6	5,0	8,7	4,5
Total aver.		1,26	1,18	1,26	1,03	1,18
Total st.d.%		3,0	3,5	3,0	7,1	2,8

2) Cross-section library not from real-80

3) Analytical input spectrum
4) Relative spectrum

not included in standard deviation calculations

Table 14 Integral parameters (calculated from the solution neutron spectra by the evaluators).

Reference values for input spectrum (as given on the magnetic tape):

	ϕ_{tot} (in $m^{-2}.s^{-1}$)	ϕ(E>1MeV) (in $m^{-2}.s^{-1}$)	ϕ(E>0,1MeV) (in $m^{-2}.s^{-1}$)	R_{Ni}	R_{dpa}
ORR	$1,932 \times 10^{17}$	$3,808 \times 10^{16}$	$8,127 \times 10^{16}$	$5,142 \times 10^{-13}$	$5,450 \times 10^{-9}$
YAYOI	$1,614 \times 10^{15}$	$7,473 \times 10^{14}$	$1,548 \times 10^{15}$	$9,632 \times 10^{-15}$	$1,031 \times 10^{-10}$

Part A: ORR

	IAEA code	relative values for				
		ϕ_{tot}	ϕ(E>1MeV)	ϕ(E>0,1MeV)	R_{Ni}	R_{dpa}
100 groups	006AB	1,00	1,06	1,03	1,03	1,04
	008FB	1,04	1,11	1,05	1,10	1,09
	019BD[1])	0,887	0,970	0,982	0,874	0,959
	023CA	1,02	1,02	1,02	1,01	1,02
	036AC	1,02	1,06	1,03	1,03	1,04
	038AC	1,03	1,06	1,03	1,03	1,04
	045BC	1,00	1,07	1,01	1,03	1,04
	049DA	1,01	1,02	1,01	1,01	1,02
	050AA	1,04	1,06	1,04	1,03	1,05
	051BA	1,04	1,04	1,04	1,00	1,03
	055BC	1,01	1,05	1,02	1,04	1,04
	062BA	1,05	1,03	1,05	1,00	1,03
	067DA	1,00	1,01	1,00	0,995	1,00
	069AC	1,03	1,06	1,03	1,03	1,04
	071AC	1,03	1,06	1,03	1,03	1,04
	074AD	1,03	1,06	1,03	1,03	1,04
	075KB	1,04	1,06	1,04	1,01	1,05
	076KA	1,03	1,06	1,04	1,02	1,05
620 groups	001BB	1,06	1,04	1,03	0,959	1,03
	018BD[2])	0,946	1,13	1,10	0,829	1,05
	020BD[2])	0,905	1,08	1,03	1,03	1,05
	021BD[2])	0,905	1,08	1,02	1,03	1,05
	064BA	1,03	1,08	1,04	1,03	1,06
	065BA	1,01	1,07	1,04	1,01	1,05
other groups structure	003EE	1,10	1,06	1,09	1,05	1,07
	005EB	1,01	1,07	0,935	1,07	1,02
	031RA	1,02	1,06	1,02	1,12	1,06 (1.04)
	032RA	1,04	1,08	1,03	1,37 (1.00)	1,16 (1.04)
	033RA	1,03	1,06	1,03	1,04	1,05 (1.04)
	034GA[3])	1,67	1,07	1,54	1,20	1,31
	035GA[3])	1,07	1,06	1,16	1,17	1,13
	040IA[4])	0,931	1,03	0,856	0,975	0,952
	043JA	1,00	1,02	0,996	0,994	1,01

Table 14 (continued)

Part B: YAYOI

	IAEA code	relative values for						
		Φ_{tot}	$\Phi(E>1MeV)$	$\Phi(E>0,1MeV)$	$R_{...}$		R_{dpa}	
100 groups	Y07AB	1,27	1,18	1,26	0,933		1,16	
	Y10FB	1,27	1,19	1,27	1,04		1,18	
	Y22BD[1])	1,19	0,993	1,17	0,793		1,03	
	Y24CA	1,27	1,19	1,26	1,06		1,19	
	Y37AC	1,24	1,15	1,23	1,05		1,15	
	Y46BC	1,29	1,21	1,28	1,09		1,21	
	Y47BC	1,28	1,21	1,28	1,09		1,21	
	Y52DA	1,23	1,22	1,23	1,03		1,17	
	Y53AA	1,25	1,15	1,25	0,948		1,14	
	Y54BA	1,24	1,13	1,23	0,996		1,15	
	Y56BC	1,25	1,17	1,25	1,05		1,18	
	Y63BA	1,25	1,14	1,24	0,994		1,15	
	Y68DA	1,20	1,18	1,20	1,08		1,16	
	Y70AC	1,24	1,15	1,23	1,04		1,15	
	Y72BD	1,28	1,20	1,26	1,10		1,20	
	Y73BD	1,28	1,20	1,26	1,08		1,20	
	Y77AD	1,28	1,21	1,28	1,08		1,21	
	Y78KB	1,28	1,18	1,28	1,06		1,20	
	Y79KA	1,29	1,19	1,28	1,07		1,20	
	Y80AD	1,29	1,22	1,28	1,10		1,22	
	Y81KB	1,29	1,21	1,29	1,10		1,22	
	Y82KA	1,30	1,21	1,29	1,10		1,22	
620 groups	Y02BB	1,34	1,22	1,32	0,809		1,15	
	Y48BC	1,23	1,22	1,23	1,13		1,20	
	Y57BC	1,20	1,17	1,20	1,07		1,16	
	Y66BA	1,30	1,18	1,32	0,915		1,17	
other groups structure	Y25HA	1,28	1,20	1,28	1,10	(1,00)	1,21	(1,18)
	Y26HA	1,28	1,21	1,28	1,19		1,24	
	Y27HA	1,24	1,10	1,23	1,46	(1,03)	1,28	(1,15)
	Y28HA	1,28	1,16	1,29	0,967	(0,955)	1,17	(1,17)
	Y29GA[3])	1,32	1,43	1,37	0,974		1,22	
	Y30GA[3])	1,24	1,08	1,29	1,42		1,21	
	Y41IA[4])	1,34	1,24	1,35	1,05		1,24	
	Y44JA	1,16	1,05	1,15	0,857		1,06	
	Y61EB	1,34	1,20	1,35	0,932		1,20	

1) relative spectrum.

2) without neutron selfshielding.

3) REAL-80 cross-section set not applied in adjustment.

4) analytical input spectrum in adjustment.

(.....) values calculated with a coarse group cross section.

Table 15. Spectrum characteristics (calculated by evaluators).

Reference values for input spectrum
(Fluence rate values are given in $m^{-2}.s^{-1}$).

	Φ_{Ni}	Φ_{Co} / R_{Co}	Φ_{int} / R_{int}	average energy (in MeV)	DAR values for $^{58}Ni(n,p)$	DAR values for $^{54}Fe(n,p)$
ORR	$4,949\times10^{16}$	$5,018\times10^{14}$	$4,725\times10^{15}$	$5,960\times10^{-1}$	1,27	1,28
		$1,279\times10^{-15}$	$9,019\times10^{-16}$			
YAYOI	$9,271\times10^{14}$			1,387	1,29	1,30

Part A: ORR

	IAEA code	relative values					
		Φ_{Ni}	Φ_{Co}	Φ_{int}	average energy	DAR values for $^{58}Ni(n,p)$	DAR values for $^{54}Fe(n,p)$
100 groups	006AB	1,03	1,07	1,08	1,01	1,02	1,02
	008FB	1,10	1,06	1,08	1,04	1,00	0,98
	019BD	0,87	0,94	0,90	1,05	1,10 *	1,11 *
	023CA	1,01	1,03	0,98	1,00	1,01	1,02
	036AC	1,03	1,04	1,10	1,02	1,01	1,02
	038AC	1,03	1,04	1,10	1,01	1,02	1,02
	045BC	1,03	1,05	1,00	1,04	1,01	1,02
	049DA	1,01	1,03	1,00	1,00	1,01	1,01
	050AA	1,03	1,07	1,07	1,00	1,02	1,02
	051BA	1,00	1,05	1,06	0,99	1,03	1,04
	055BC	1,04	1,04	0,98	1,03	0,99	1,00
	062BA	1,00	1,05	1,05	0,98	1,03	1,04
	067DA	0,99	1,02	1,02	1,00	1,01	1,01
	069AC	1,02	1,07	1,07	1,01	1,02	1,02
	071AC	1,03	1,07	1,07	1,01	1,02	1,02
	074AD	1,03	1,06	1,09	1,18	1,02	1,02
	075KB	1,01	1,06	1,10	1,17	1,04	1,04
	076KA	1,02	1,06	1,10	1,18	1,03	1,04
other groups structure 620 groups	001BB	0,96	1,25	0,99	0,94	1,08	1,09
	018BD	0,83	0,95	0,91	1,08	1,28	1,32
	020BD	1,03	0,95	0,87	1,16	1,02	1,02
	021BD	1,03	0,96	0,87	1,15	1,02	1,02
	064BA	1,03	1,12	0,93	1,02	1,03	1,04
	065BA	1,01	1,05	0,94	1,04	1,03	1,04
	003EB	1,04	1,04	1,20	0,96	1,03	1,03
	005EB	1,07	1,04	1,22	1,03	0,96	0,96
	031HA	1,12	1,17	1,34	1,06	0,94	0,94
	032HA	1,37	0,58	0,76	1,20	0,84	0,83
	033HA	1,03	1,11	1,29	1,01	1,02	1,02
	034GA	1,20	1,01	0,93	0,73	1,09	1,08
	035GA	1,17	1,09	1,00	1,06	0,97	0,95
	040IA	0,97	1,03	0,95	1,05	0,98	0,98
	043JA	0,99	0,62	0,80	1,00	1,02	1,02

* Considered as outlier in the series of 100 groups values.

Table 15 (continued).

Part B: YAYOI

	IAEA code	relative values					
		ϕ_{Ni}	R_{Co}	R_{int}	average energy	DAR values for $^{58}Ni(n,p)$	DAR values for $^{54}Fe(n,p)$
100 groups	Y07AB	0,93	1,30	1,31	0,89	1,23	1,27
	Y10FB	1,04	1,30	1,31	0,91	1,13	1,15
	Y22BD	0,79	1,31	1,41	0,82	1,29	1,32
	Y24CA	1,06	1,30	1,33	0,92	1,12	1,14
	Y37AC	1,05	1,29	1,33	0,91	1,09	1,11
	Y46BC	1,09	1,32	1,35	0,92	1,11	1,12
	Y47BC	1,09	1,31	1,34	0,92	1,11	1,12
	Y52DA	1,03	1,24	1,22	0,93	1,14	1,16
	Y53AA	0,95	1,30	1,32	0,89	1,20	1,22
	Y54BA	1,00	1,29	1,34	0,90	1,15	1,16
	Y56BC	1,05	1,29	1,32	0,92	1,12	1,13
	Y63BA	0,99	1,30	1,34	0,90	1,15	1,17
	Y68DA	1,08	1,22	1,22	0,95	1,07	1,08
	Y70AC	1,04	1,28	1,31	0,91	1,11	1,12
	Y72BD	1,10	1,36	1,41	0,92	1,09	1,10
	Y73BD	1,09	1,36	1,41	0,91	1,10	1,12
	Y77AD	1,08	1,30	1,31	0,92	1,12	1,13
	Y78KB	1,06	1,32	1,36	0,91	1,12	1,14
	Y79KA	1,07	1,34	1,38	0,91	1,12	1,14
	Y80AD	1,10	1,30	1,31	0,93	1,10	1,12
	Y81KB	1,10	1,33	1,36	0,92	1,10	1,12
	Y82KA	1,10	1,33	1,37	0,92	1,10	1,12
620 groups	Y02BB	0,81	1,42	1,42	0,82	1,42	1,47
	Y48BC	1,13	1,22	1,22	0,96	1,06	1,08
	Y57BC	1,07	1,20	1,20	0,95	1,08	1,09
	Y66BA	0,91	1,31	1,32	0,87	1,28	1,31
other groups structure	Y25HA	1,10	1,30	1,33	0,94	1,10	1,11
	Y26HA	1,19	1,29	1,32	0,97	1,04	1,04
	Y27HA	1,46	1,28	1,43	1,09	0,88	0,86
	Y28HA	0,97	1,31	1,33	0,86	1,20	1,23
	Y29GA	0,97	1,23	1,08	0,90	1,25	1,28
	Y30GA	1,42	1,14	1,22	0,98	0,85	0,83
	Y41IA	1,05	1,37	1,40	0,90	1,18	1,20
	Y44JA	0,86	1,21	1,25	0,88	1,23	1,25
	Y61EB	0,93	1,34	1,35	0,87	1,29	1,32

Table 16. Definition of some important quantities.

parameter	definition formula
nickel activation rate	$R_{Ni} = \int_0^{20MeV} \sigma_{Ni}(E).\phi_E(E).dE$
nickel fluence rate	$\phi_{Ni} = \int_0^{20MeV} \sigma_{Ni}(E).\phi_E(E).dE / \langle\sigma_{Ni}\rangle^{fission}$
total cobalt activation rate	$R_{Co} = \int_0^{20MeV} \sigma_{Co}(E).\phi_E(E).dE$
intermediate cobalt activation rate	$R_{Co}^{int} = \int_{0,55eV}^{1\ MeV} \sigma_{Co}(E).\phi_E(E).dE$
cobalt fluence rate	$\phi_{Co} = R_{Co} / \langle\sigma_{Co}\rangle^{2200}$
intermediate cobalt fluence rate	$\phi_{Co}^{int} = R_{Co}^{int} / \int_{0,563eV}^{1,05MeV} \sigma(E).\frac{dE}{E}$
mean spectrum energy	$\langle E\rangle = \int_0^{20MeV} E.\phi(E).dE / \int_0^{20MeV} \phi(E).dE$
displacement rate for steel	$R_{dpa} = \int_0^{20MeV} \sigma_d(E).\phi_E(E).dE$
damage-to-activation ratio (DAR) for nickel	$DAR = \frac{R_{dpa}/R_{Ni}}{\langle\sigma_d\rangle^{fission} / \langle\sigma_{Ni}\rangle^{fission}}$

Table 17. Standard deviations in participants values for integral parameters.

Part A: ORR

Group	standard deviation in participants values (in per cent)				
structures	$s(\phi_{tot})$	$s(\phi>1MeV)$	$s(\phi>0,1MeV)$	$s(R_{Ni})$	$s(R_{dpa})$
100 groups	1,4	1,8	1,4	1,4	1,3
620 groups	2,6	1,6	0,5	2,0	3,4
other groups	3,3	3,9	5,2	1,5	1,7
total	2,1	2,5	2,8	1,7	2,2

Part B: YAYOI

Group	standard deviation in participants values (in per cent)				
structures	$s(\phi_{tot})$	$s(\phi>1MeV)$	$s(\phi>0,1MeV)$	$s(R_{Ni})$	$s(R_{dpa})$
100 groups	2,0	2,4	1,8	4,6	2,4
620 groups	5,2	2,0	4,9	11	1,4
other groups	4,7	5,6	5,0	8,7	4,5
total	3,0	3,5	3,0	7,1	2,8

Table 18. Comparison of predicted and measured activation rates in nickel. The measured reaction rates per target atom of nickel are $5,310 \times 10^{-13} s^{-1}$ and $1,070 \times 10^{-14} s^{-1}$ for ORR and YAYOI respectively. The coefficients of variation are 5 and 2,4 per cent respectively.

	R_{Ni} predicted/R_{Ni} measured	
	ORR	YAYOI
for all solutions:		
average value	0,99	0,93
standard deviation	0,017	0,071
lowest value	0,96	0,77
highest value	1,04	0,99

Table 19. Uncertainty data in integral parameters as supplied by the participants.
Reference values for the input spectrum (in per cent).

spectrum	IAEA code	$s(\phi_{tot})$	$s(\phi(E>1MeV))$	$s(\phi(E>0,1MeV))$	$s(R_{Ni})$	$s(R_{dpa})$
ORR	000XX	12,8	18,0	13,1	21,4	18,3
YAYOI	Y00XX	13,8	19,7	14,1	28,6	20,5

Part A: ORR

spectrum	IAEA code	relative standard deviation in integral parameter *				
		ϕ_{tot}	$\phi(E>1MeV)$	$\phi(E>0,1MeV)$	R_{Ni}	R_{dpa}
100 groups	006AB	0,41	0,33	0,65	0,35	0,44
	008FB	0,41	0,33	0,66	0,22	0,24
	036AC	0,43	0,37	0,69	-	0,85
	038AC	0,43	0,37	0,70	-	0,85
	045BC	0,28	0,30	0,29	0,13	0,19
	050AA	0,43	0,37	0,70	0,47	0,71
	055BC	0,10	0,12	0,13	0,12	0,09
	062BA	0,68	0,86	0,78	0,83	0,89
	074AC	0,41	0,30	0,63	0,40	0,55
	075KB	0,41	0,31	0,63	0,40	0,54
620 gr.	001BB	0,19	0,32	0,31	0,21	0,24
others	031HA	0,39	0,32	0,66	0,29	0,39
	043JA	0,46	0,34	0,64	0,30	0,34

Part B: YAYOI

100 groups	Y07AB	0,42	0,57	0,49	0,30	0,45
	Y10FB	0,29	0,39	0,34	0,27	0,21
	Y37AC	0,41	0,60	0,48	-	0,80
	Y46BC	0,14	0,15	0,14	0,14	0,12
	Y47BC	0,18	0,25	0,19	0,16	0,17
	Y53AA	0,45	0,63	0,50	0,42	0,69
	Y56BC	0,18	0,19	0,17	0,17	0,10
	Y63BA	0,74	0,84	0,74	0,68	0,82
	Y77AD	0,38	0,43	0,45	0,27	0,50
	Y80AD	0,37	0,41	0,44	0,27	0,50
	Y78KB	0,34	0,41	0,38	0,27	0,49
	Y81KB	0,34	0,39	0,42	0,27	0,49
620 gr.	Y02BB	0,32	0,38	0,33	0,25	0,25
	Y48BC	0,20	0,19	0,22	0,13	0,15
	Y57BC	0,15	0,20	0,17	0,15	0,10
others	Y25HA	0,33	0,48	0,39	0,31	0,38
	Y44JA	0,74	0,63	0,79	0,61	0,59

*relative to the corresponding value for the input spectrum.

Table 20. Uncertainty data in integral parameters as calculated by the evaluators from the solution neutron spectra and uncertainty data. Reference values for input spectrum in percent (calculated with correlations).

spectrum	IAEA code	$s(\phi_{tot})$	$s(\phi(E>1MeV))$	$s(\phi(E>0,1MeV))$	$s(R_{Ni})$	$s(R_{dpa})$
ORR	000XX	12,8	18,0	13,1	21,4	18,3
YAYOI	Y00XX	13,8	19,7	14,1	28,6	20,5

Part A: ORR

	IAEA code	relative standard deviation in integral parameter *									
		ϕ_{tot}		$\phi(E>1MeV)$		$\phi(E>0,1MeV)$		R_{Ni}		R_{dpa}	
		with correlations	without correlations	with correlations	without correlations	with correlations	without correlations	with correlations	without correlations	with correlations	without correlations
100 groups	006AB	0,43	0,27	0,34	0,31	0,67	0,37	0,47	0,27	0,70	0,28
	008FB	0,42	0,27	0,33	0,32	0,65	0,37	0,49	0,30	0,71	0,30
	036AC	0,43	0,27	0,37	0,32	0,70	0,33	0,46	0,28	0,71	0,28
	038AC	0,43	0,27	0,37	0,32	0,70	0,38	0,46	0,28	0,71	0,28
	05BC	0,29	0,24	0,21	0,11	0,41	0,12	0,42	0,16	0,69	0,19
	050AA	0,45	0,25	0,38	0,32	0,71	0,38	0,48	0,28	0,71	0,28
	055BC	0,10	0,04	0,11	0,05	0,12	0,04	0,42	0,13	0,66	0,17
	062BA	-	0,39	-	0,47	-	0,45	-	0,43	-	0,37
	069AC	0,44	0,25	0,38	0,32	0,71	0,38	0,48	0,28	0,71	0,28
	071AC	0,44	0,27	0,38	0,32	0,71	0,38	0,47	0,28	0,71	0,28
	074AD	0,42	0,26	0,31	0,29	0,65	0,36	0,46	0,25	0,69	0,27
	075KB	0,42	0,26	0,32	0,29	0,65	0,36	0,46	0,25	0,69	0,27

Part B: YAYOI

100 groups	Y07AB	0,45	0,37	0,58	0,39	0,50	0,37	0,38	0,24	0,68	0,29
	Y10FB	0,40	0,36	0,52	0,37	0,46	0,37	0,34	0,24	0,66	0,28
	Y37AC	0,41	0,37	0,60	0,39	0,47	0,38	0,37	0,26	0,68	0,29
	Y46BC	0,14	0,07	0,16	0,08	0,13	0,06	0,34	0,14	0,61	0,16
	Y47BC	0,16	0,11	0,26	0,13	0,17	0,12	0,35	0,16	0,62	0,18
	Y53AA	0,48	0,38	0,64	0,41	0,53	0,38	0,42	0,26	0,70	0,30
	Y56BC	0,12	0,09	0,14	0,18	0,12	0,07	0,37	0,14	0,61	0,17
	Y63BA	-	0,42	-	0,65	-	0,31	-	0,41	-	0,36
	Y70AC	0,47	0,37	0,61	0,55	0,52	0,27	0,38	0,26	0,69	0,29
	Y77AD	0,41	0,37	0,44	0,35	0,46	0,35	0,32	0,22	0,64	0,26
	Y78KB	0,37	0,34	0,41	0,34	0,44	0,35	0,32	0,23	0,64	0,26
	Y80AD	0,40	0,35	0,42	0,34	0,45	0,35	0,32	0,22	0,64	0,26
	Y81KB	0,37	0,34	0,40	0,34	0,43	0,34	0,32	0,23	0,64	0,26

*relative to the corresponding value for the input spectrum.

Table 21. Effect of covariance information on the uncertainties in integral spectrum characteristics (shown for the input neutron spectra).

IAEA code	corr. matrix for ϕ	corr. matrix for σ_{Ni} and σ_{dpa}	standard deviation in percent for								
			ϕ_{tot}	ϕ(E>1MeV)	ϕ(E>0,1MeV	R_{Ni}			R_{dpa}		
						total	due to contribution of ϕ	due to contribution of σ	total	due to contribution of ϕ	due to contribution of σ
000XX	var.+cov.*	var.+cov.*	12,75	18,01	13,13	21,40	19,65	8,47	18,31	13,93	11,89
000XX	diag.	diag.	6,13	8,42	5,78	9,20	8,85	2,49	6,82	6,14	2,97
000XX	diag.	var.+cov.	6,13	8,42	5,78	12,25	8,85	8,47	13,38	6,14	11,89
000XX	var.+cov.	diag.	12,75	18,01	13,13	19,81	19,65	2,49	14,24	13,93	2,97
Y00XX	var.+cov.*	var.+cov.*	13,77	19,65	14,06	28,60	27,32	8,47	20,47	16,37	12,29
Y00XX	diag.	diag.	6,01	9,26	6,18	12,71	12,47	2,48	7,86	7,25	3,03
Y00XX	diag.	var.+cov.	6,01	9,26	6,18	15,08	12,47	8,47	14,27	7,25	12,29
Y00XX	var.+cov.	diag.	13,77	19,65	14,06	27,43	27,32	2,48	16,65	16,37	3,03

* This situation refers to the REAL-80 input data set.

able 22: Solutions supplying correlation matrices

art A: ORR

IAEA code	adjust-ment code	groups	remarks
000XX	-	100	input spectrum
006AB	STAY'SL	100	
008FB	NEUPAC	100	numbering of groups starting at maximum energy
031HA	LSL	20	
036AC	STAY'SL	100	
038AC	STAY'SL	100	uncorrected nuclear data
043JA	SENSAK	40	
045BC	SANDBP	100	18 reactions (Fe58GC deleted)
050AA	STAY'SL	100	
055BC	SANDBP	100	
069AC	STAY'SL	100	
071AC	STAY'SL	100	20 reactions (Ni58P used)
074AD	STAY'SL	100	
075KB	ITER-3	100	

Part B: YAYOI

IAEA code	adjust-ment code	groups	remarks
Y00XX	-	100	input spectrum
Y07AB	STAY'SL	100	
Y10FB	NEUPAC	100	see: 008FB
Y25HA	LSL	20	
Y37AC	STAY'SL	100	13 reactions (Ni58P used)
Y44JA	SENSAK	40	
Y46BC	SANDBP	100	11 reactions (Ti47P deleted)
Y47BC	SANDBP	100	11 reactions (Ti47P deleted) 5-points smoothing
Y53AA	STAY'SL	100	
Y56BC	SANDBP	100	
Y70AC	STAY'SL	100	13 reactions (Ni58P used)
Y77AD	STAY'SL	100	13 reactions (Ni58P used)
Y78KB	ITER-3	100	13 reactions (Ni58P used)
Y80AD	STAY'SL	100	(Ni58P used) (Ti47P deleted)
Y81KB	ITER-3	100	(Ni58P used) (Ti47P deleted)

Table 23. Average correlation coefficients and the variance of all element values in the correlation matrix

Part A: ORR

IAEA code	fission region (E>0,8 MeV)			slowing down region (0,5 eV<E<0,8 MeV)			thermal region (E<0,5 eV)			total		
	m	$\overline{r_{ij}}$	$s^2(r_{ij})$	m	$\overline{r_{ij}}$	$s^2(r_{ij})$	m	$\overline{r_{ij}}$	$s^2(r_{ij})$	m	$\overline{r_{ij}}$	$s^2(r_{ij})$
000XX (input)	31	0,167	0,057	61	0,088	0,051	8	0,522	0,120	100	0,057	0,033
006AB	31	0,045	0,100	61	0,054	0,052	8	0,084	0,393	100	0,025	0,033
008FB	31	0,040	0,100	61	0,052	0,052	8	0,078	0,394	100	0,069	0,035
031HA	6	0,063	0,229	13	0,069	0,084	1	1,000		20	0,033	0,063
036AC	31	0,046	0,101	61	0,052	0,053	8	0,065	0,411	100	0,024	0,034
038AC	31	0,046	0,101	61	0,052	0,053	8	0,065	0,411	100	0,024	0,034
043JA	22	0,160	0,069	16	0,174	0,073	2	0,625	0,141	40	0,107	0,031
045BC	31	0,172	0,341	61	0,308	0,214	8	0,536	0,244	100	0,144	0,220
050AA	31	0,050	0,098	61	0,056	0,053	8	0,086	0,391	100	0,026	0,033
055BC	31	0,278	0,240	61	0,504	0,191	8	0,247	0,637	100	0,211	0,230
074AD	31	0,037	0,105	61	0,053	0,053	8	0,073	0,405	100	0,023	0,034
075KB	31	0,037	0,105	61	0,053	0,053	8	0,073	0,405	100	0,023	0,034

m = number of energy groups involved in the matrix.

$\overline{r_{ij}}$ = average correlation coefficient

$s^2(r_{ij})$ = the variance of all element values

Table 23. (Continued)

Part B: YAYOI

	fission region (E>0,8 MeV)			slowing down region (0,5 eV<E<0,8 MeV)			thermal region (E<0,5 eV)			total		
	m	$\overline{r_{ij}}$	$s^2(r_{ij})$	m	$\overline{r_{ij}}$	$s^2(r_{ij})$	m	$\overline{r_{ij}}$	$s^2(r_{ij})$	m	$\overline{r_{ij}}$	$s^2(r_{ij})$
Y00XX (input)	31	0,164	0,087	61	0,087	0,052	8	0,520	0,123	100	0,055	0,033
Y07AB	31	0,056	0,103	61	0,057	0,057	8	0,520	0,123	100	0,034	0,036
Y10FB	31	0,048	0,102	61	0,055	0,056	8	0,514	0,122	100	0,069	0,035
Y25HA	6	0,068	0,240	13	0,083	0,088	1	1,000	0	20	0,040	0,061
Y37AC	31	0,057	0,106	61	0,058	0,059	8	0,520	0,122	100	0,030	0,035
Y44JA	22	0,148	0,073	16	0,130	0,076	2	0,750	0,063	40	0,076	0,022
Y46BC	31	0,250	0,299	61	0,087	0,643	8	1,000	0	100	0,104	0,528
Y47BC	31	0,248	0,383	61	0,033	0,755	8	0,999	0	100	0,062	0,599
Y53AA	31	0,064	0,101	61	0,059	0,056	8	0,520	0,123	100	0,031	0,035
Y56BC	31	0,177	0,477	61	0,096	0,701	8	1,000	0	100	0,120	0,613
Y77AD	31	0,045	0,106	61	0,056	0,056	8	0,520	0,122	100	0,029	0,035
Y78KB	31	0,045	0,106	61	0,056	0,057	8	0,520	0,122	100	0,029	0,035
Y80AD	31	0,045	0,106	61	0,056	0,057	8	0,520	0,122	100	0,029	0,035
Y81KB	31	0,045	0,106	61	0,056	0,057	8	0,520	0,122	100	0,029	0,035

m = number of energy groups involved in the matrix.

$\overline{r_{ij}}$ = average correlation coefficient

$s^2(r_{ij})$ = the variance of all element values

Table 24: Cumulative percentage of eigen values.

Part A: ORR

IAEA code	number of ordered eigen values contributing to the trace of the correlation matrix for a fraction of						number of eigen values greater than unity
	60 %	70 %	80 %	90 %	95 %	98 %	
000XX (input)	13	16	20	26	32	40	28
006AB	14	17	22	30	38	52	28
008FB	14	17	22	30	39	54	27
031HA	8	10	12	15	17	18	10
036AC	14	17	22	30	38	52	29
038AC	14	17	22	30	41	52	29
043JA	12	17	21	27	31	35	18
045BC	2	3	4	5	6	7	7
050AA	14	17	22	30	38	52	28
055BC	2	3	4	5	7	8	8
074AD	13	17	22	30	39	54	27
075KB	13	17	22	30	39	54	27

Table 24: (Continued)

Part B: YAYOI

IAEA code	number of ordered eigen values contributing to the trace of the correlation matrix for a fraction of						number of eigen values greater than unity
	60 %	70 %	80 %	90 %	95 %	98 %	
Y000X (input)	13	16	20	26	33	40	28
Y07AB	13	17	21	27	34	45	29
Y10FB	13	17	21	28	35	49	27
Y25HA	8	10	13	15	17	18	9
Y37AC	13	16	21	27	36	45	27
Y44JA	13	16	21	26	31	34	18
Y46BC	1	1	2	4	5	6	6
Y47BC	1	1	2	3	4	5	5
Y53AA	13	17	21	28	34	45	28
Y56BC	1	1	2	3	5	6	5
Y77AD	13	16	21	27	34	56	28
Y78KB	13	16	21	27	34	56	28
Y80AD	13	16	21	27	34	56	28
Y81KB	13	16	21	27	34	56	28

Table 25: Average communalities.

Part A: ORR

IAEA code	number of factor loading vector consi-dered	fission region	slowing-down region	thermal region	total
000XX (input)	20	0,797	0,806	0,775	0,801
006AB	20	0,720	0,784	0,783	0,764
008FB	20	0,723	0,777	0,781	0,762
031HA	10	0,776	0,682	0,843	0,718
036AC	20	0,765	0,758	0,791	0,763
038AC	20	0,762	0,762	0,799	0,765
043JA	10	0,473	0,602	0,548	0,529
045BC	20	1,000	1,000	1,000	1,000
050AA	20	0,751	0,772	0,745	0,764
055BC	20	1,000	0,999	1,000	1,000
074AD	20	0,757	0,768	0,808	0,768
075KB	20	0,757	0,758	0,808	0,768

Table 25: (Continued)

Part B: YAYOI

IAEA code	number of factor loading vectors consi-dered	fission region	slowing-down region	thermal region	total
Y00XX (input)	20	0,797	0,806	0,775	0,801
Y07AB	20	0,756	0,808	0,784	0,790
Y10FB	20	0,777	0,799	0,773	0,790
Y25IIA	10	0,756	0,673	0,634	0,699
Y37AC	20	0,777	0,807	0,786	0,796
Y44JA	10	0,433	0,591	0,565	0,503
Y46BC	20	1,000	1,000	1,000	1,000
Y47BC	20	1,000	1,000	1,000	1,000
Y53AA	20	0,757	0,805	0,786	0,789
Y56BC	20	0,999	1,000	1,000	1,000
Y77AD	20	0,748	0,814	0,790	0,792
Y78KB	20	0,748	0,814	0,790	0,792
Y80AD	20	0,748	0,814	0,790	0,792
Y81KB	20	0,748	0,814	0,790	0,792

Table 20. Rotated factor loading vectors in the input spectrum correlation matrix and their replication in the different code solutions.

Part A: ORR

serial number of Rflv for 000XX *	IAEA code 006AB	008FB	036AC	038AC	050AA	074AD	075KB
1	y	y	y	y	-	y	y
2	-	-	-	-	-	-	-
3	-	-	-	-	-	-	-
4	y	y	y	y	y	y	y
5	y	y	y	-	-	y	y
6	-	-	-	-	-	-	-
7	-	-	-	-	-	-	-
8	-	-	-	-	-	-	-
9	-	-	-	-	-	-	-
10	y	y	y	-	-	y	y
11	y	y	y	y	y	y	y
12	-	-	-	-	-	-	-
13	y	y	y	y	-	y	y
14	-	-	-	-	-	-	-
15	y	y	y	y	y	y	y
16	-	-	-	-	-	-	-
17	y	y	y	y	-	y	y
18	y	y	y	-	-	y	y
19	-	-	-	-	-	-	-
20	-	-	-	-	-	-	-

Part B: YAYOI

serial number of Rflv for Y00XX *	IAEA code Y07AB	Y10FB	Y37AC	Y53AA	Y77AD	Y78KB	Y81KB
1	-	-	-	-	-	-	-
2	-	-	-	-	-	-	-
3	y	y	y	y	y	y	y
4	y	y	y	y	y	y	y
5	y	y	y	y	y	y	y
6	-	-	-	-	-	-	-
7	-	-	-	-	-	-	-
8	y	y	y	y	y	y	y
9	y	y	y	y	y	y	y
10	-	-	-	-	-	-	-
11	y	y	y	y	y	y	y
12	-	-	-	-	-	-	-
13	y	y	y	y	y	-	-
14	y	y	y	y	y	y	y
15	y	y	y	y	y	y	y
16	y	y	y	y	y	y	y
17	y	y	y	y	y	y	y
18	y	y	y	y	y	y	y
19	y	y	y	y	y	y	y
20	-	-	-	-	-	-	-

* Rflv means: Rotated factor loading vector
y means that this rotated factor loading vector is present also in the solution

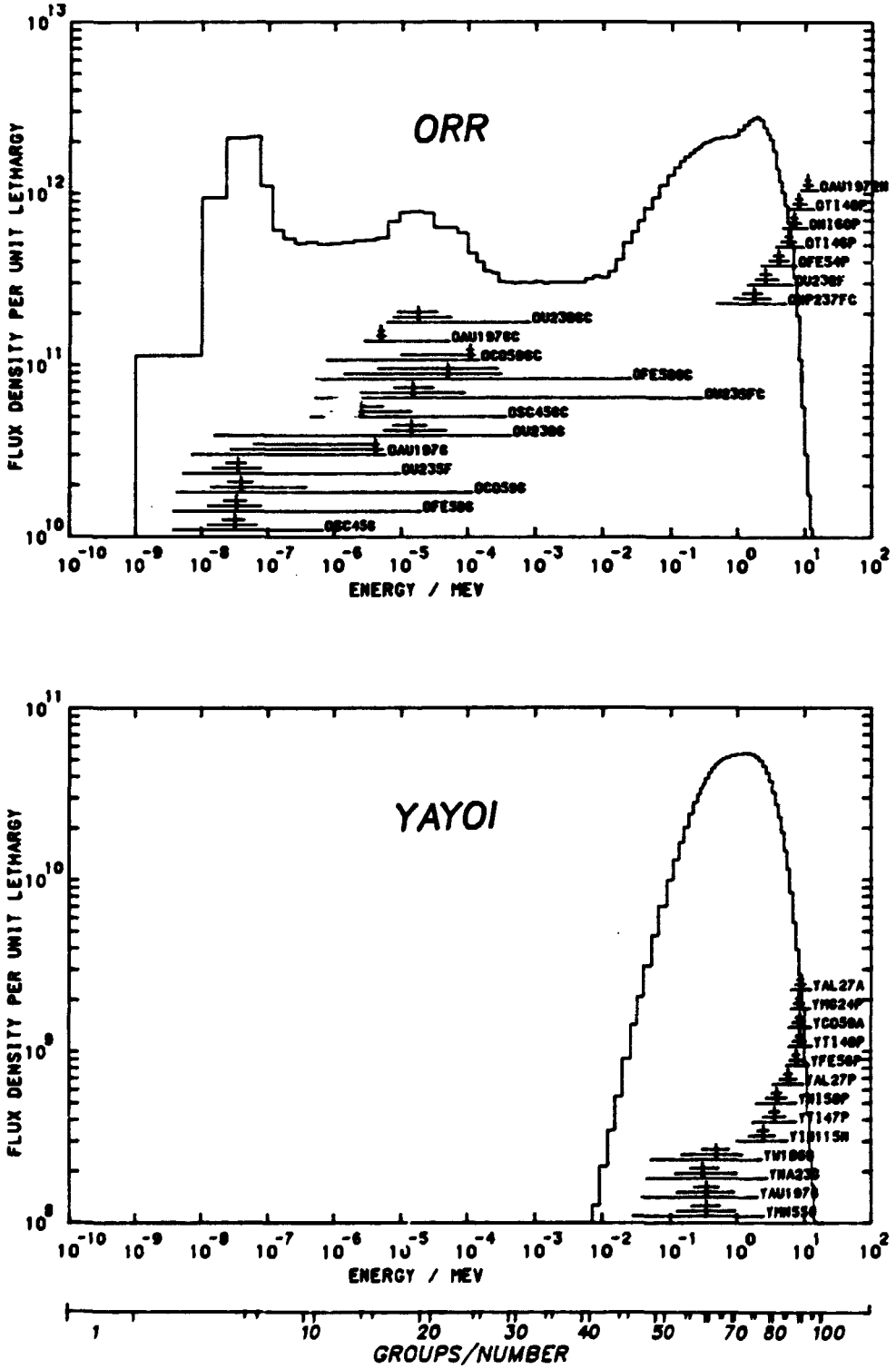

For each reaction a set of 4 lines is given.
The vertical line indicates the median response energy ,i e the energy for which the response on both sides is 50% from the total.
The horizontal lines indicate response regions with 30, 60 and 90% of the total response with 35,20 and 5% of the response outside the interval on either side resp..

Fig.: 1 Energy response regions.

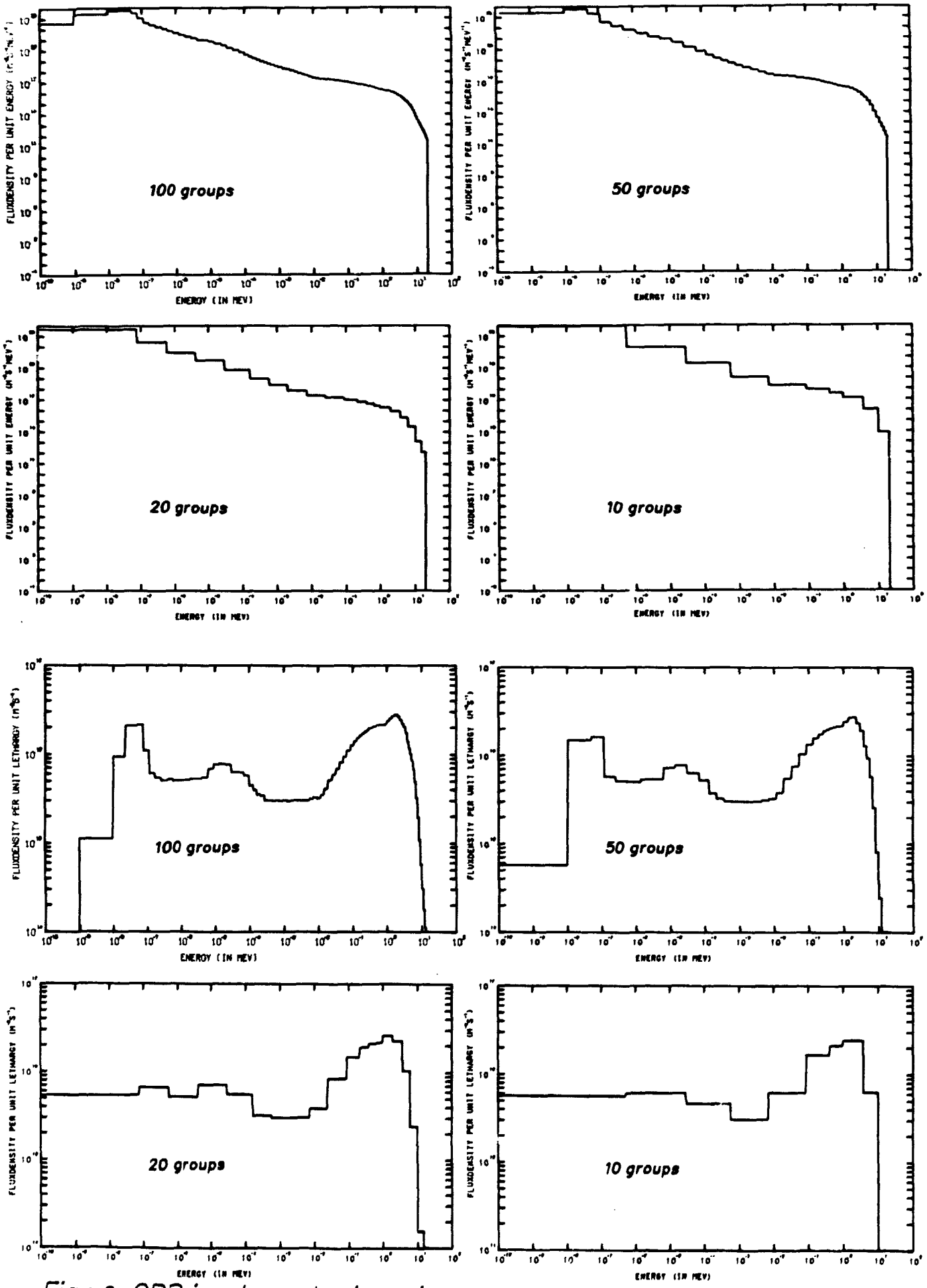

Fig.: 2 ORR input spectra in various group structures.

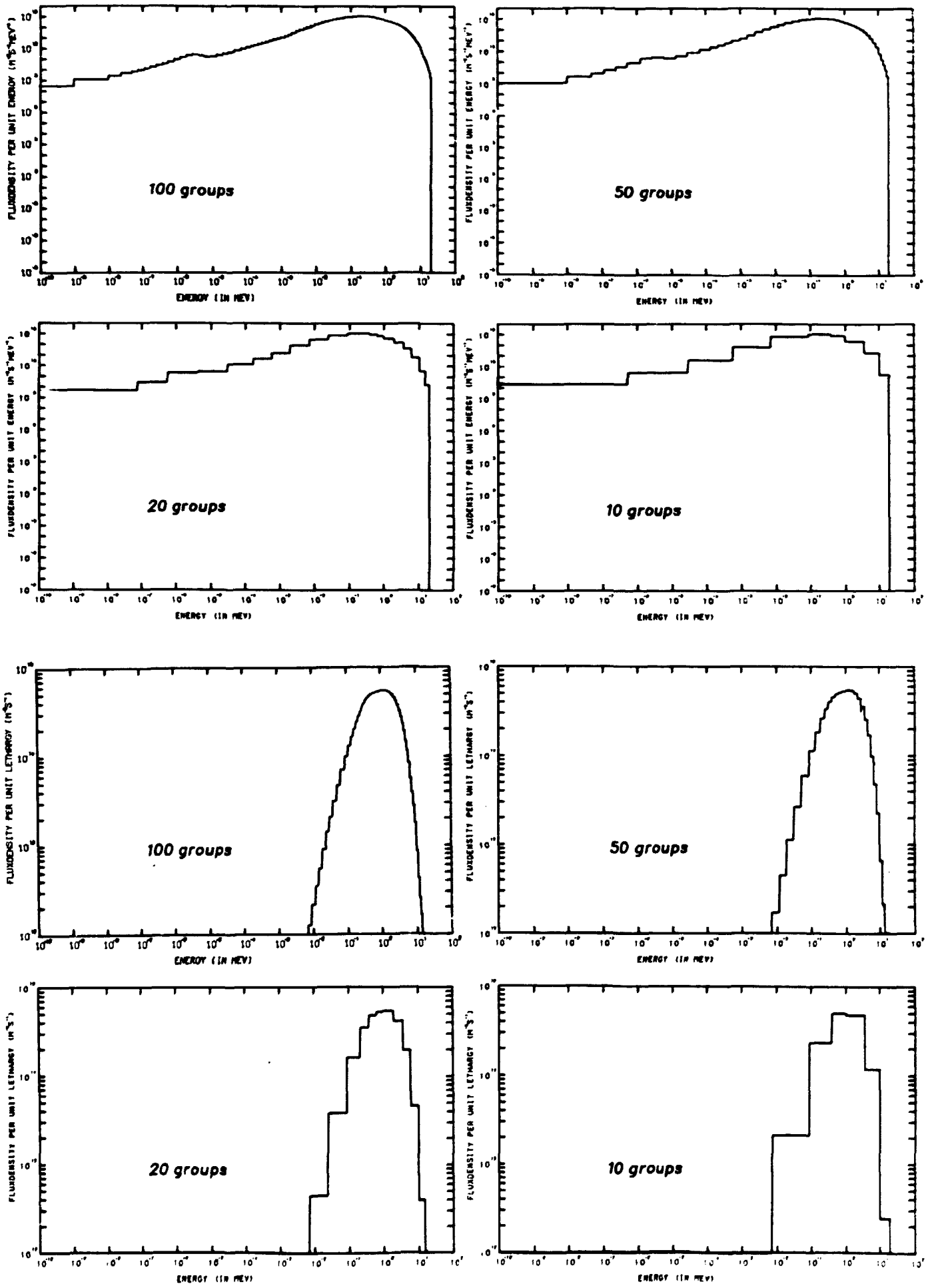

Fig.: 3 YAYOI input spectra in various group structures.

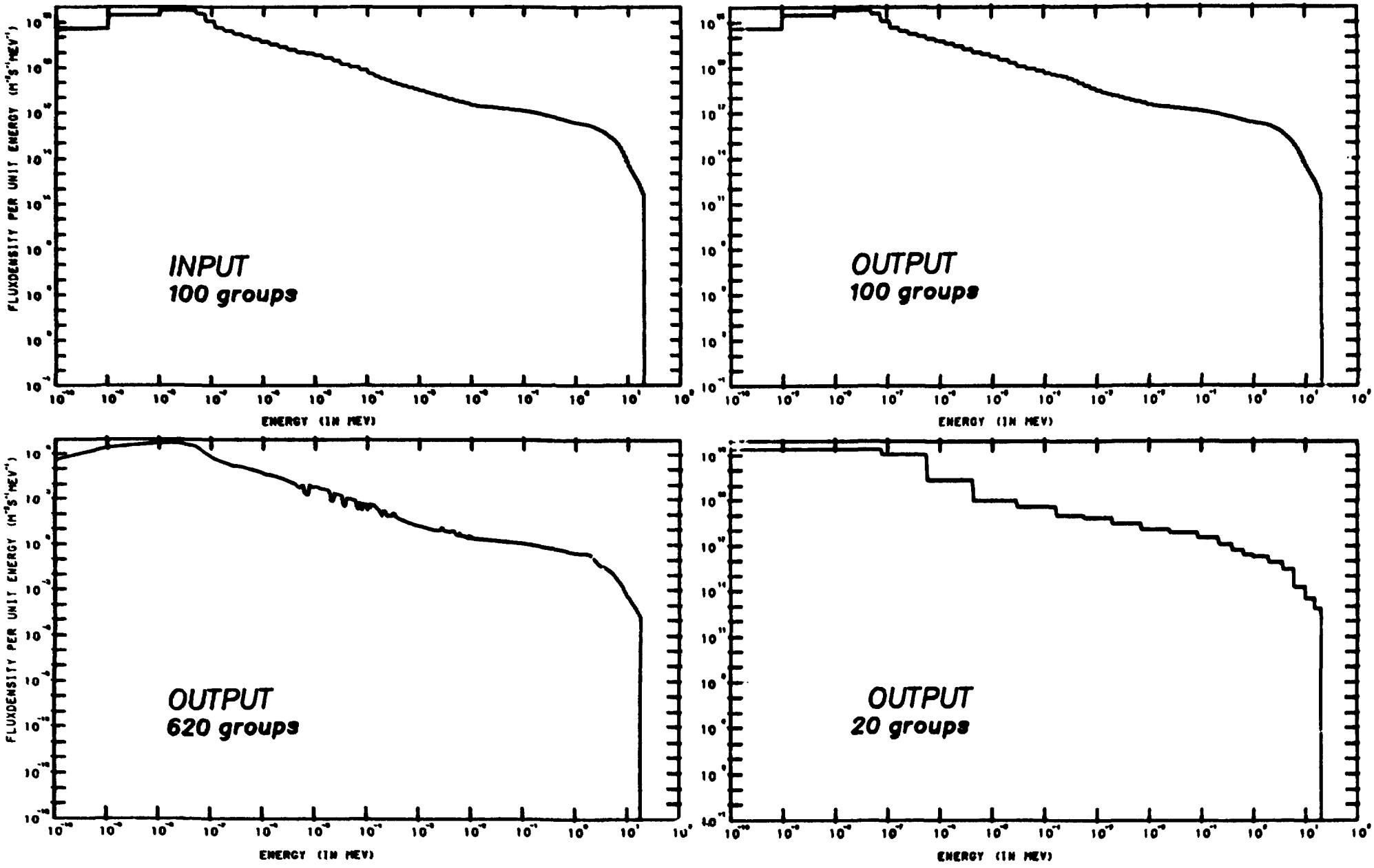

Fig.: 4 Examples of ORR spectra ($\varphi_E(E)$ representation).

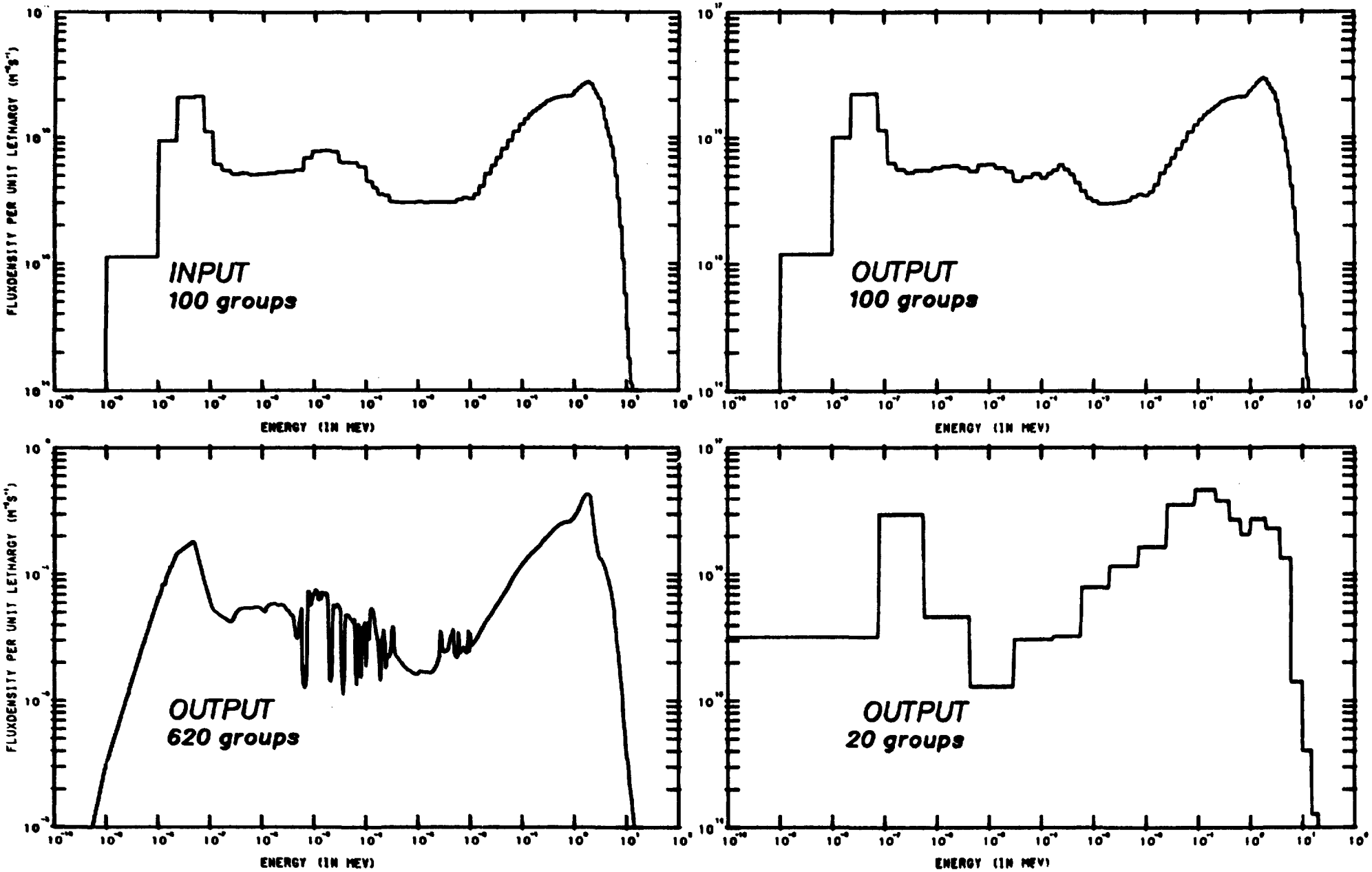

Fig.: 5 Examples of ORR spectra ($\varphi_U(E)$ representation).

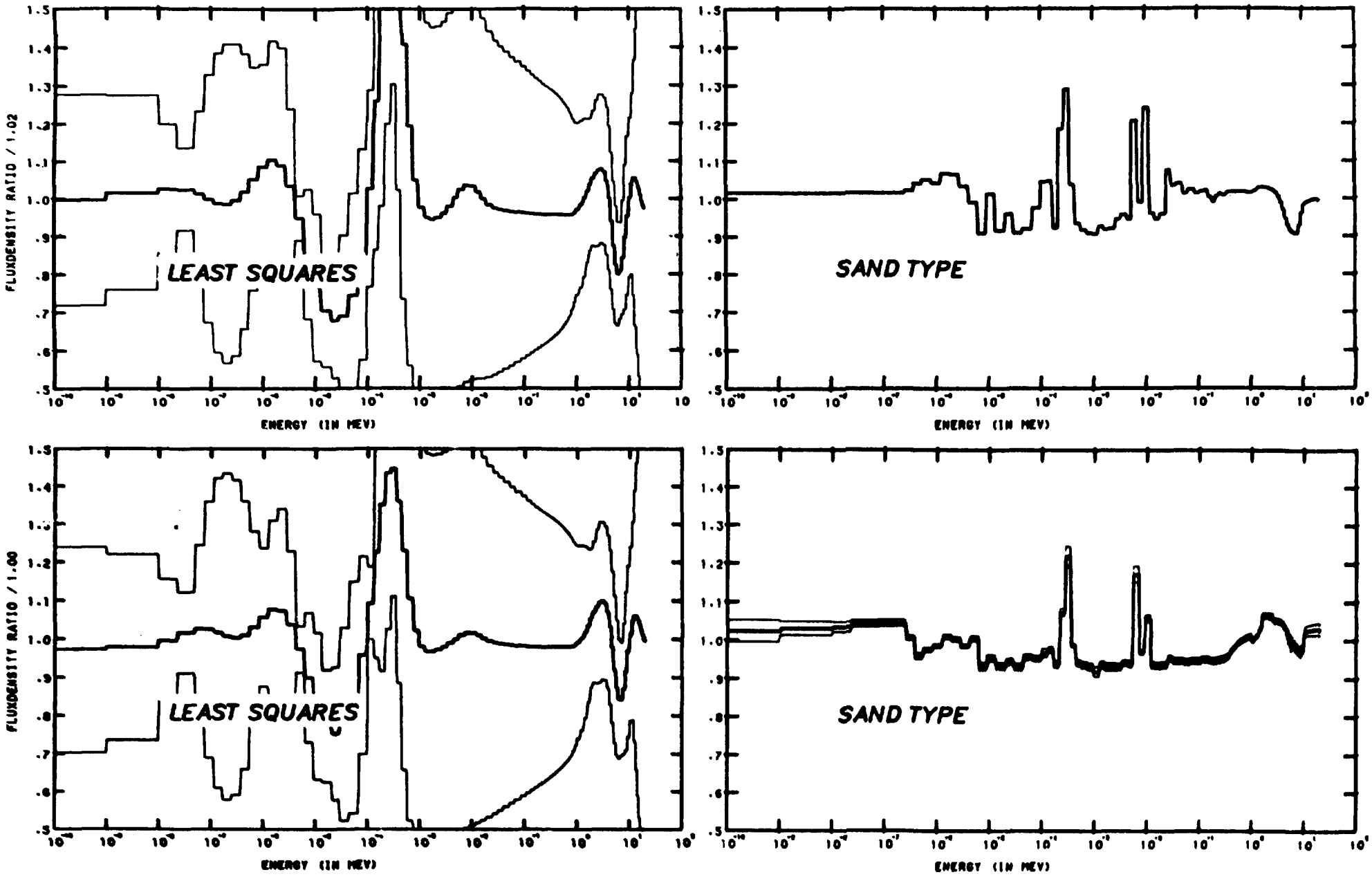

Fig.: 6 Two different modifications for two types of codes. ORR (100 GROUPS)

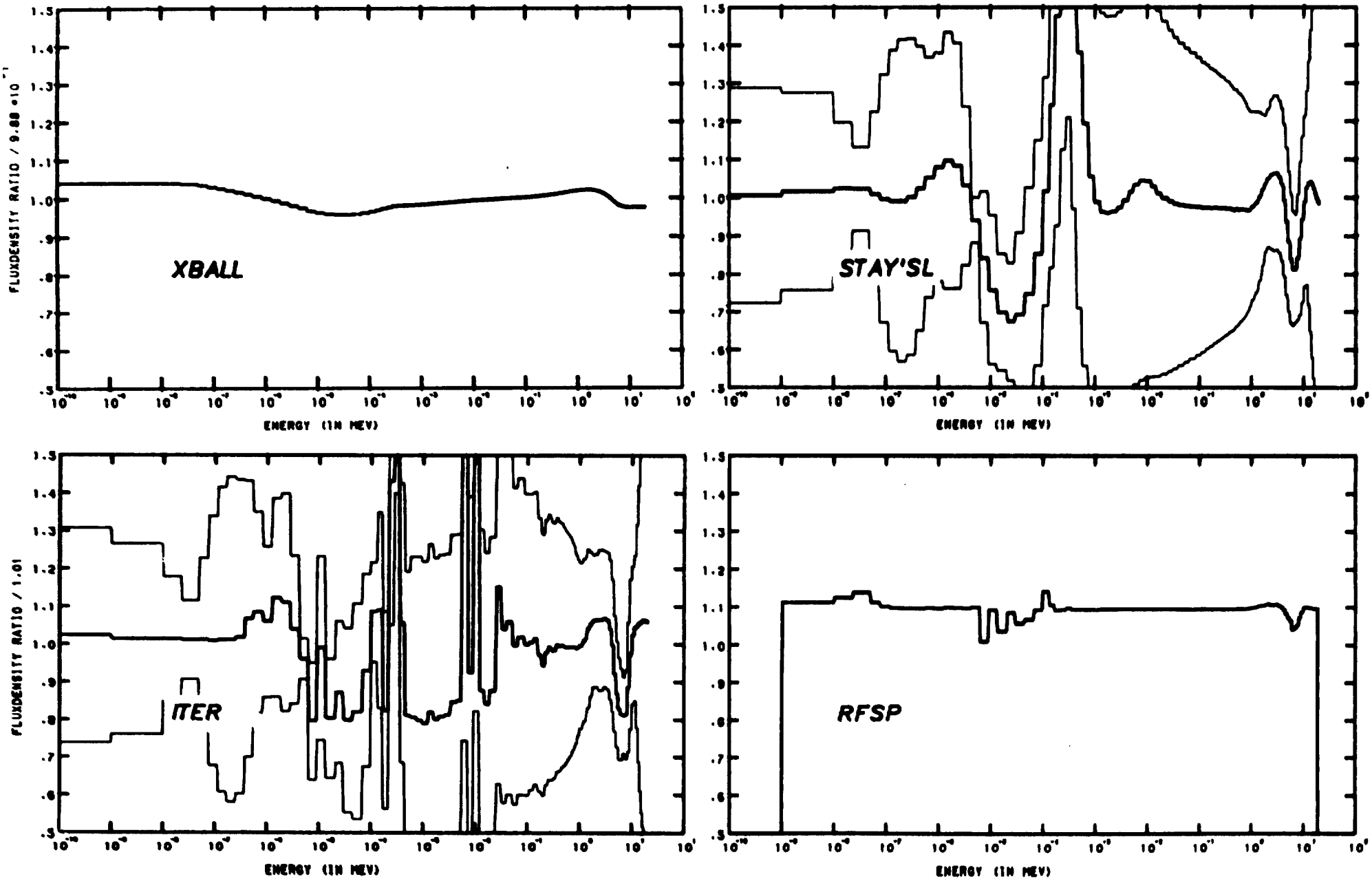

Fig.: 7 Modifications for different codes. ORR (100 GROUPS)

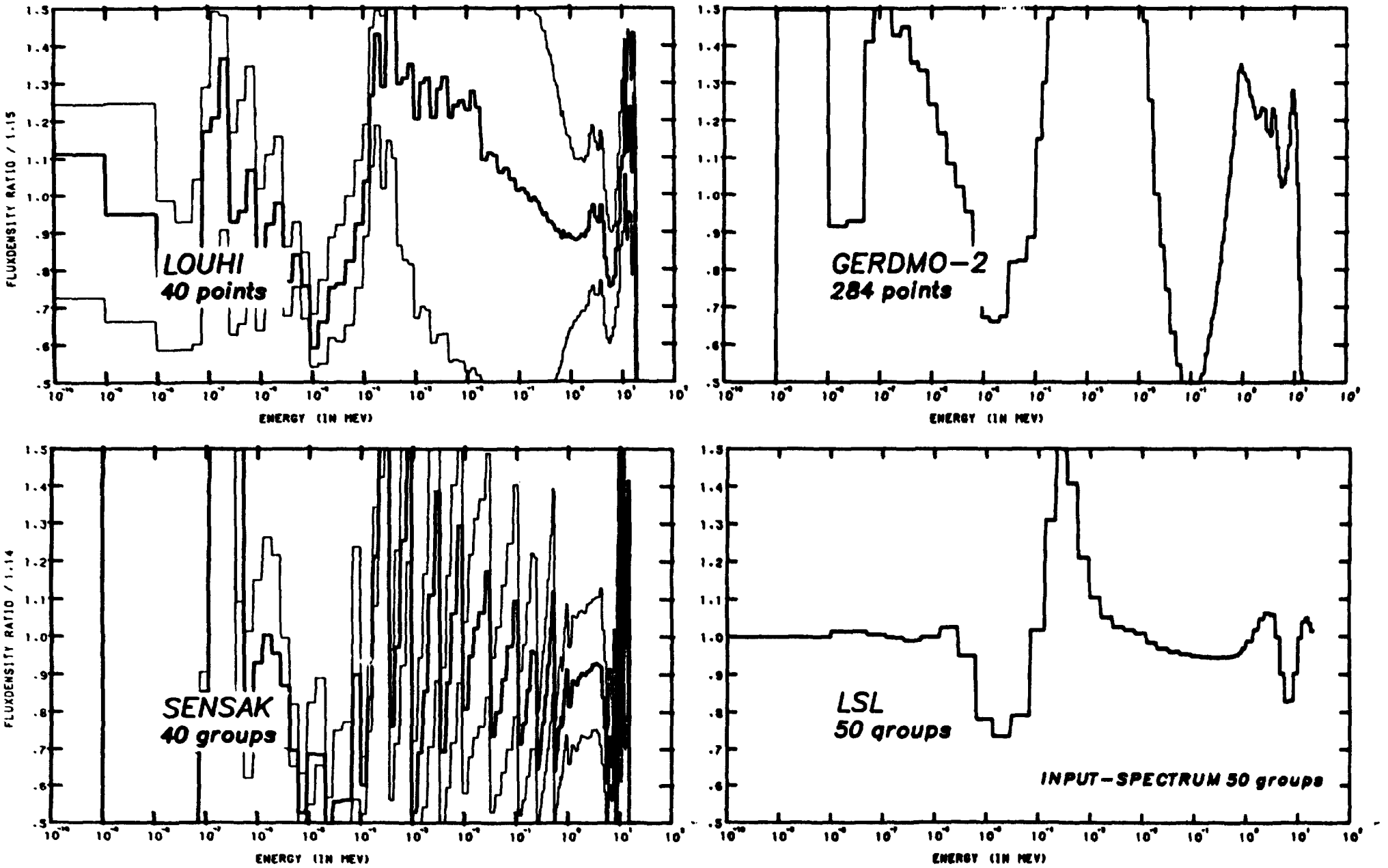

Fig.: 8 Modifications for different codes. ORR

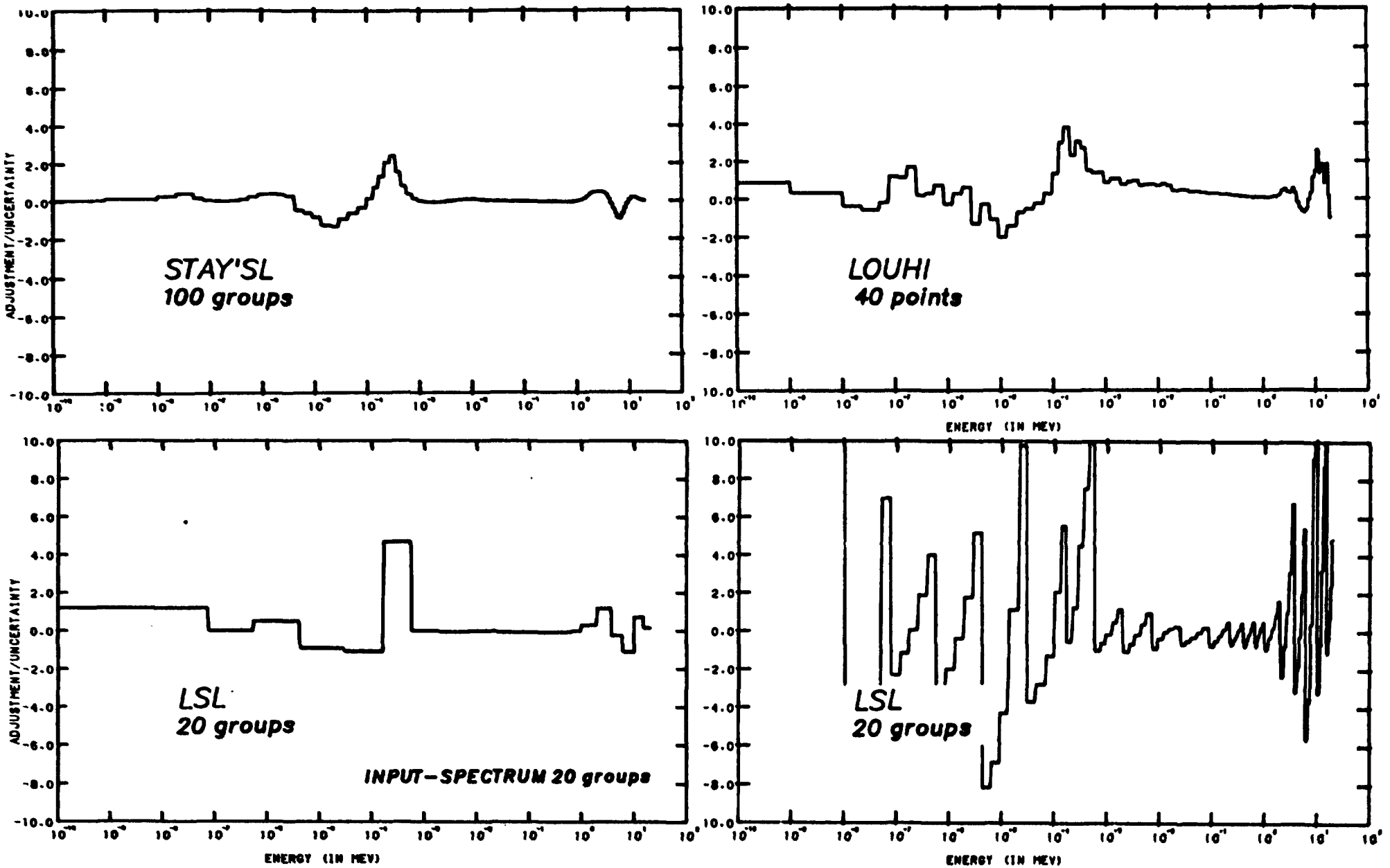

Fig.: 9 Significance of modifications. ORR

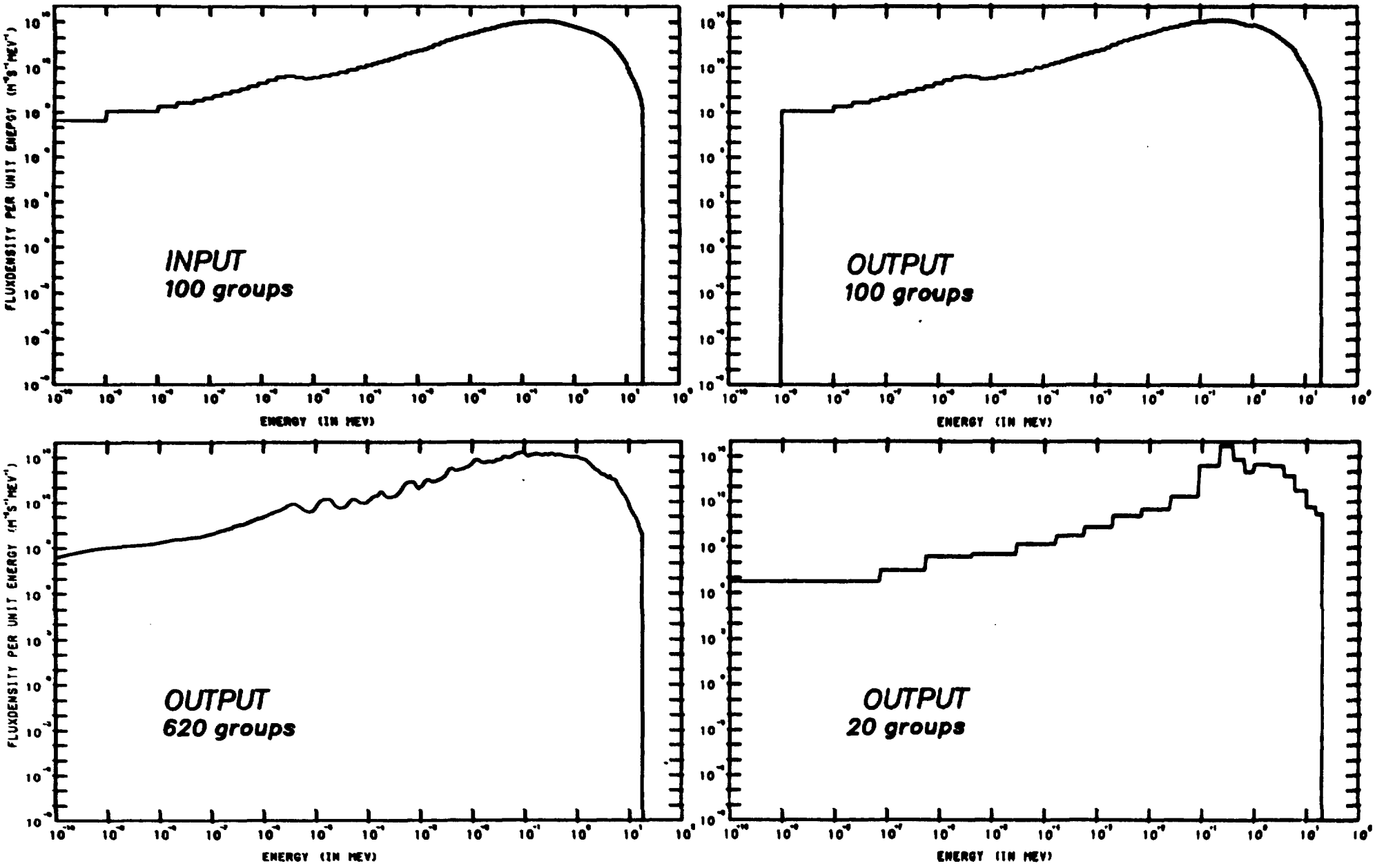

Fig.: 10 Examples of YAYOI spectra ($\varphi_E(E)$ representation).

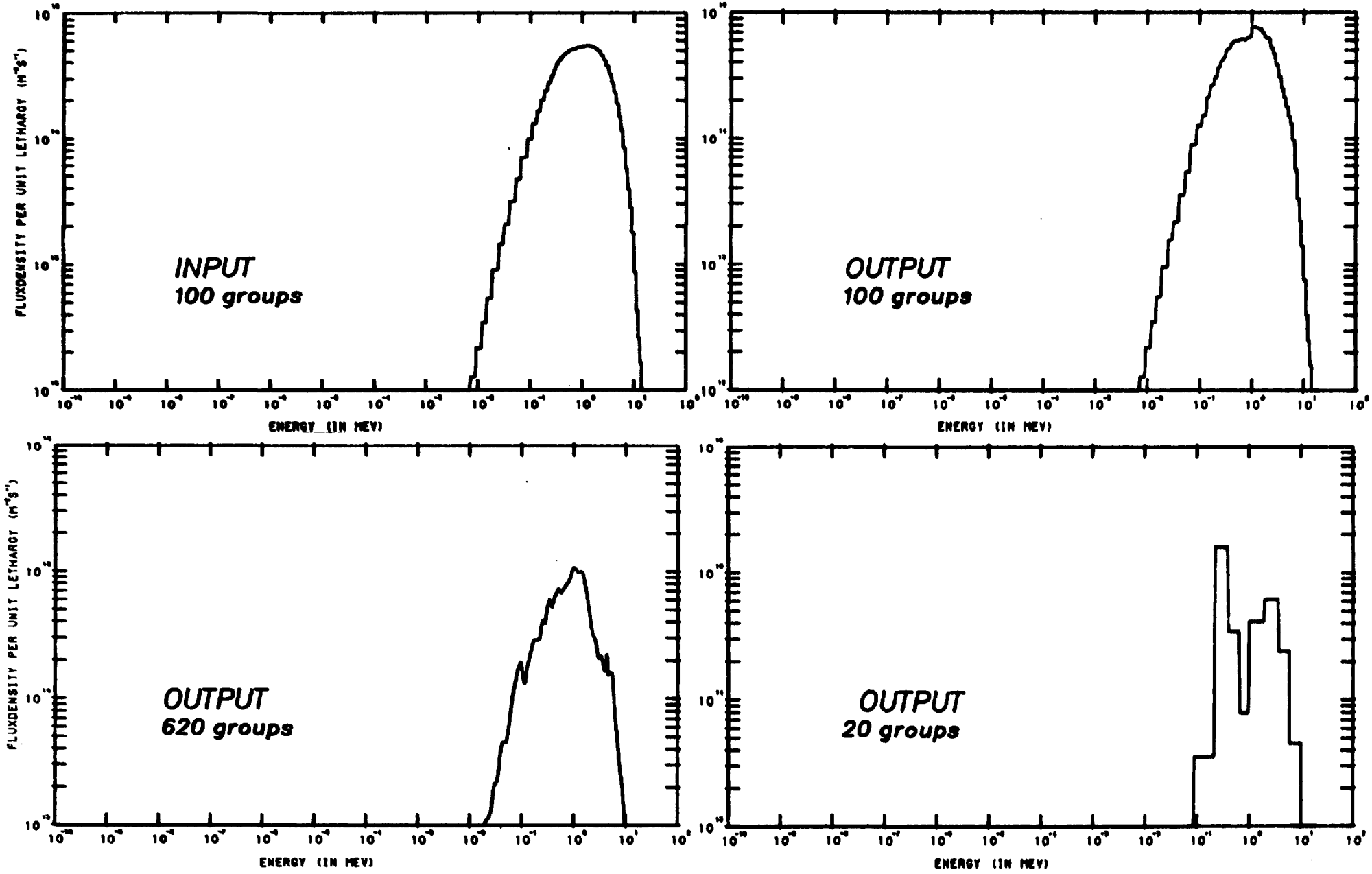

Fig.: 11 Examples of YAYOI spectra ($\varphi_U(E)$ representation).

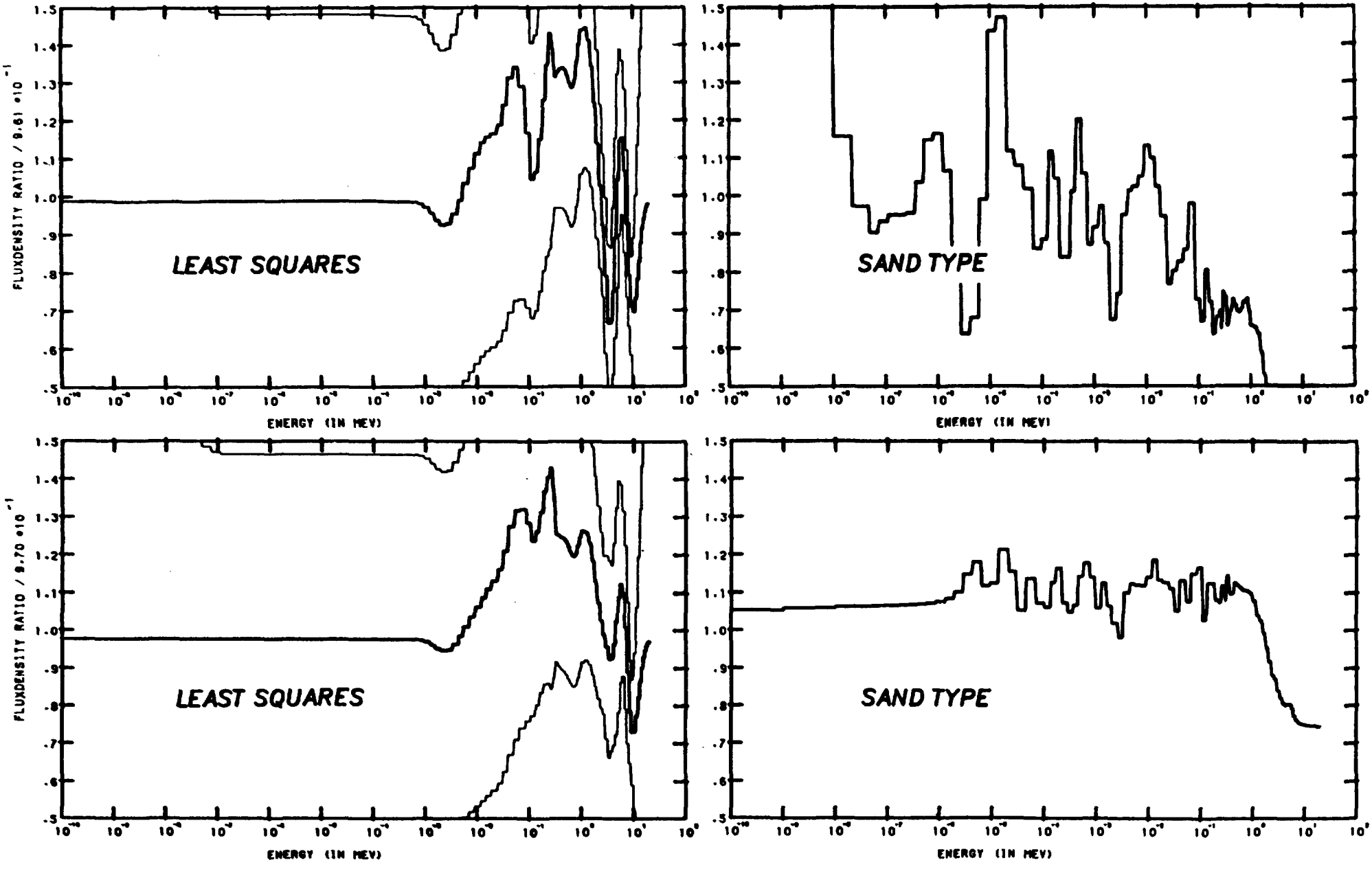

Fig.: 12 Two different modifications for two types of codes. YAYOI (100 GROUPS)

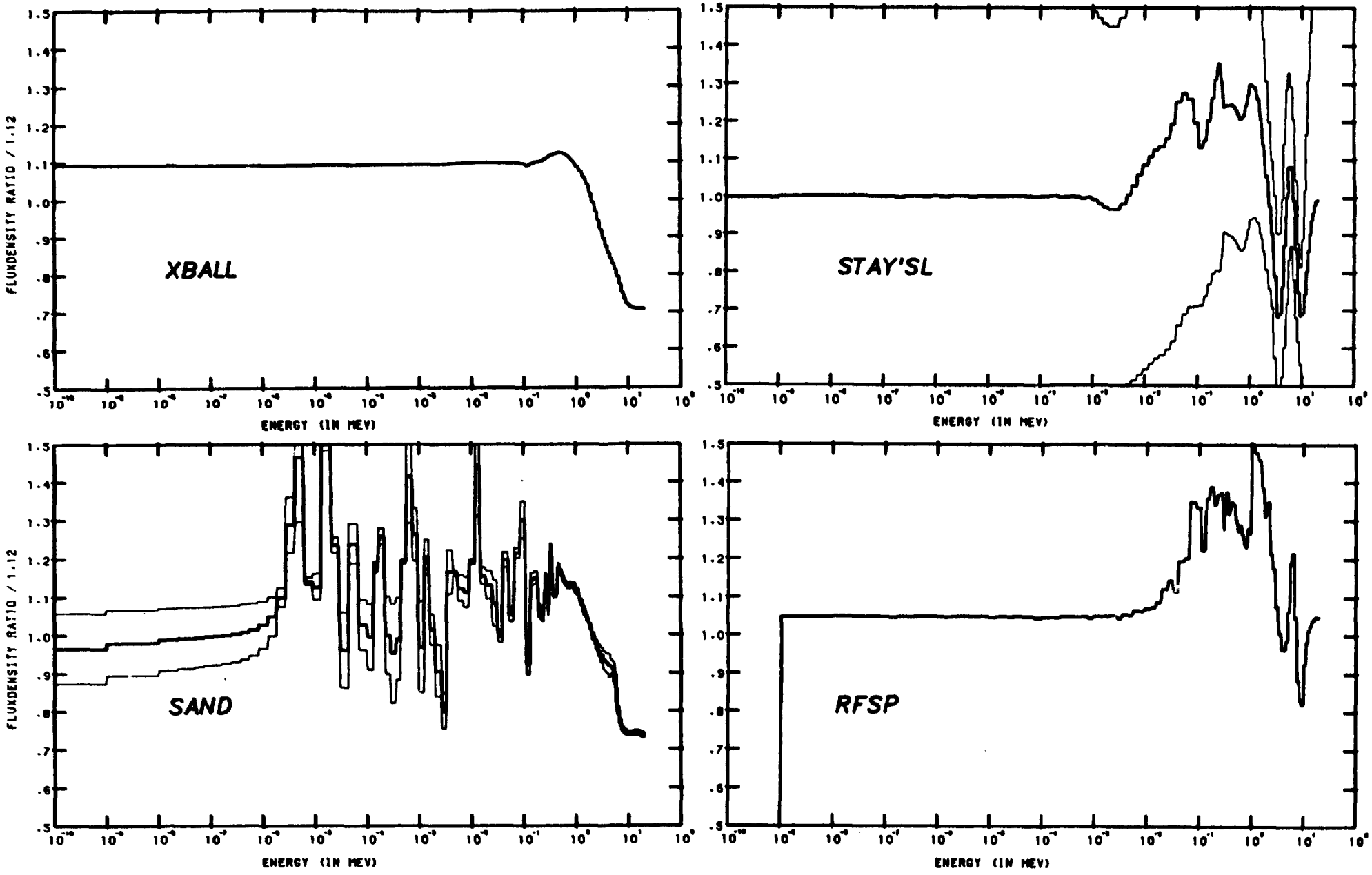

Fig.: 13 Modifications for different codes. YAYOI (100 GROUPS)

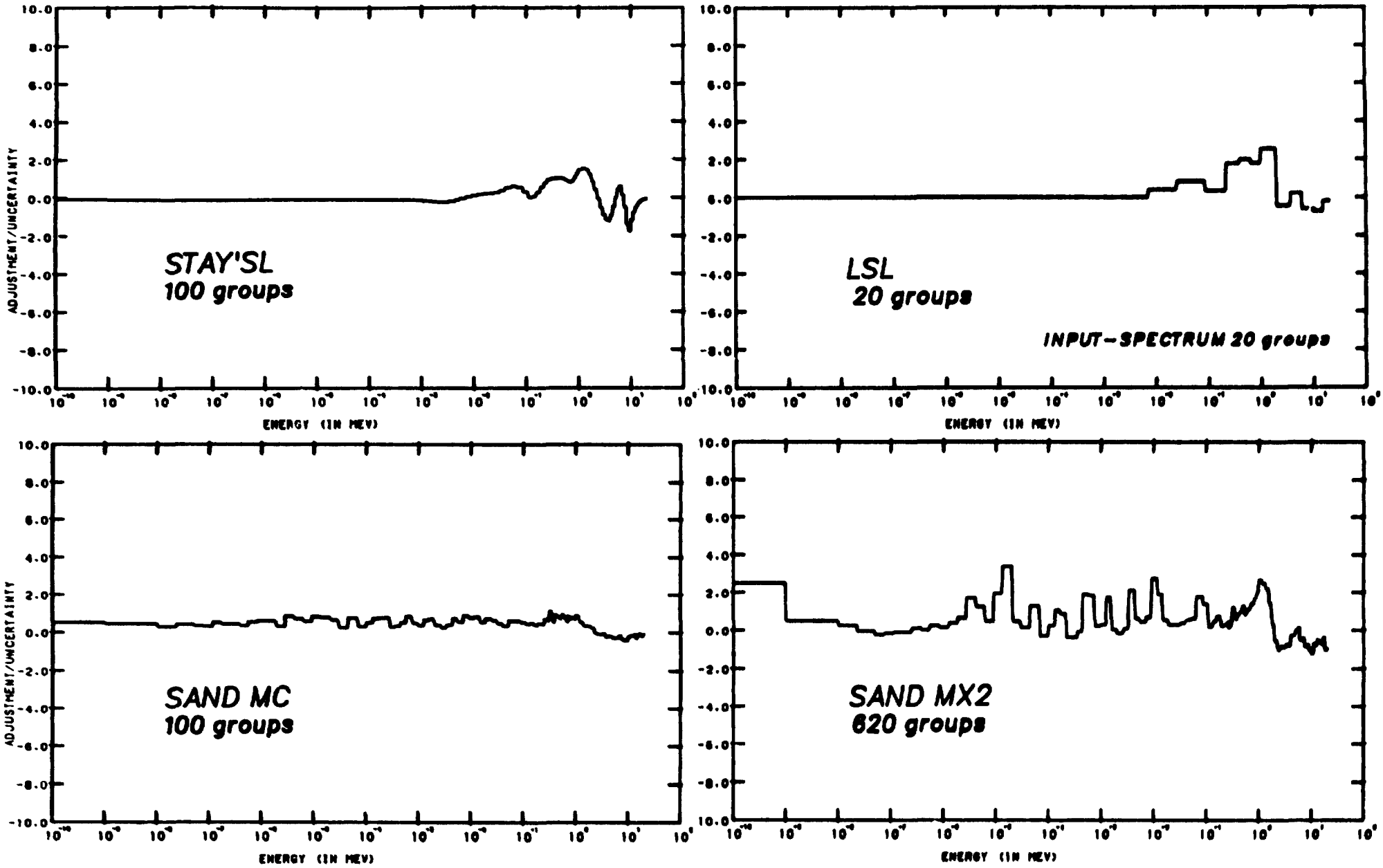

Fig.: 14 Significance of modifications. YAYOI

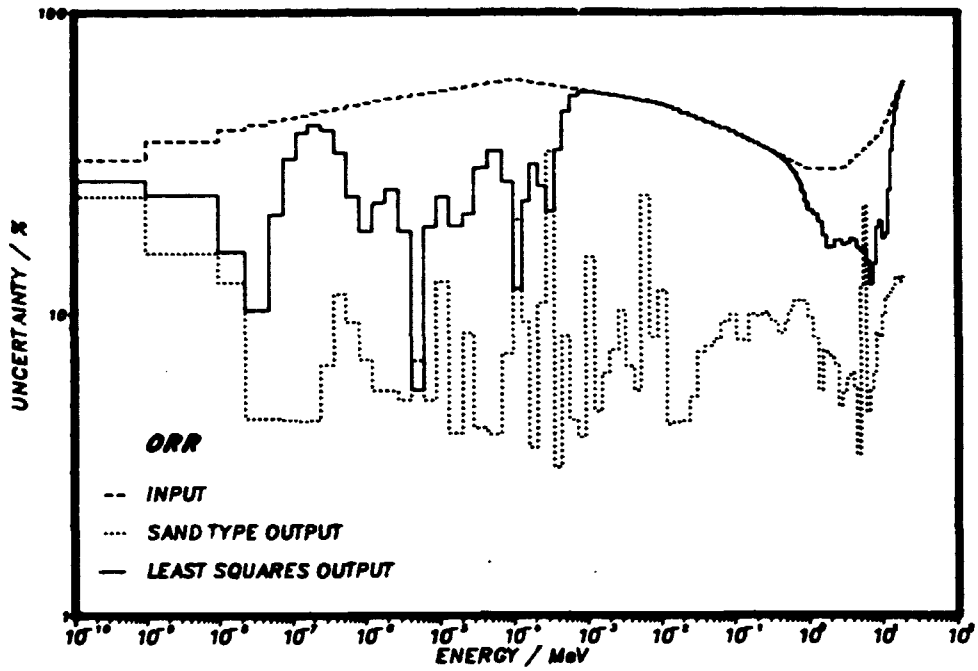

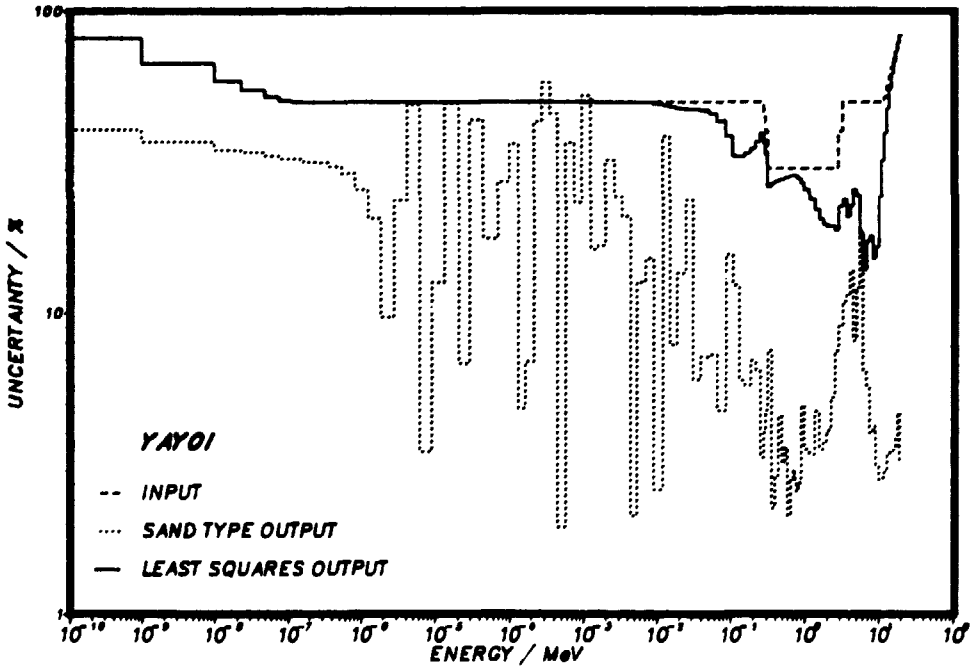

Fig.: 15 Uncertainties as a function of energy.

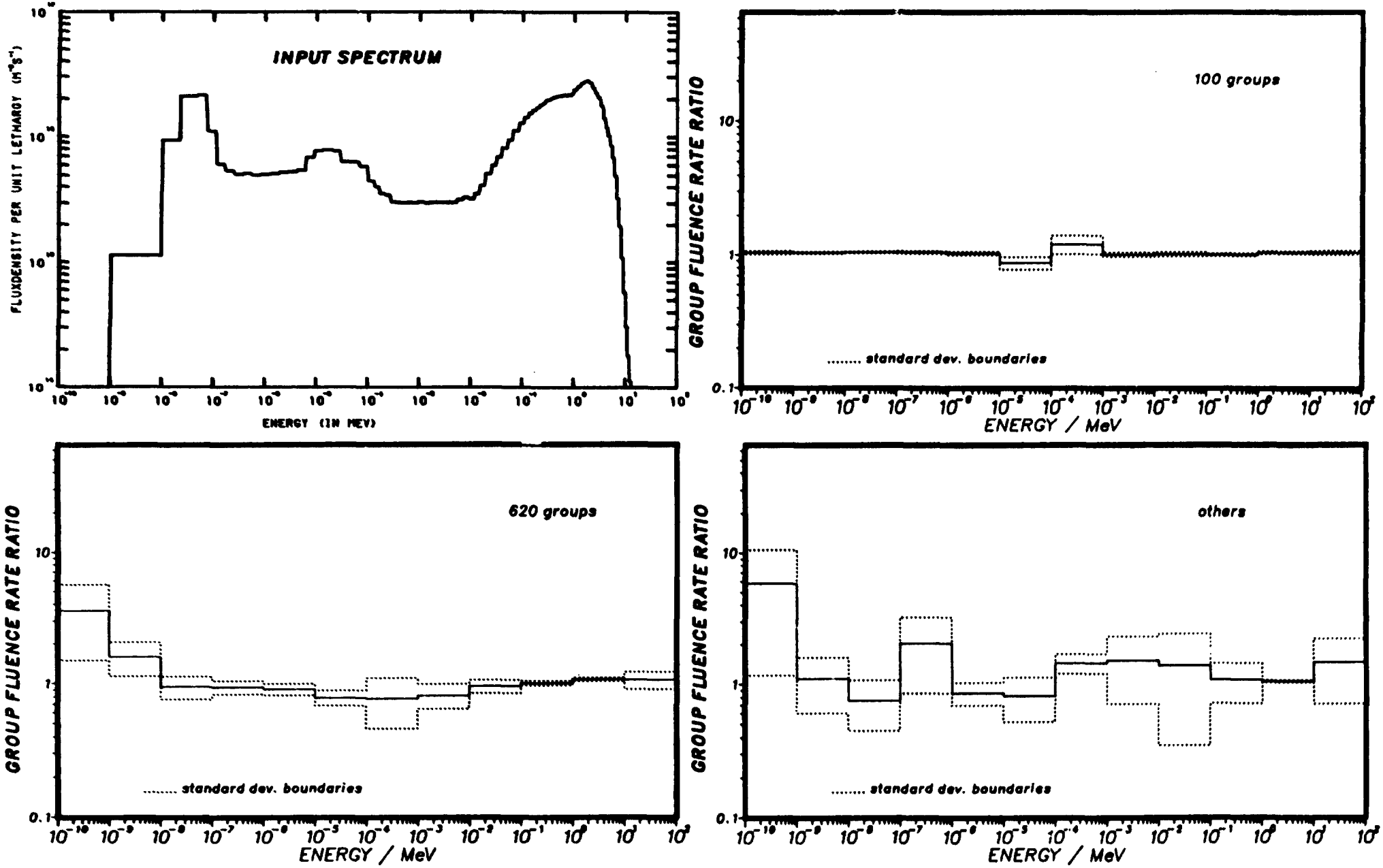

Fig.: 16 Ratios and standard deviations for decade groups for ORR.

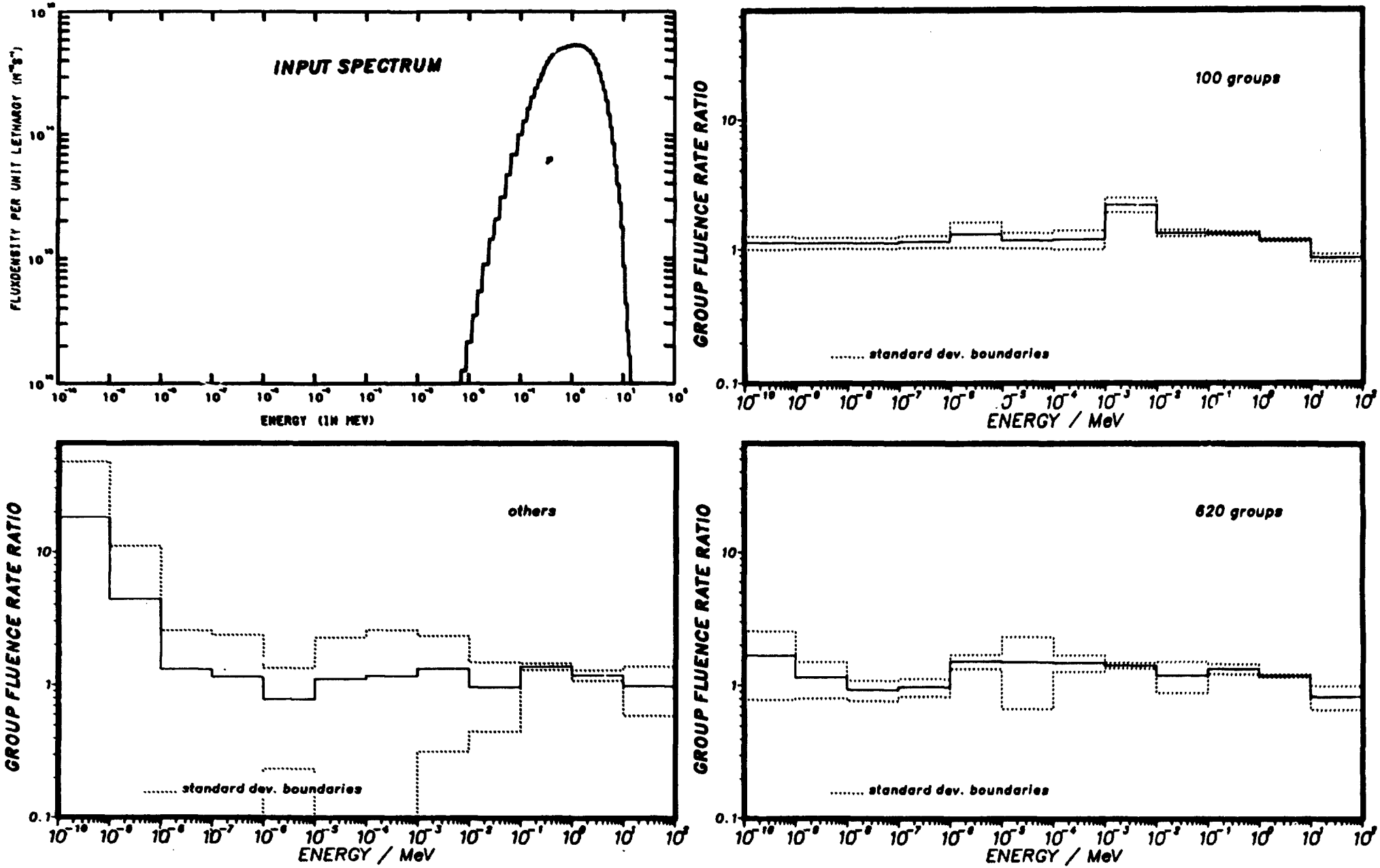

Fig.: 17 Ratios and standard deviations for decade groups for YAYOI.

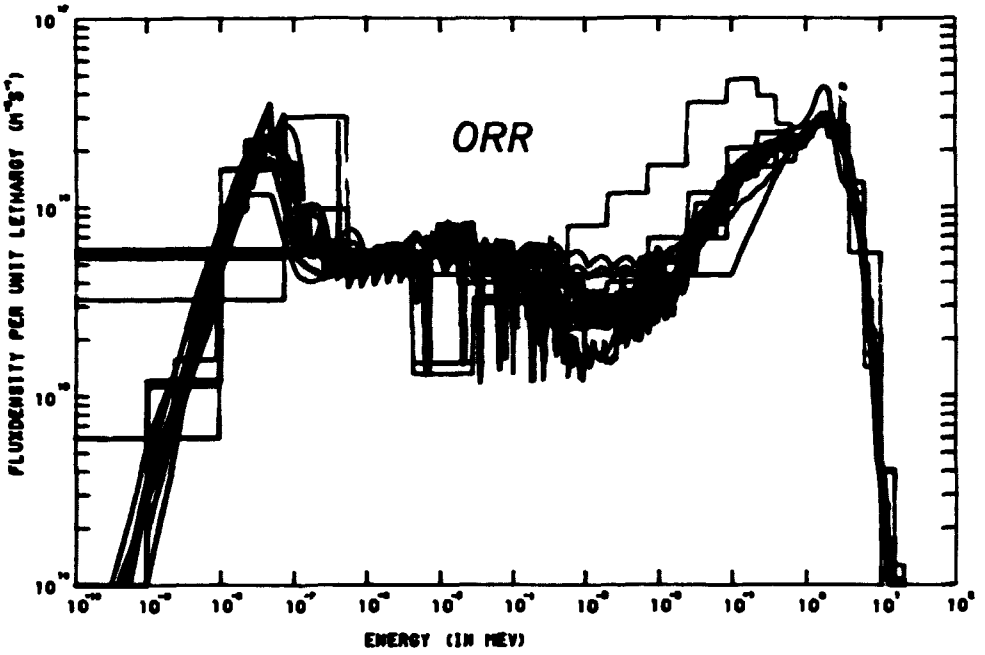

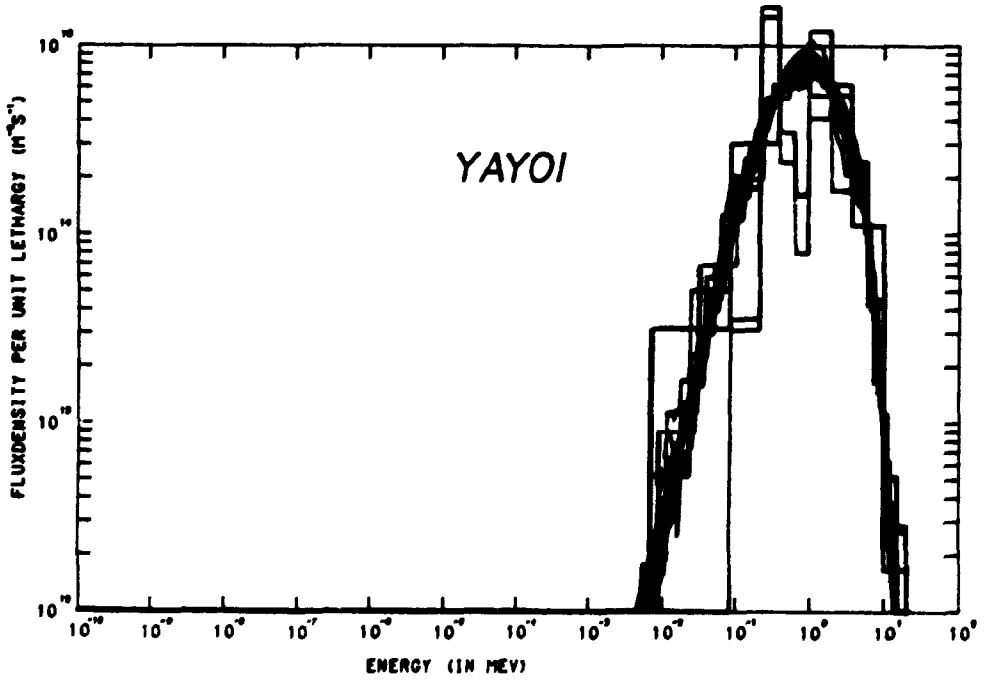

Fig.: 18 Comparison of all output spectra.

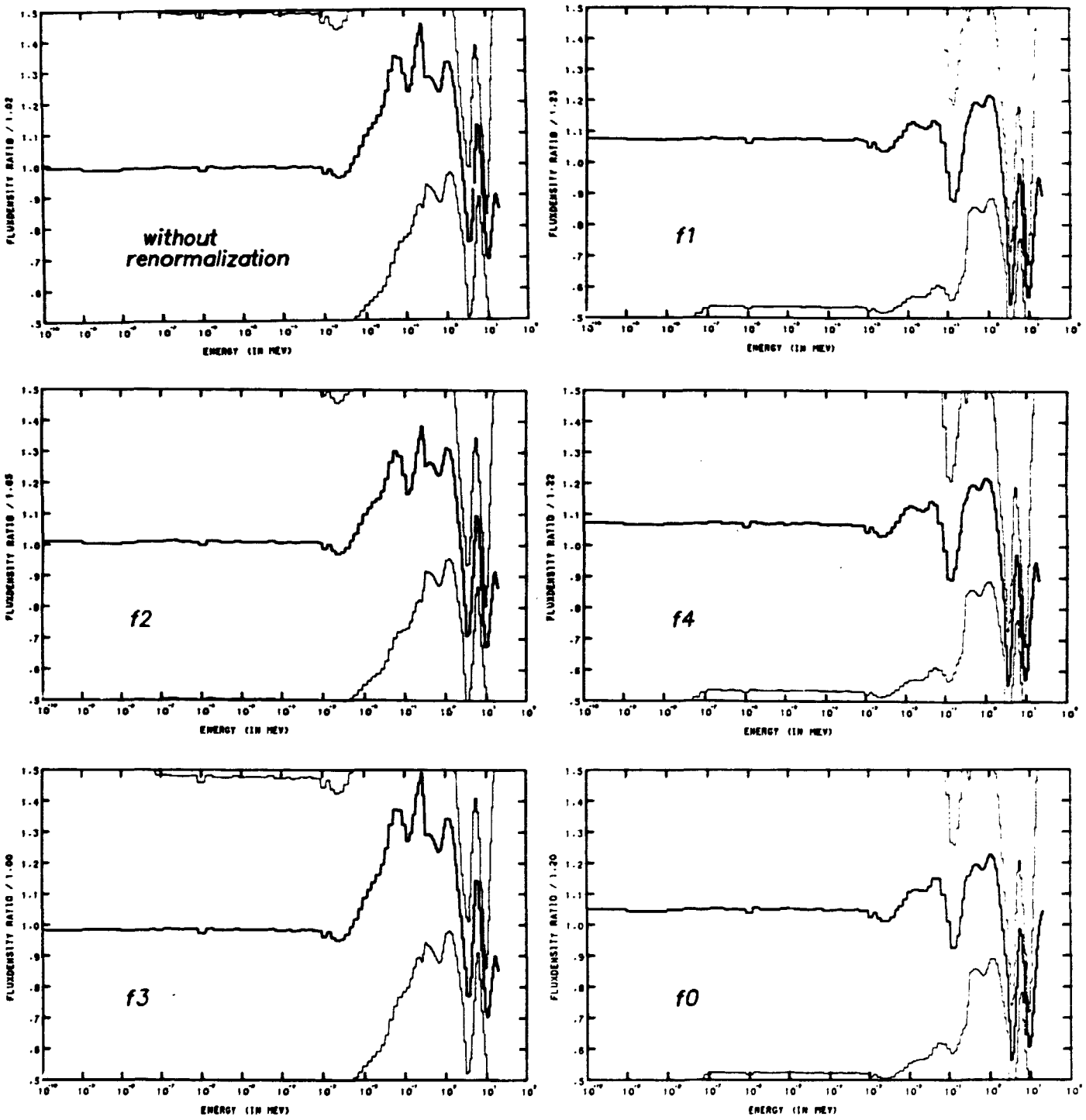

To facilitate the display a vertical scaling factor has been used.
For the expressions of the various normalization factors see appendix 1.

Fig.: 19 Influence of normalization on modification factor. Generalized least squares algorithm applied to YAYOI.

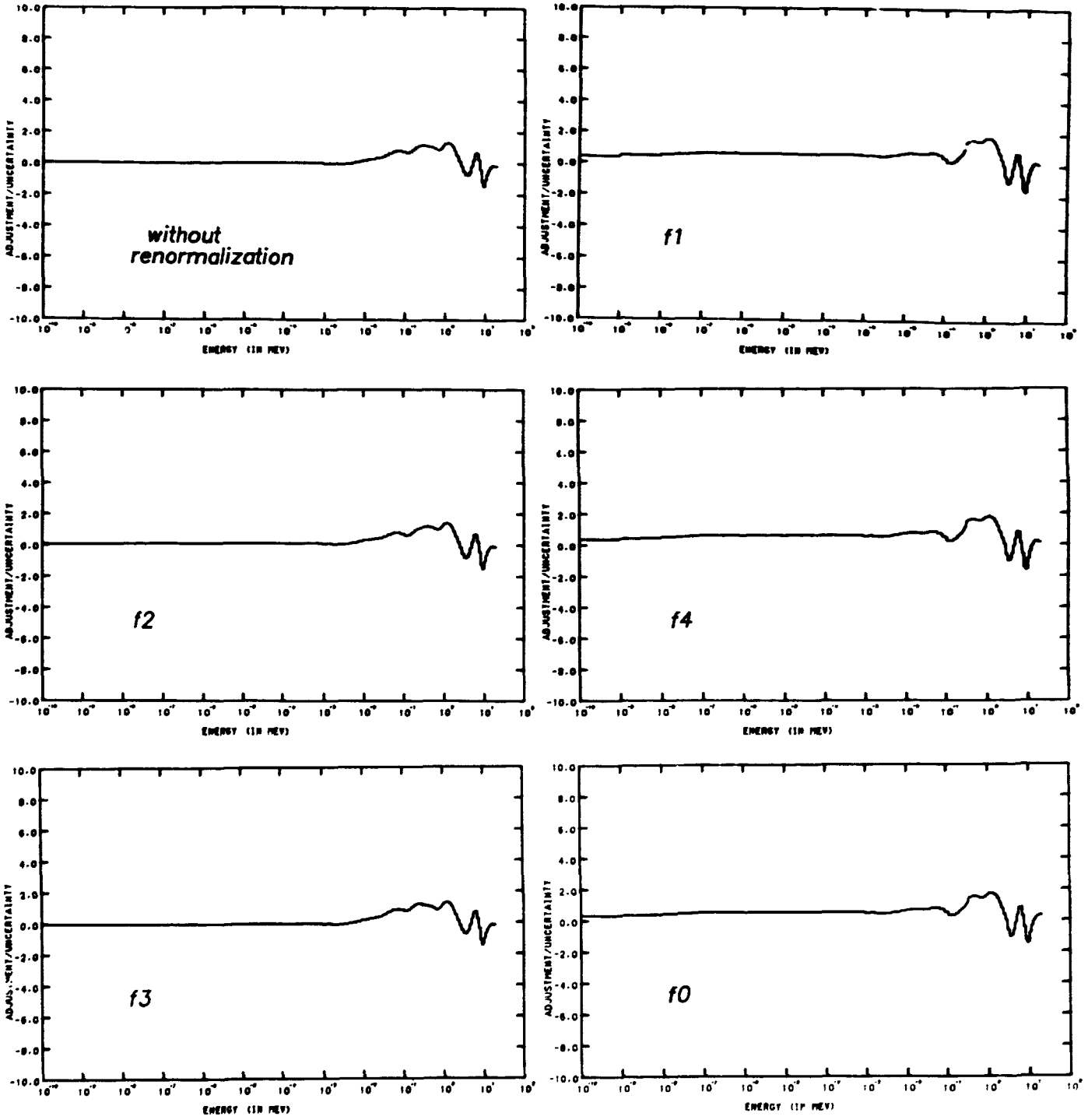

Fig.: 20 Influence of normalization on the ratio of adjustment and uncertainty.
Generalized least squares algorithm applied to YAYOI.

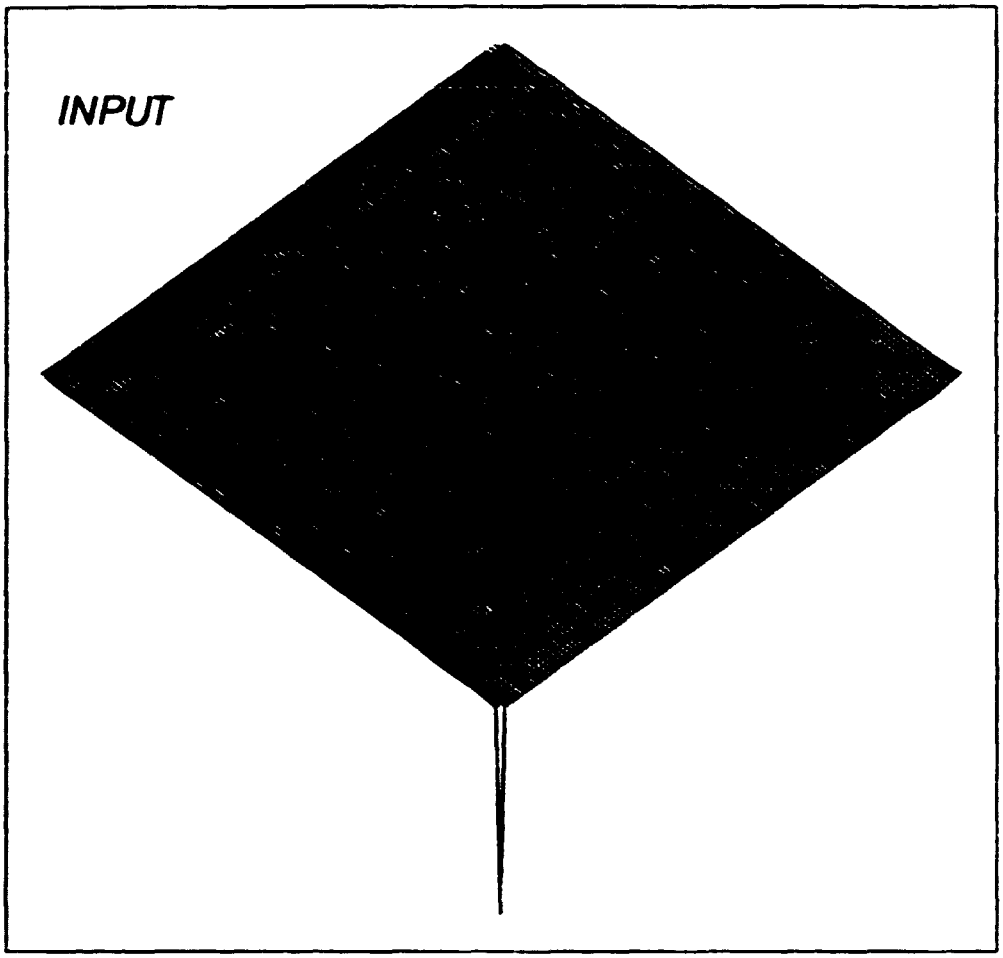

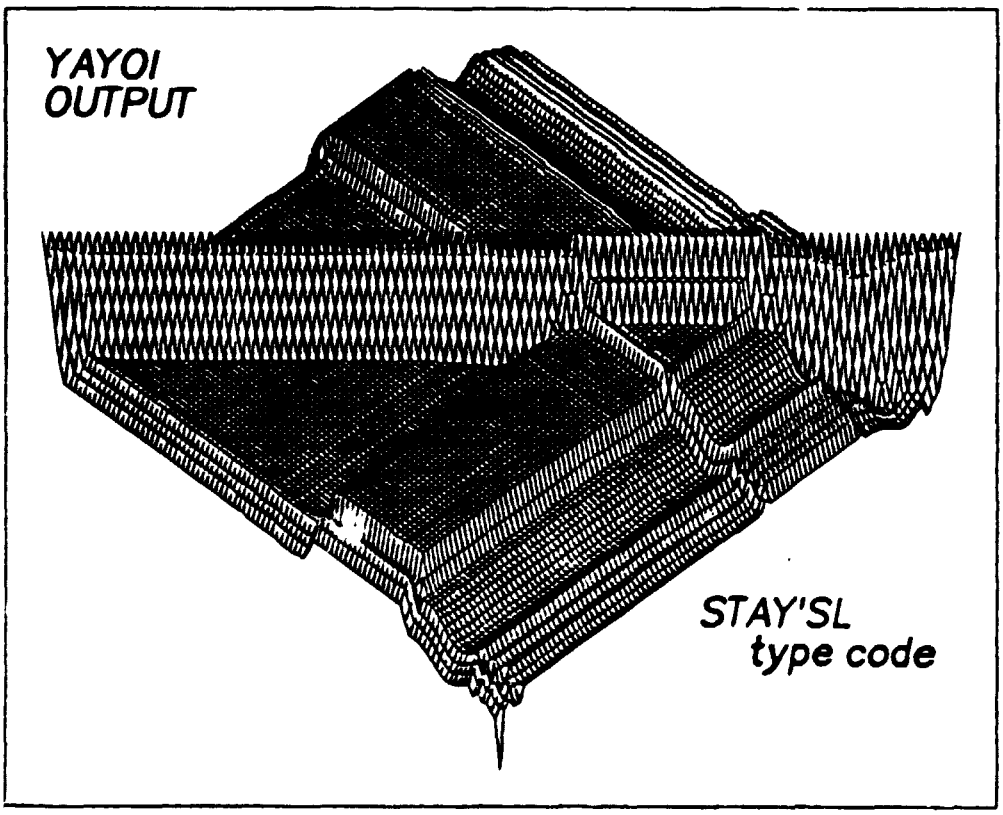

Fig.: 21 Fluence rate correlation matrices with strong correlation.

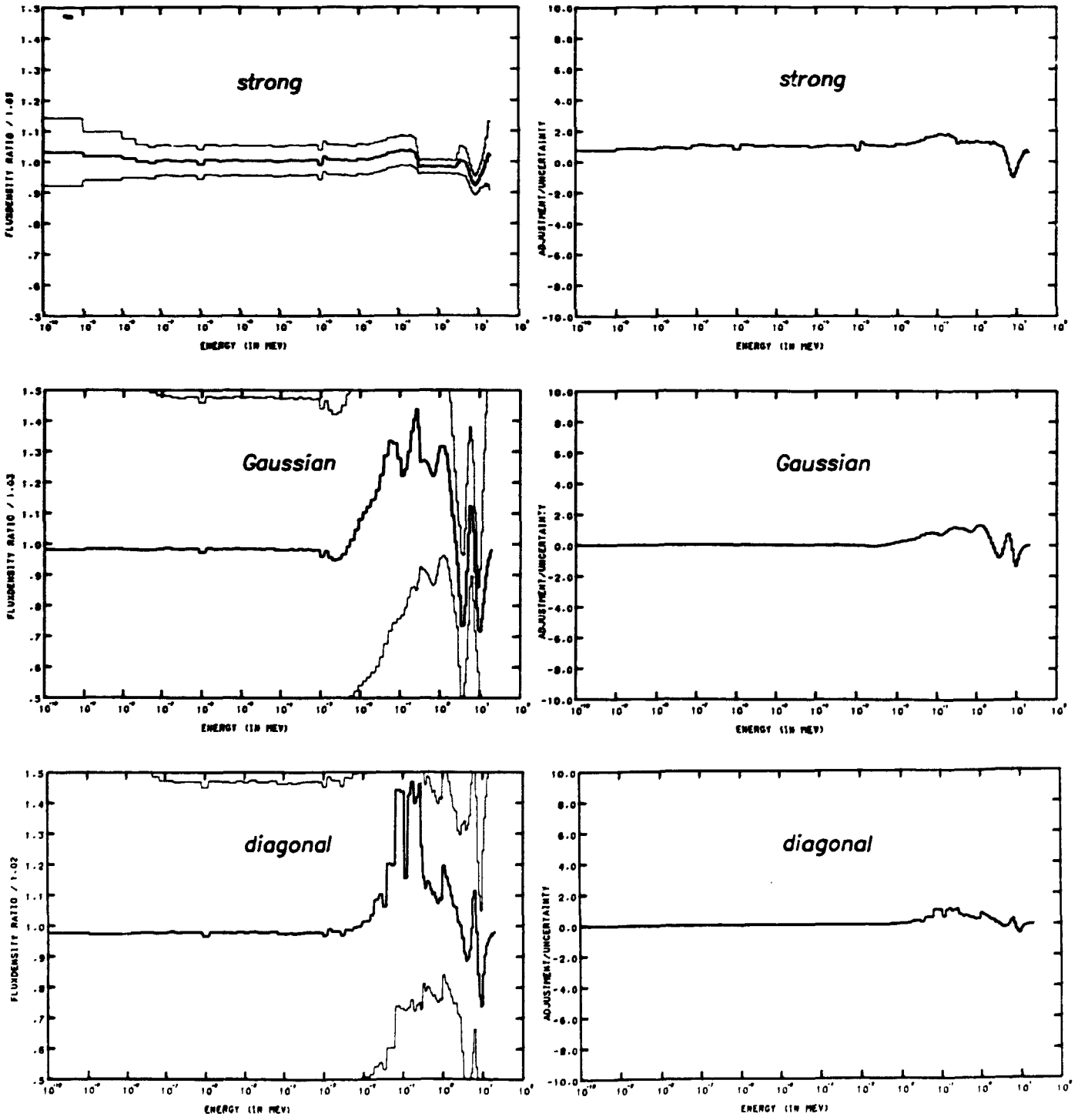

Fig.: 22 Influence of the input fluence rate correlation matrix on the neutron spectrum adjustment.

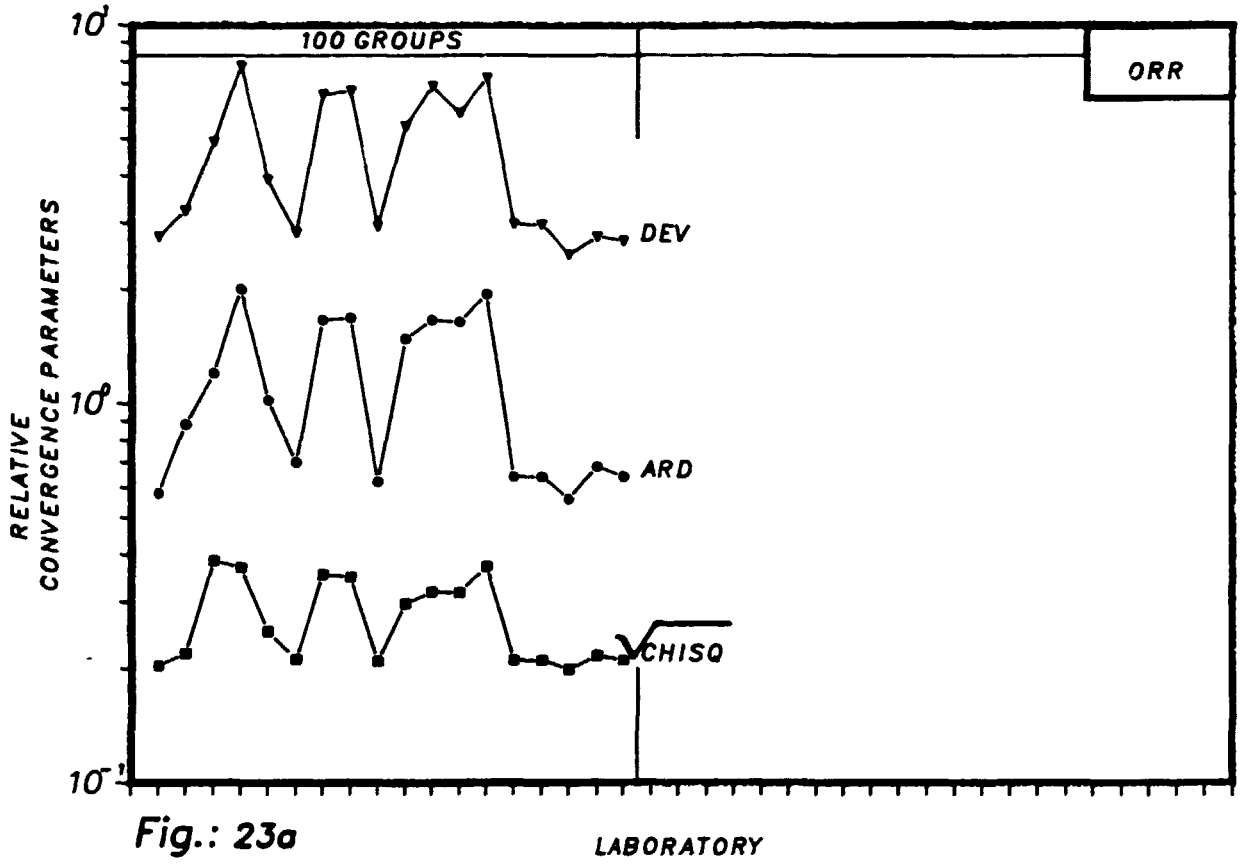

Fig.: 23a

Convergence parameters as calculated by the evaluators

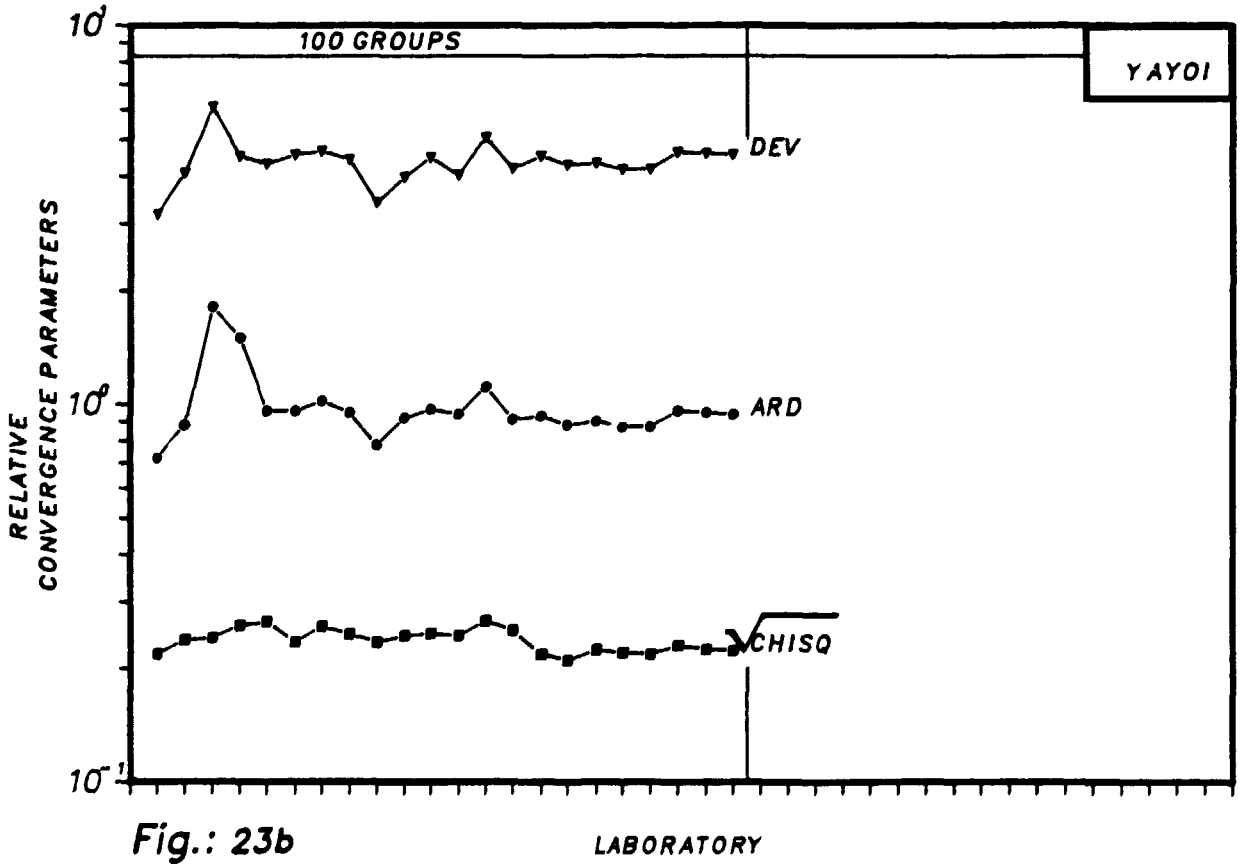

Fig.: 23b

Convergence parameters as calculated by the evaluators

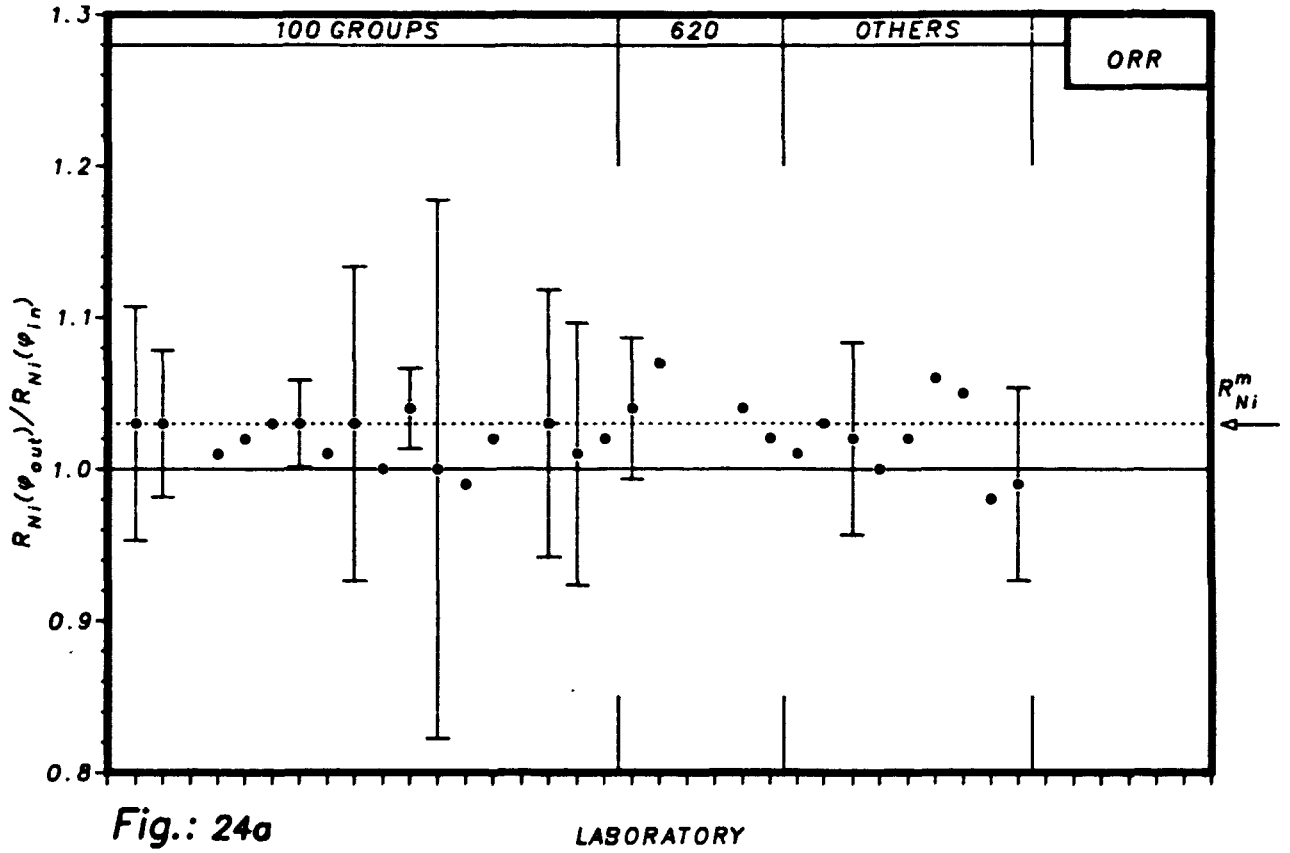

Fig.: 24a

Activation rate in nickel as given by the participants

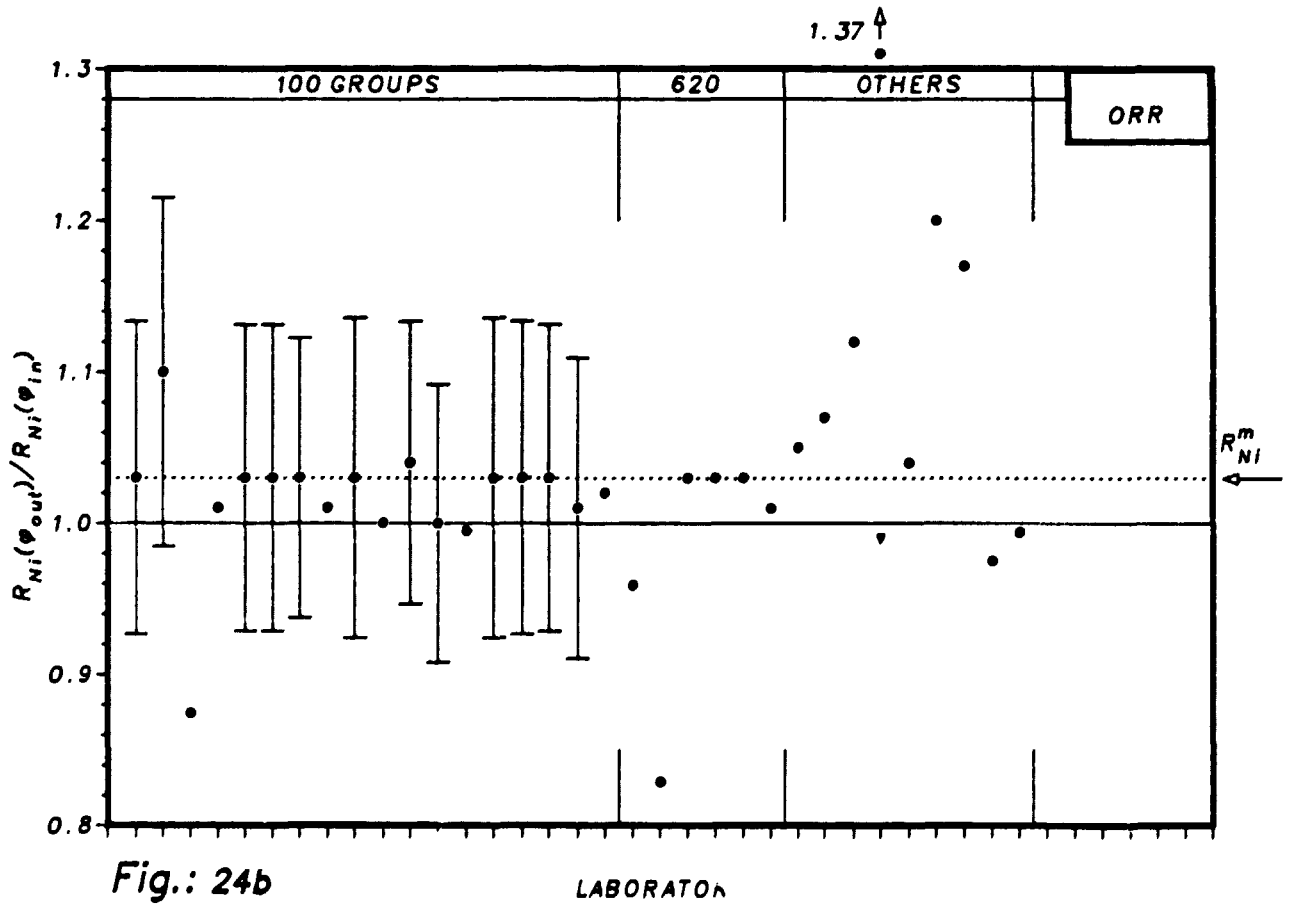

Fig.: 24b

Activation rate in nickel as calculated by the evaluators

• = *Calculated with 100 groups structure library*
▾ = *Calculated with groups structure used by participant*

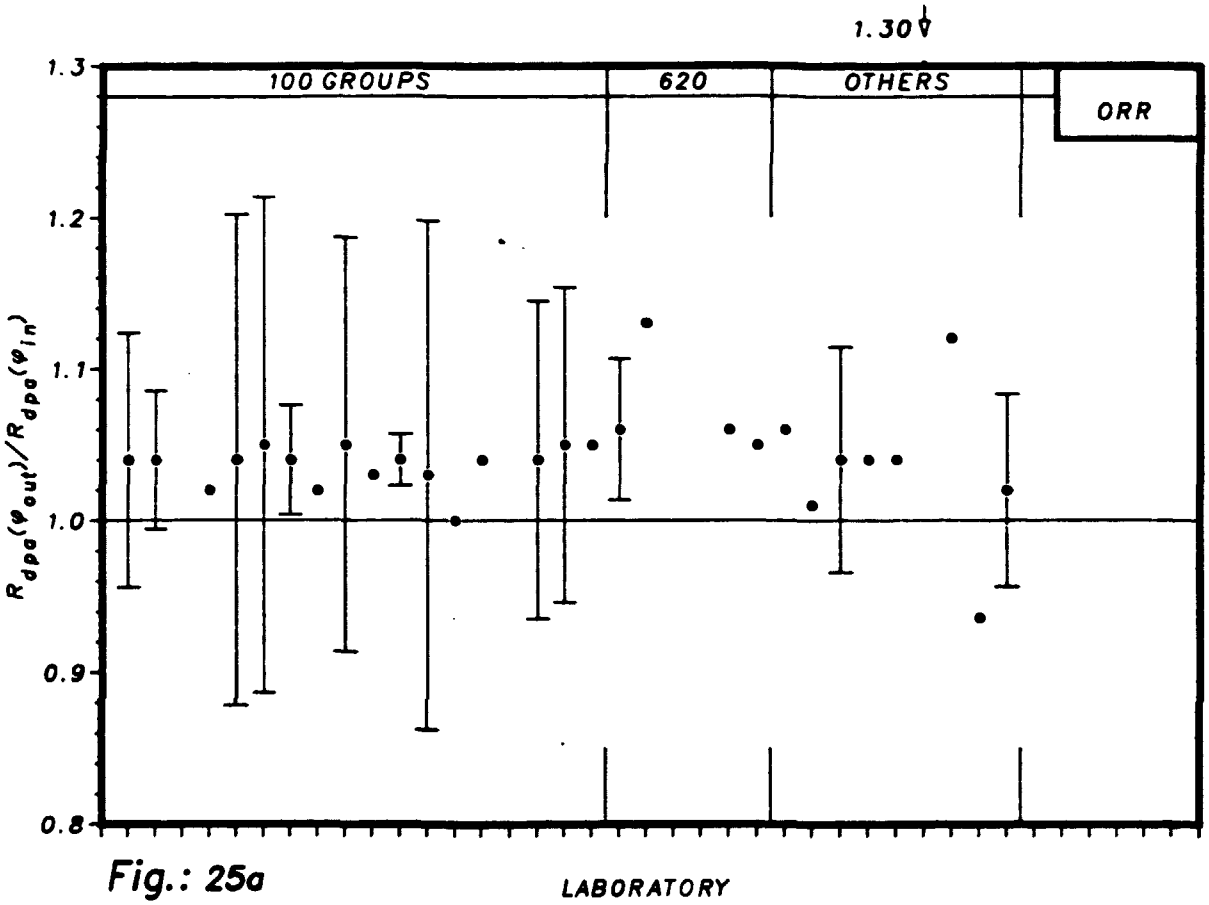

Fig.: 25a

Displacement rate in steel as given by the participants

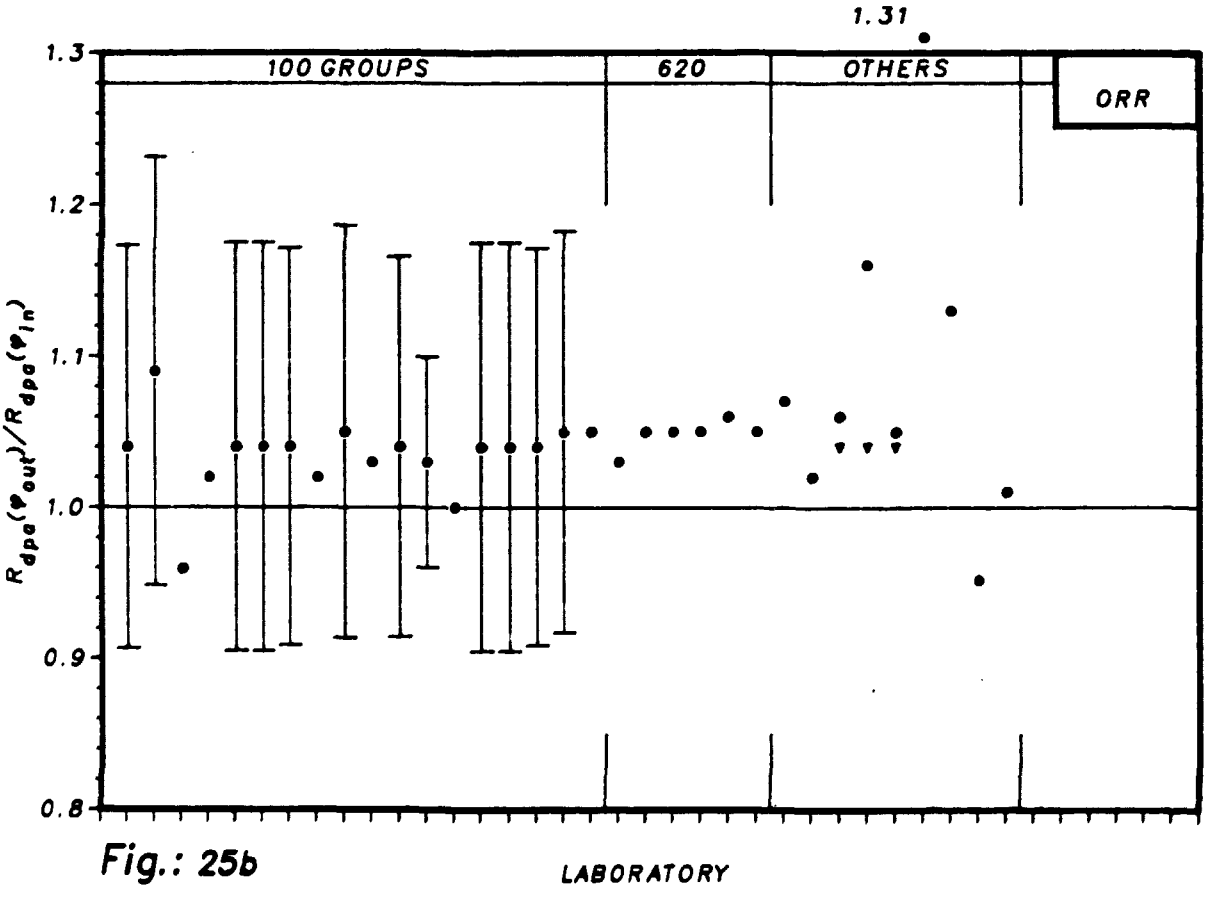

Fig.: 25b

Displacement rate in steel as calculated by the evaluators

• = *Calculated with 100 groups structure library*
▾ = *Calculated with groups structure used by participant*

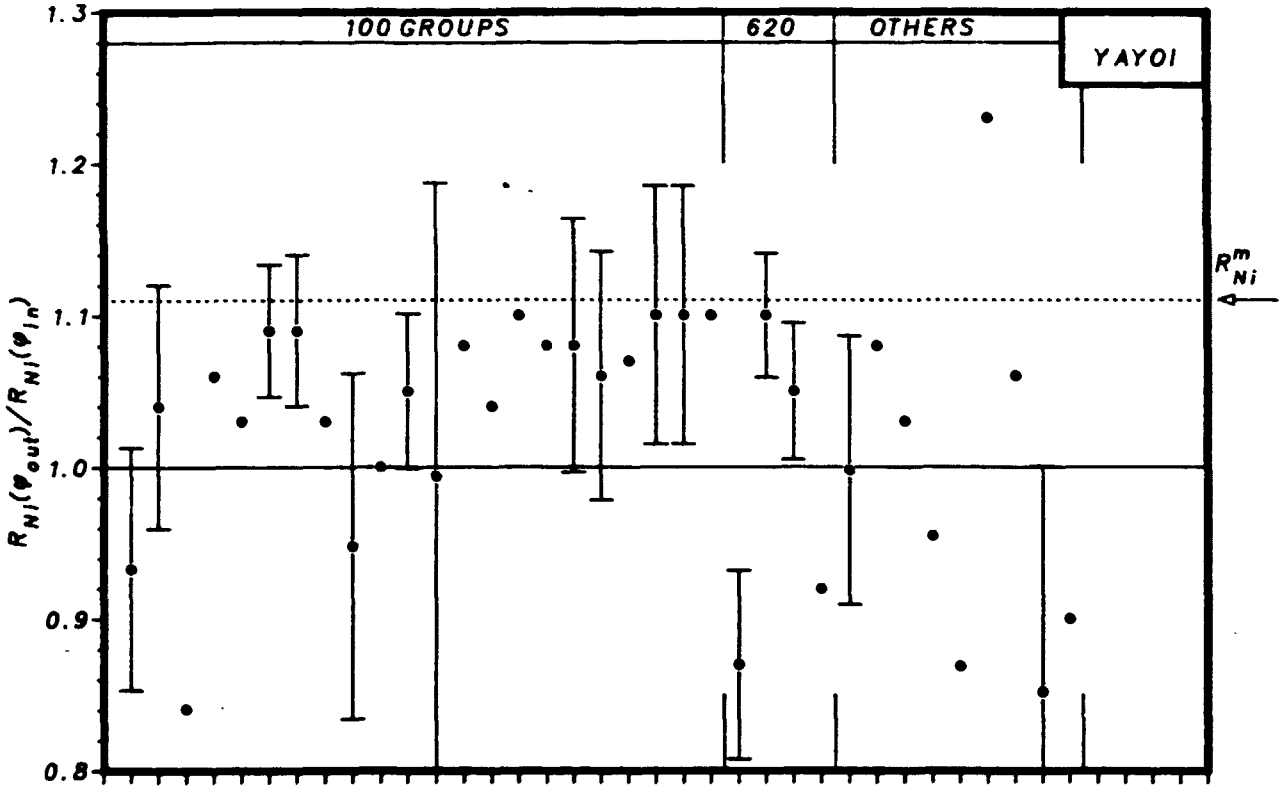

Fig.: 26a

Activation rate in nickel as given by the participants

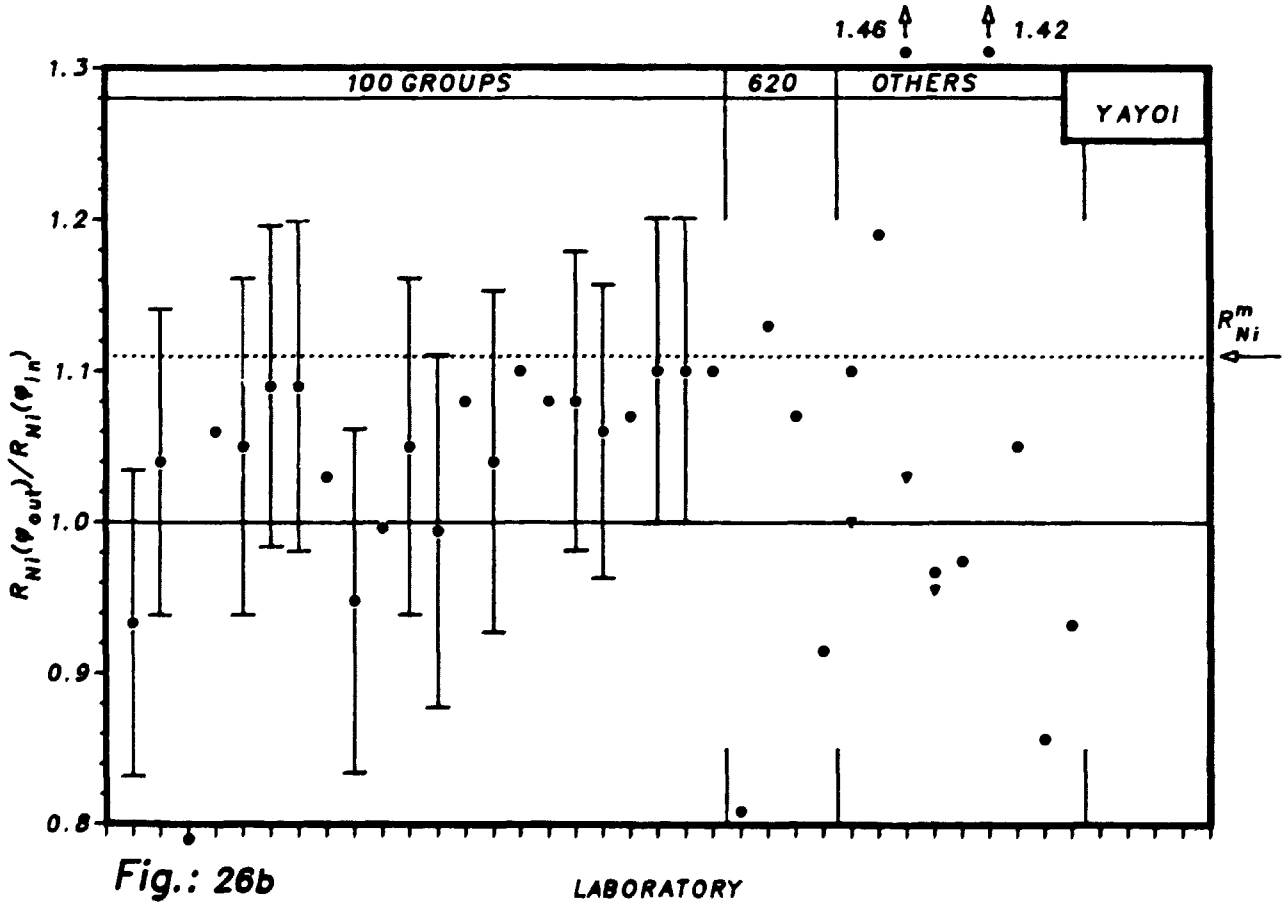

Fig.: 26b

Activation rate in nickel as calculated by the evaluators

• = Calculated with 100 groups structure library
▾ = Calculated with groups structure used by participant

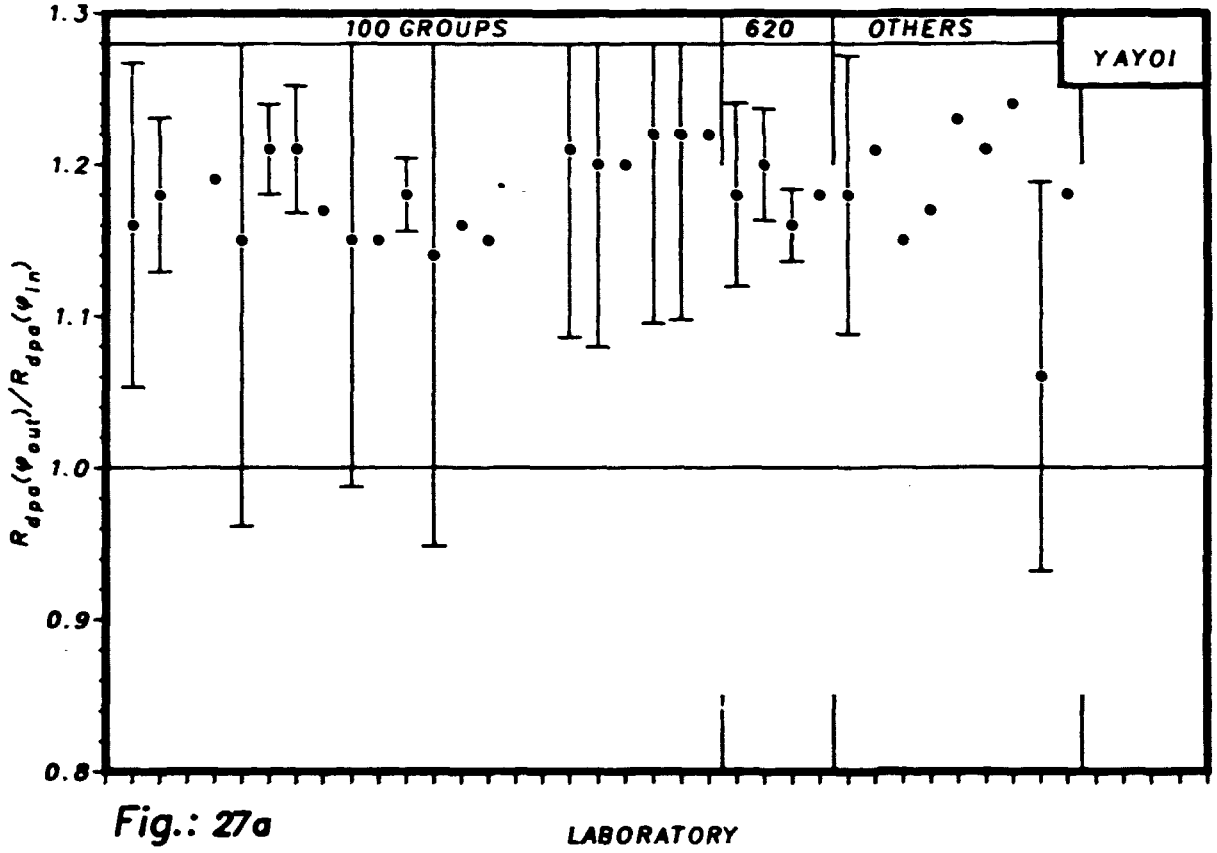

Fig.: 27a

Displacement rate in steel as given by the participants

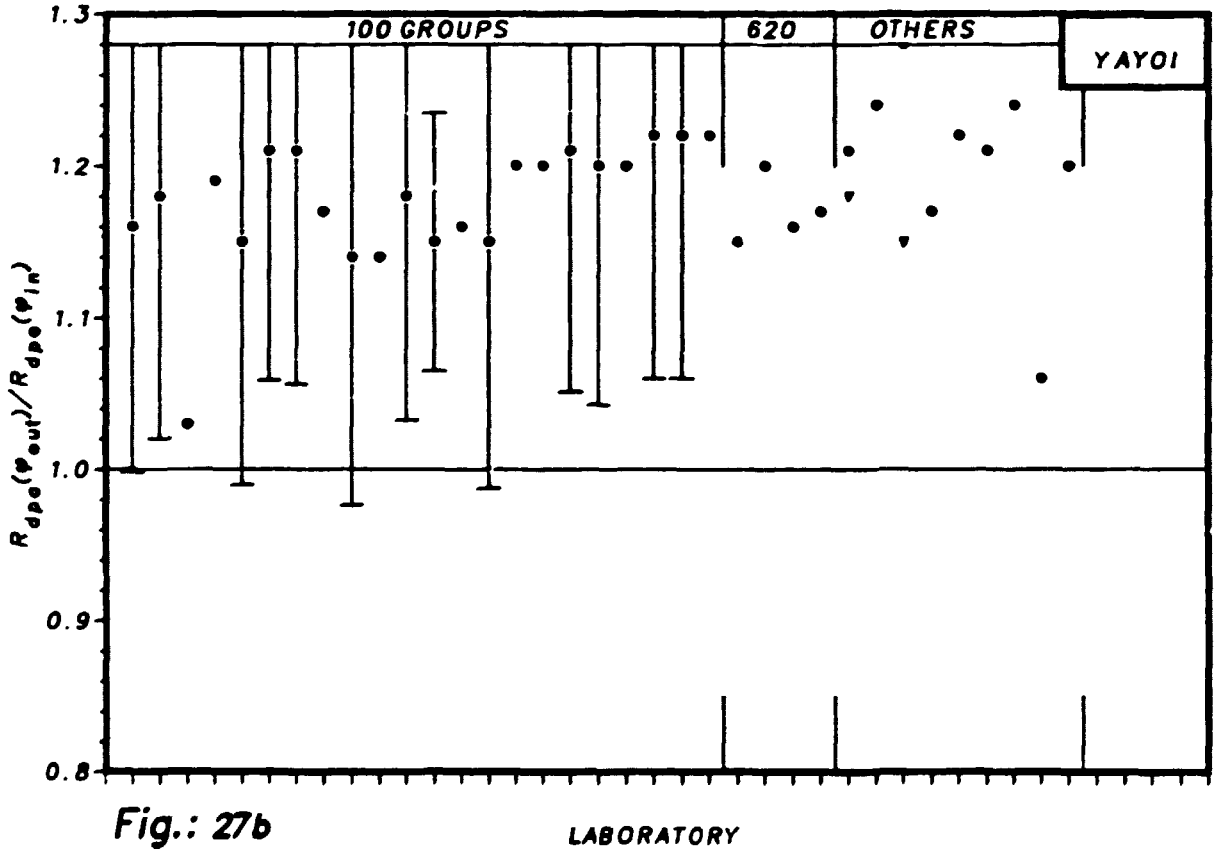

Fig.: 27b

Displacement rate in steel as calculated by the evaluators

• = Calculated with 100 groups structure library
▾ = Calculated with groups structure used by participant

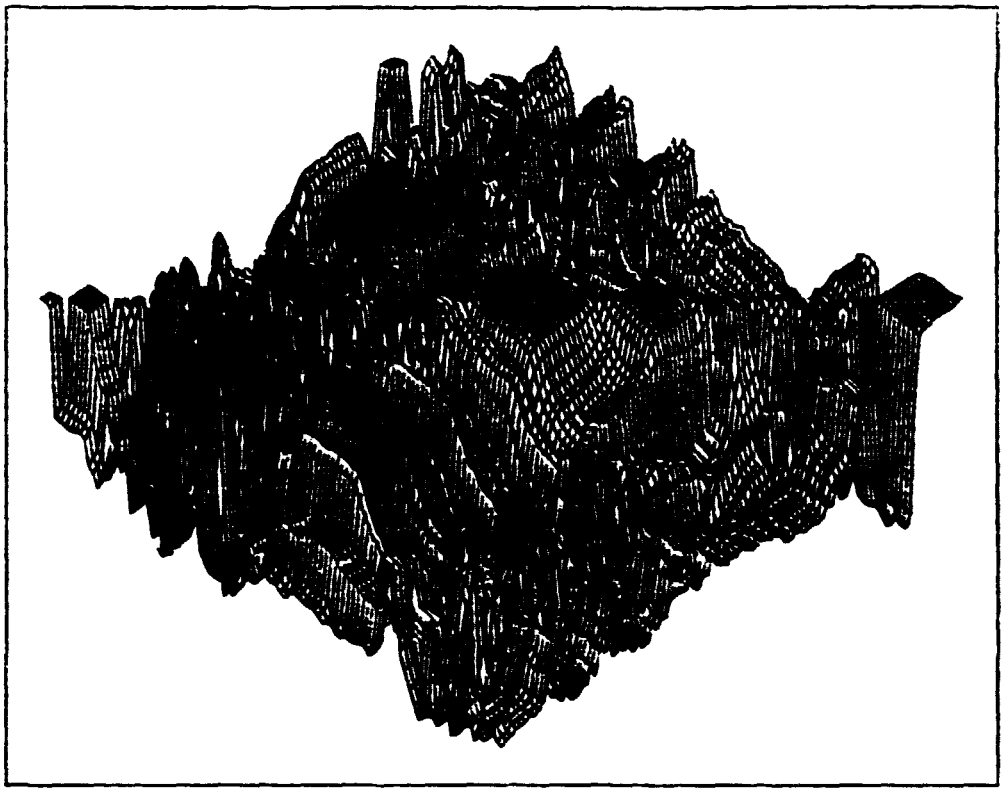

Fig.: 28 Output spectrum correlation matrix for ORR.
(stochastic model solution in 100 groups)

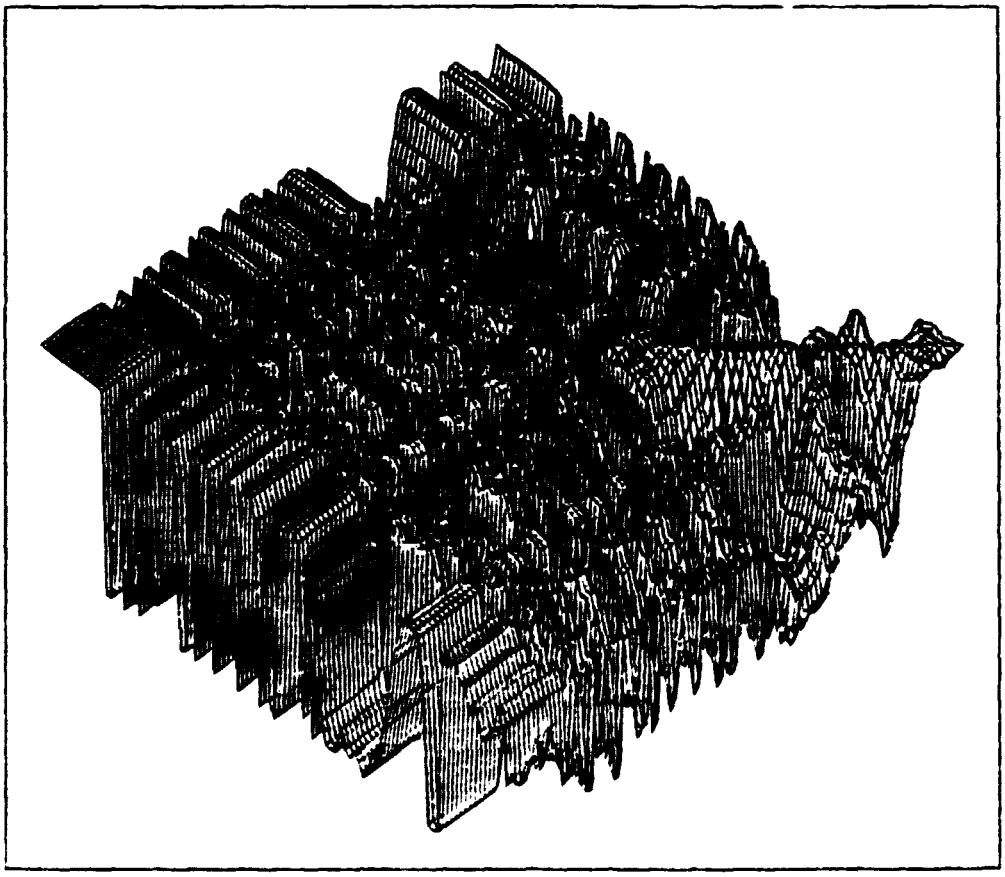

Fig.: 29 Output spectrum correlation matrix for YAYOI.
(stochastic model solution in 100 groups)

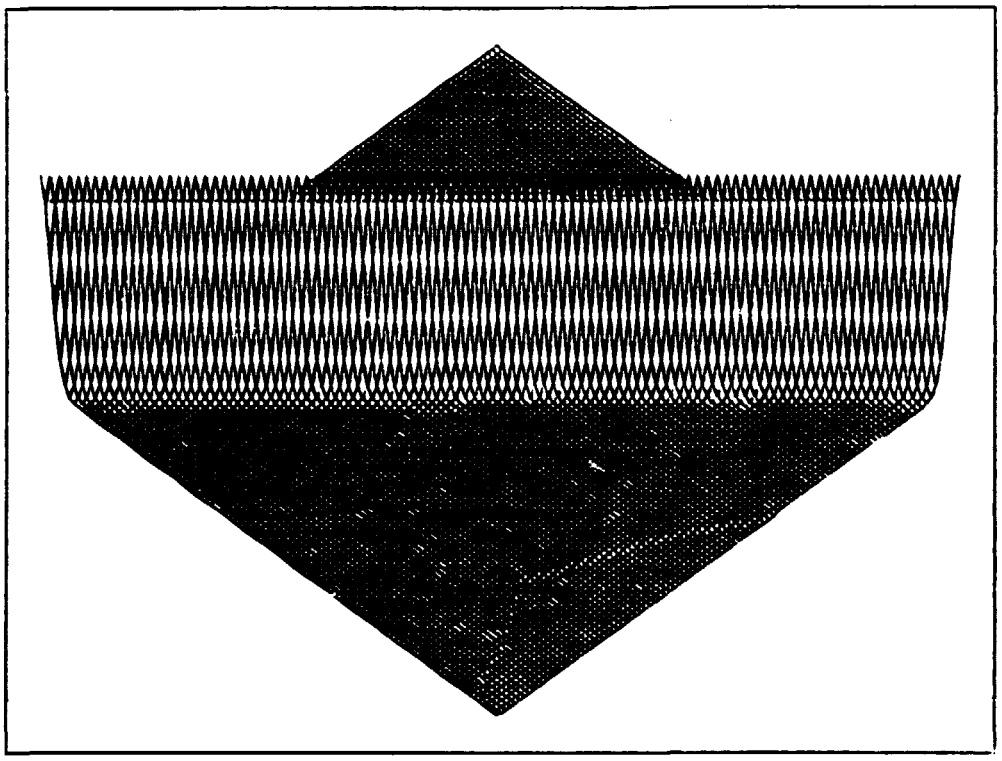

Fig.: 30 Input spectrum correlation matrix for ORR. (in 100 groups)

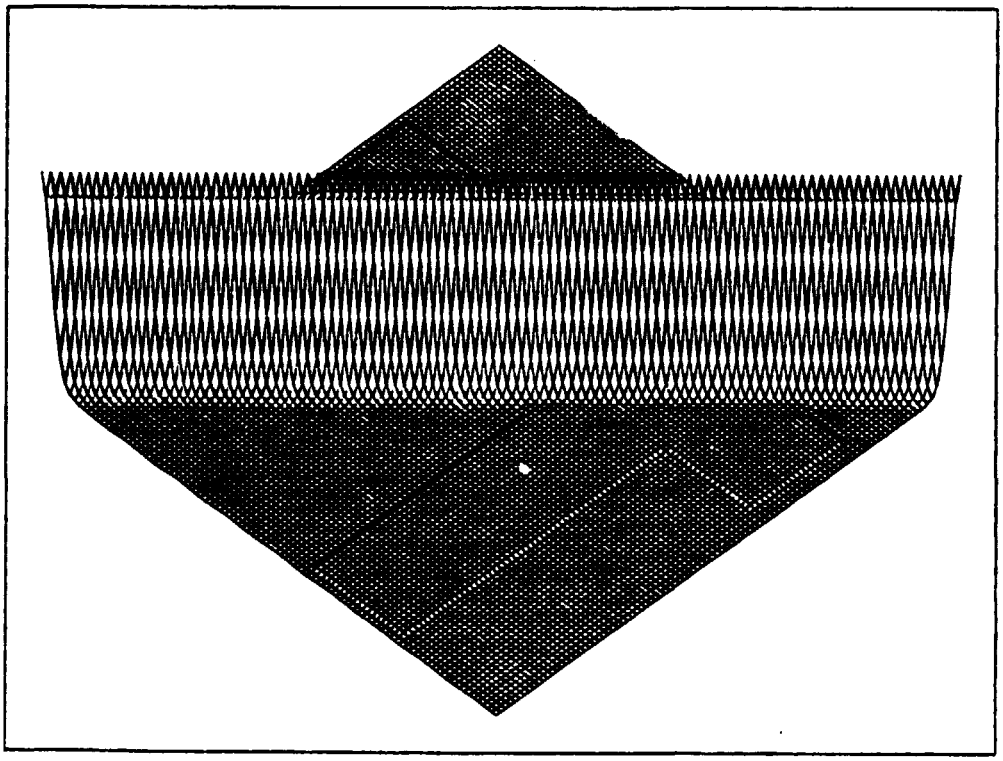

Fig.: 31 Input spectrum correlation matrix for YAYOI. (in 100 groups)

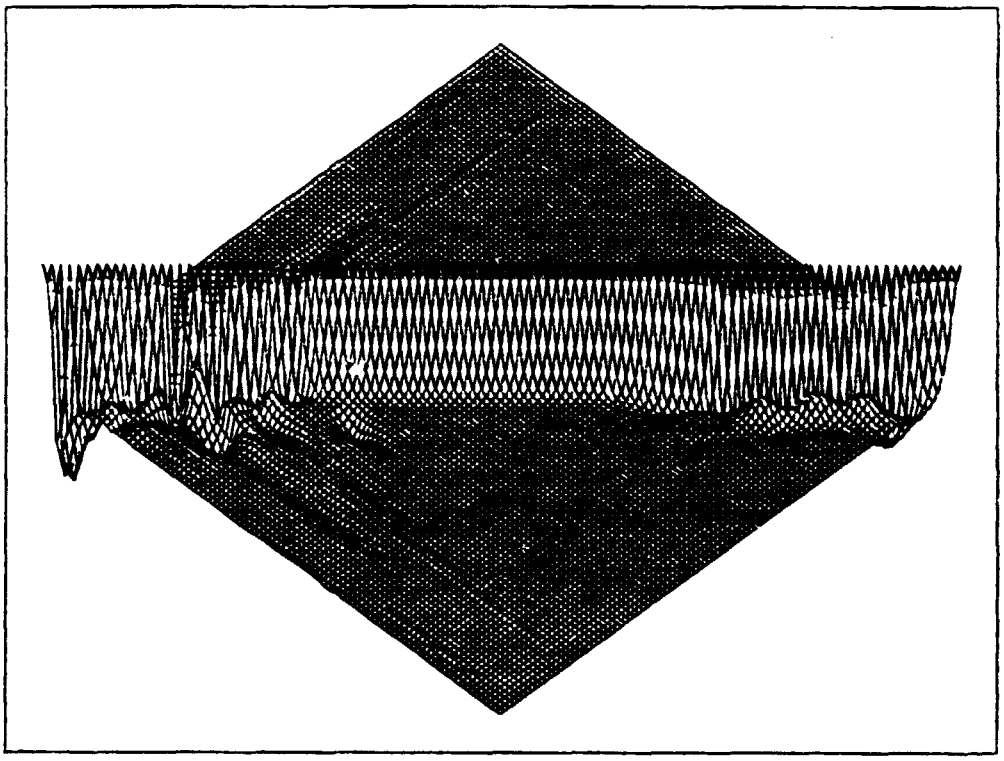

Fig.: 32 Output spectrum correlation matrix for ORR. (deterministic model solution in 100 groups)

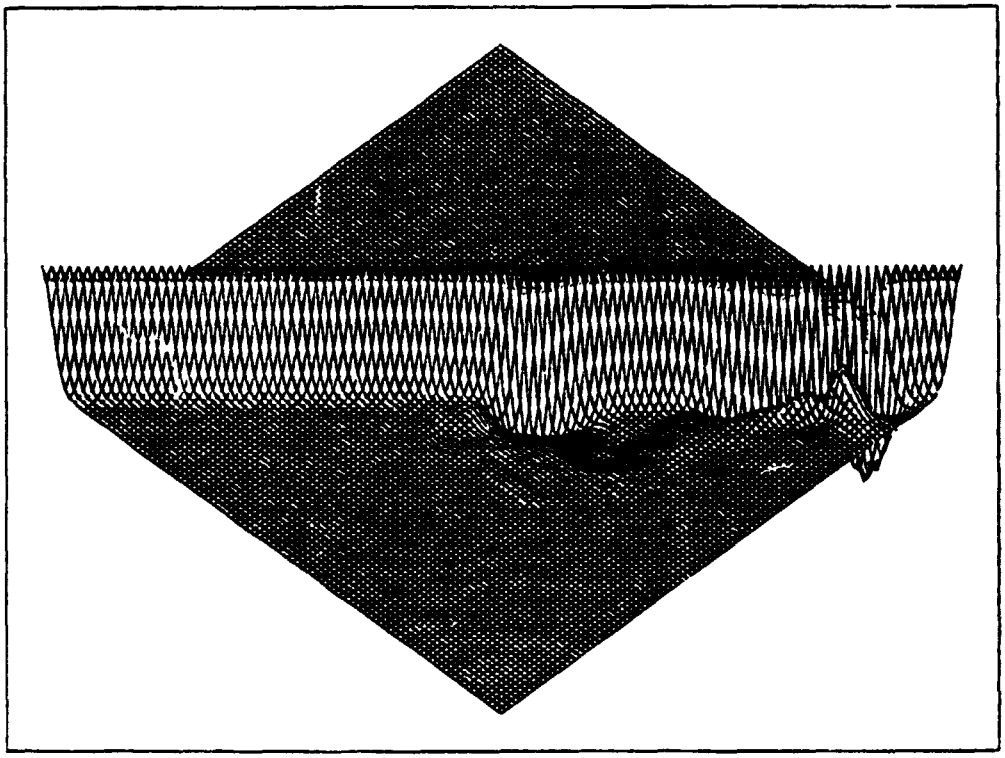

Fig.: 33 Output spectrum correlation matrix for YAYOI. (deterministic model solution in 100 groups)

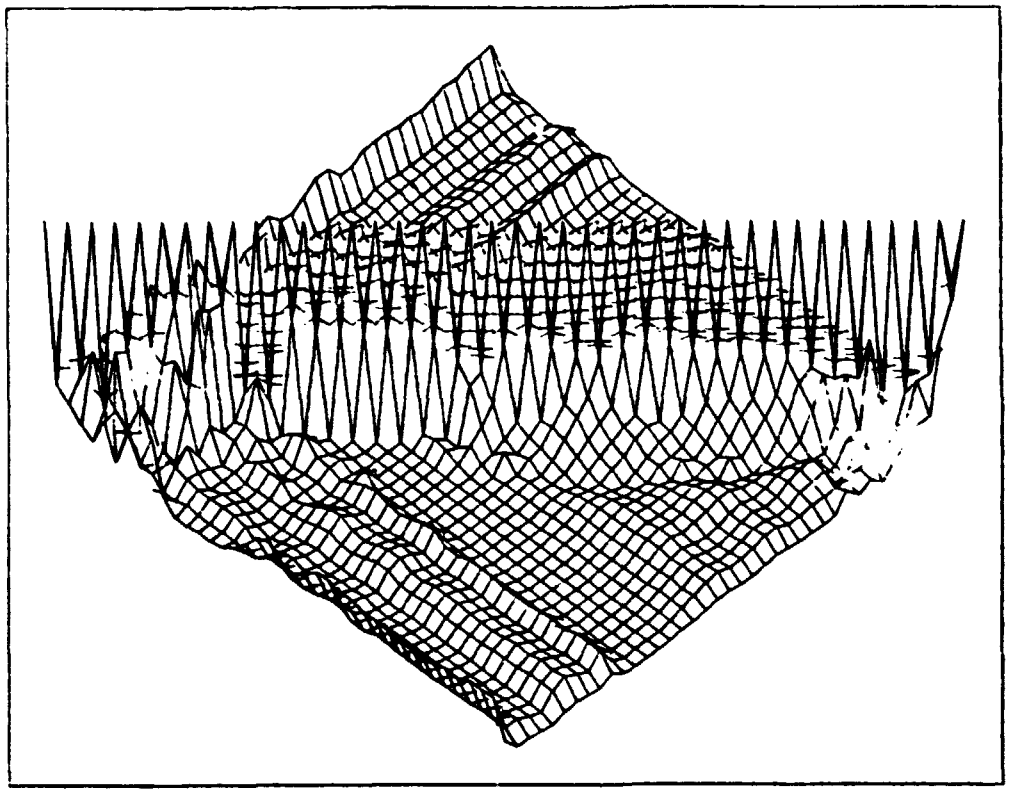

Fig.: 34 Output spectrum correlation matrix for ORR. (deterministic model solution in 40 groups)

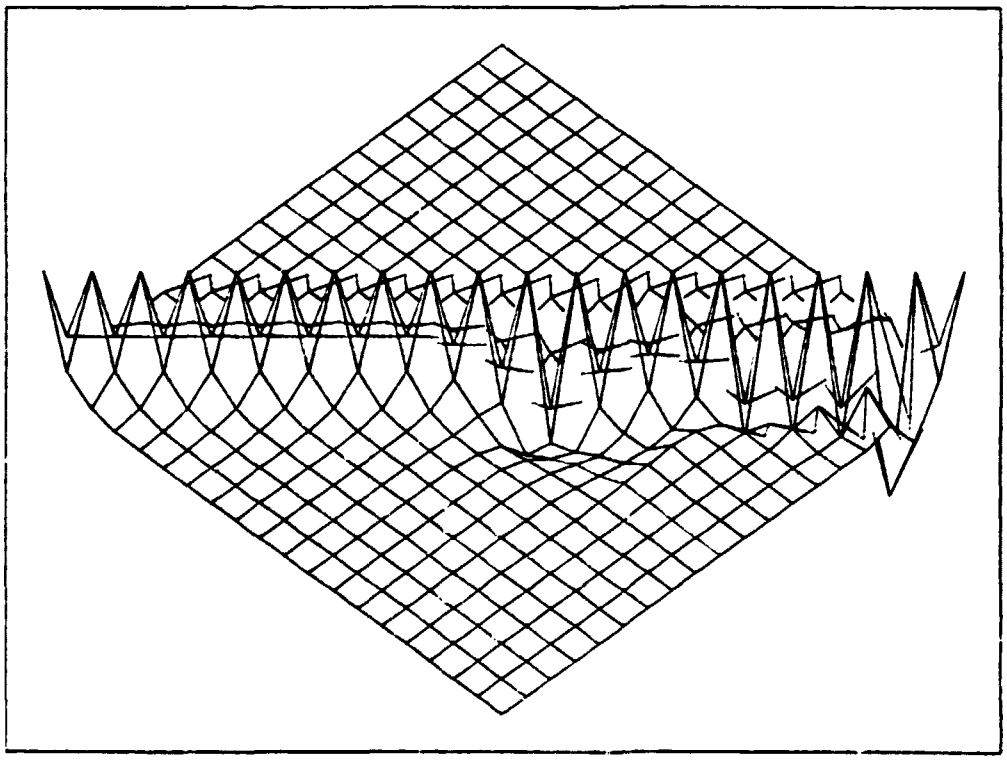

Fig.: 35 Output spectrum correlation matrix for YAYOI. (deterministic model solution in 20 groups)

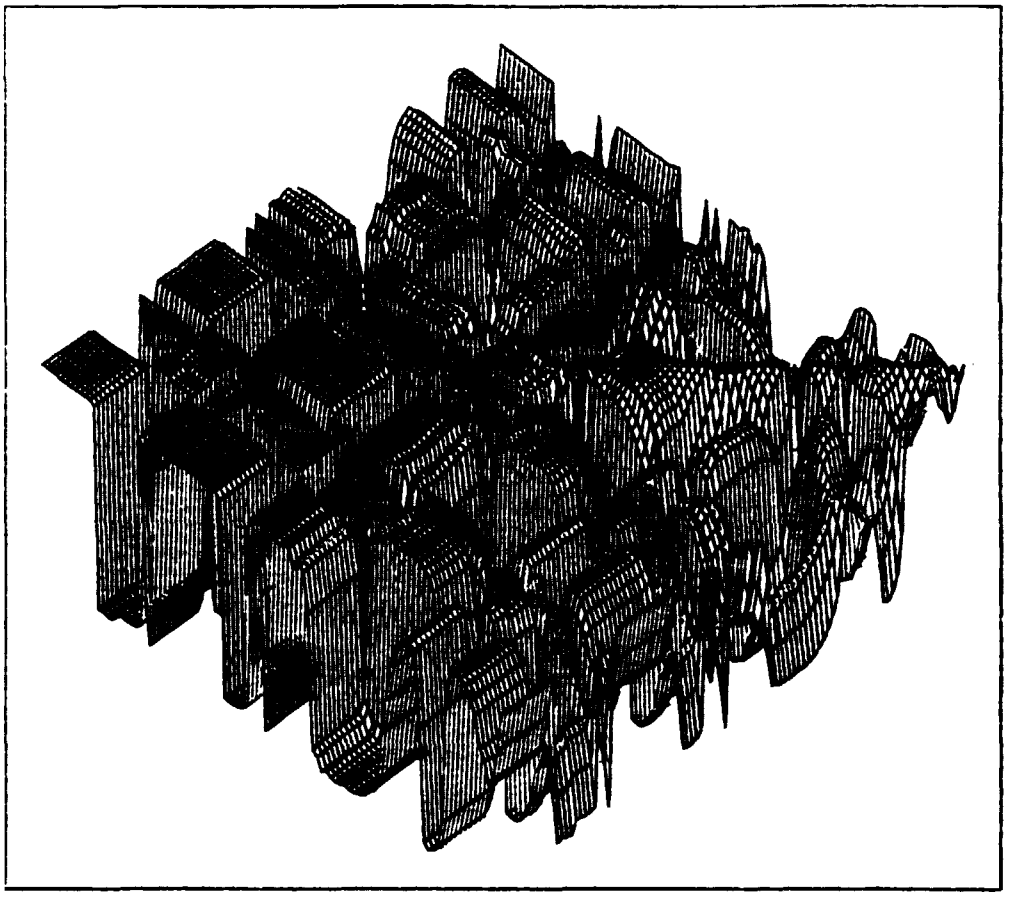

Fig.: 36 Output spectrum correlation matrix for YAYOI.
(stochastic model solution in 100 groups with smoothing)

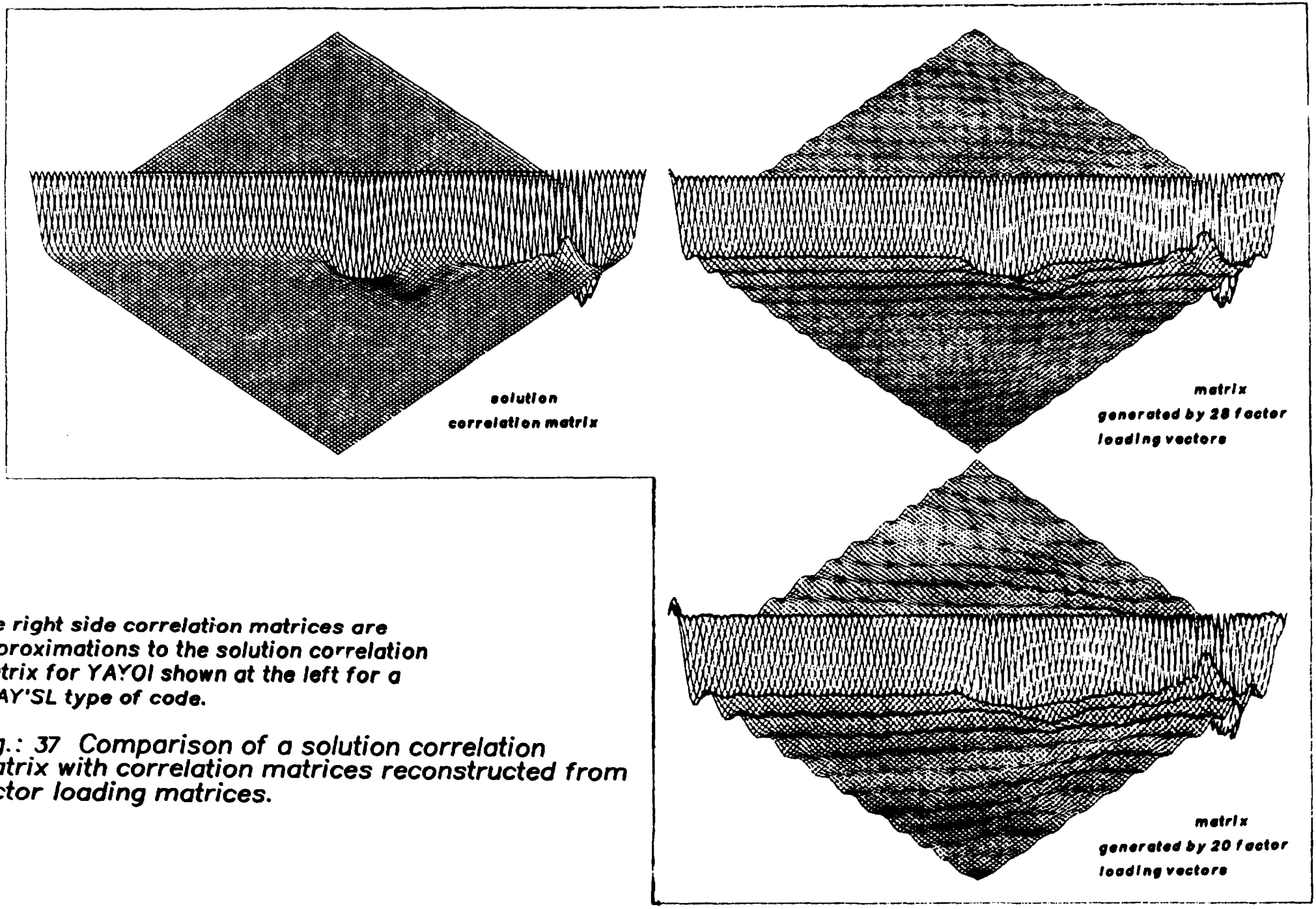

he right side correlation matrices are pproximations to the solution correlation natrix for YAYOI shown at the left for a TAY'SL type of code.

ig.: 37 Comparison of a solution correlation natrix with correlation matrices reconstructed from actor loading matrices.

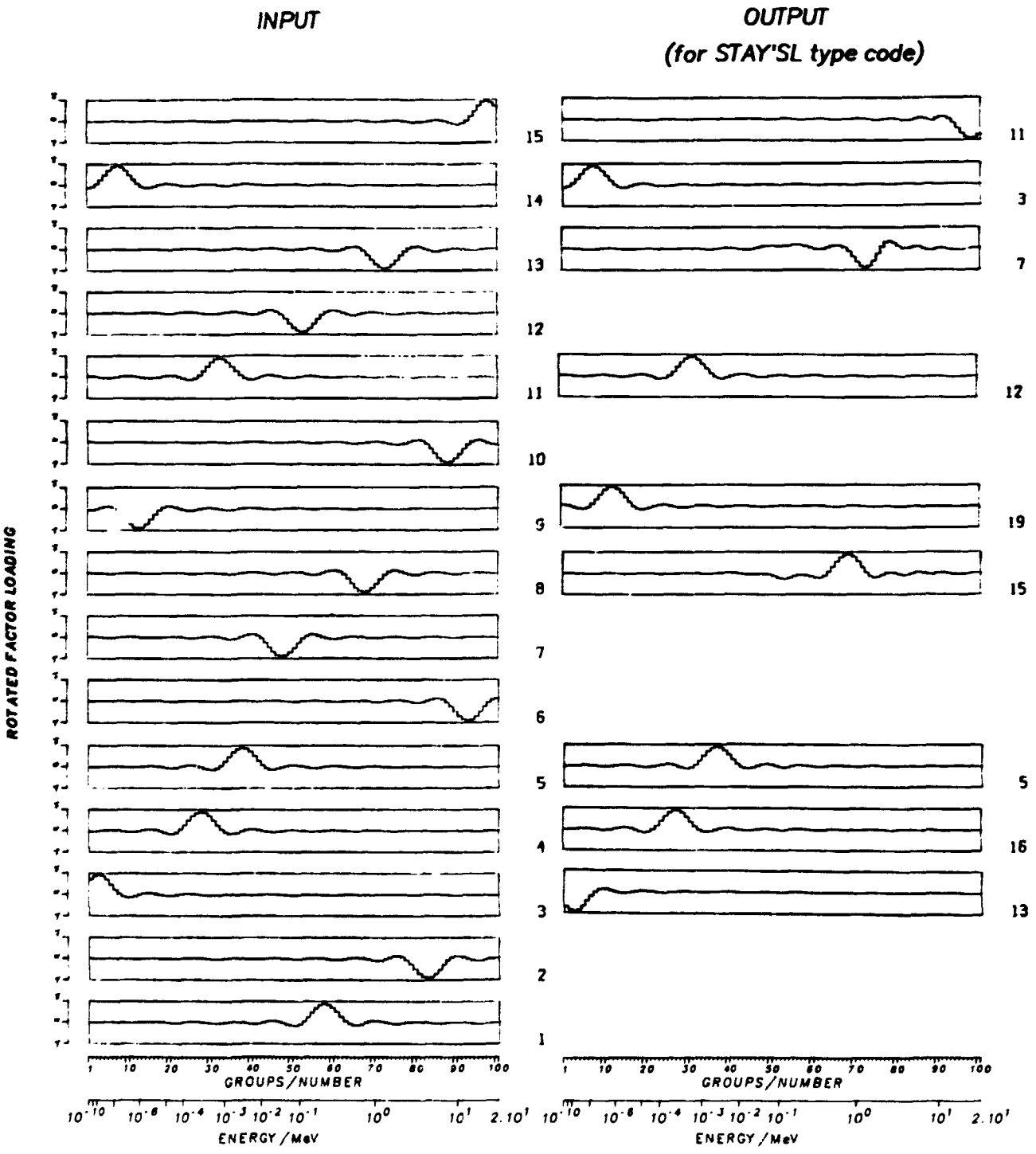

Pictures on the left show the first 20 ordered vectors for the input matrix.
Pictures at the right show the corresponding vectors, if present, and their serial number for the output matrix.

Fig.: 38 Rotated factor loadings for YAYOI input and output correlation matrices.

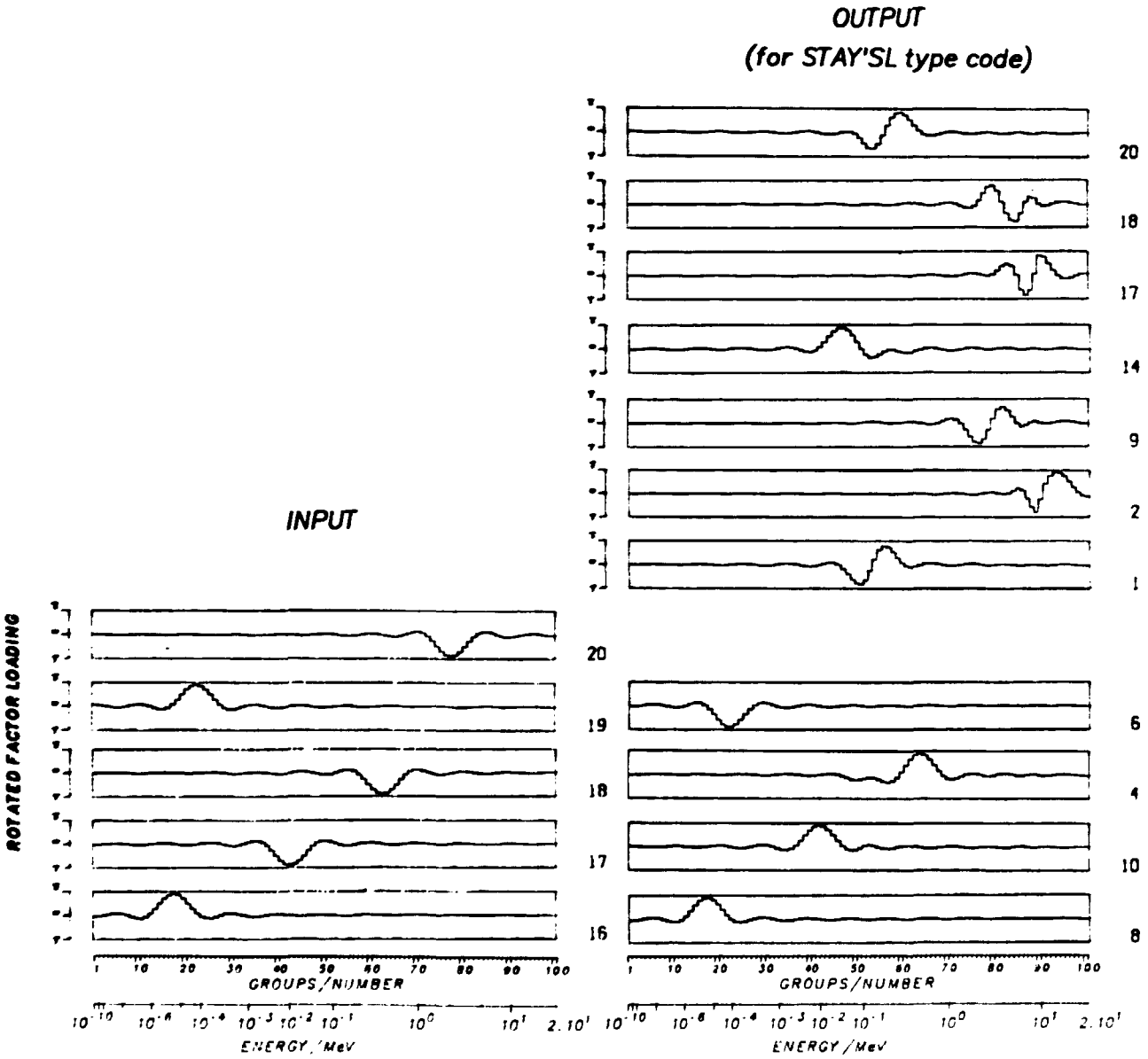

Fig.: 38 (continued)

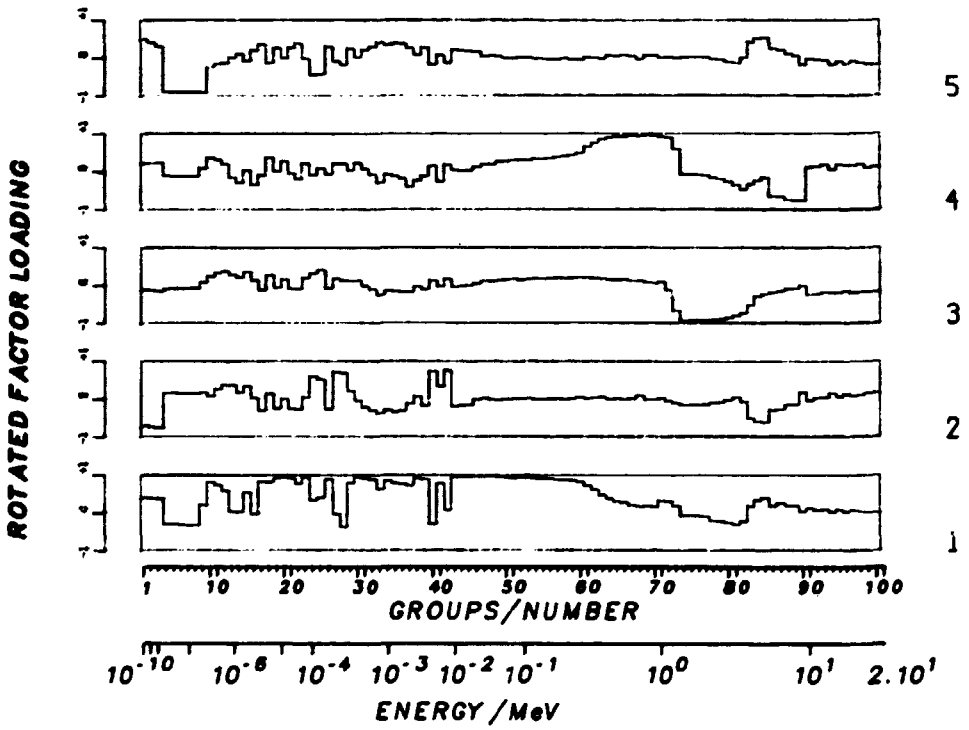

Fig.: 39 The first rotated factor loading vectors. (stochastic model solution in 100 groups for ORR)

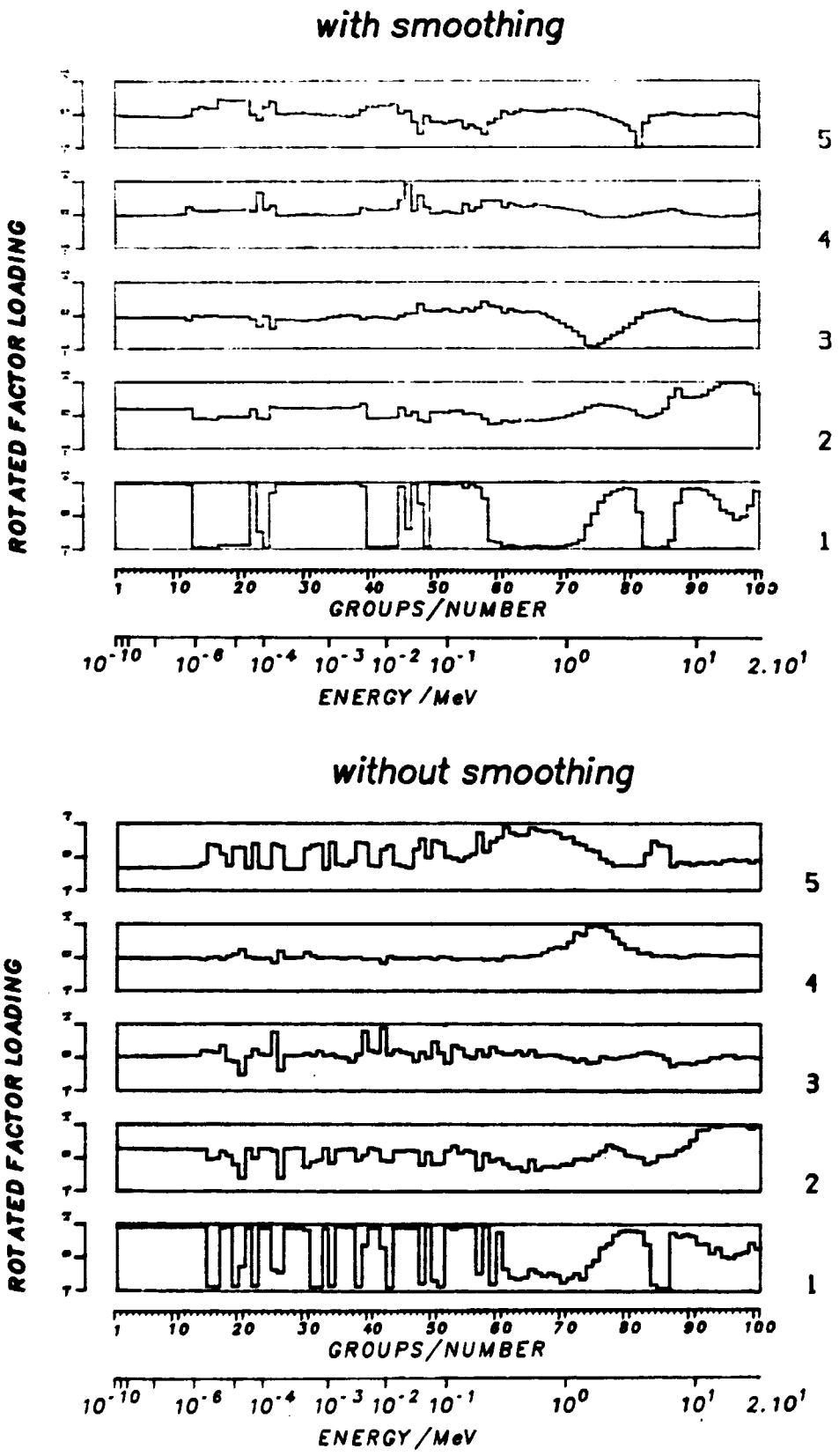

Fig.: 40 The first rotated factor loading vectors.
(stochastic model solutions in 100 groups for YAYOI)

APPENDICES

Appendix 1. The spectrum normalization factor

Often the input spectrum is not normalized, and has to be multiplied with a factor f, the normalization factor, in order that reaction rates α_i^c, calculated with the input spectrum, fit best to the experimentally determined input reaction rates α_i^m.
This normalization factor is of the order of α_i^m/α_i^c, and can be written as an appropriately weighted average of the α_i^m/α_i^c values.
We will derive some expressions for this f-factor, starting from the least squares principle for uncorrelated deviations:

$$S = \sum_{i=1}^{n} w_i(\alpha_i^m - f.\alpha_i^c)^2 = \sum_{i=1}^{n} p_i\ (\alpha_i^m/\alpha_i^c - f)^2 \qquad (A1.1)$$

with

$$p_i = w_i\alpha_i^c.\alpha_i^c \qquad (A1.2)$$

where S = weighted sum of squares of deviations;
n = number of experimental reaction rates;
a_i^m = measured reaction rate for i-th reaction;
α_i^c = $\sum \sigma_i^g.\phi^g$ = calculated reaction rate, based on input values for group cross-sections and group fluence rates;
f = normalization factor;
w_i = statistical weighting factor for the i-th reaction rate.
p_i = statistical weighting factor for the ratio α_i^m/α_i^c.

The least squares approach leads to that value of f, for which $\frac{dS}{df} = 0$.
This leads immediately to the general solution

$$f = \frac{\sum_{i=1}^{n} w_i \cdot \alpha_i^m \cdot \alpha_i^c}{\sum_{i=1}^{n} w_i \cdot \alpha_i^c \cdot \alpha_i^c} = \frac{\sum_{i=1}^{n} p_i \, (\alpha_i^m / \alpha_i^c)}{\sum_{i=1}^{n} p_i} \qquad \text{(A1.3)}$$

We will now consider various choices for the weighting factors.

a. If $w_i = 1$, then $p_i = (\alpha_i^c)^2$.

$$f_1 = \frac{\sum \alpha_i^c \cdot \alpha_i^m}{\sum (\alpha_i^c)^2} \qquad \text{(A1.4)}$$

b. If $w_i = 1/(\alpha_i^c)^2$, then $p_i = 1$ for all i, so that

$$f_2 = \frac{\sum \alpha_i^m / \alpha_i^c}{n} \qquad \text{(A1.5)}$$

With this special choice for the weights, f can be written as the unweighted average of the α_i^m/α_i^c values.

c. If $w_i = 1/(\alpha_i^m)^2$, then $p_i = (\alpha_i^c/\alpha_i^m)^2$. In this case one arrives at

$$f_3 = \frac{\sum (\alpha_i^c / \alpha_i^m)}{\sum (\alpha_i^c / \alpha_i^m)^2} \qquad \text{(A1.6)}$$

d. If $w_i = 1/\alpha_i^c$, then $p_i = \alpha_i^c$. Then

$$f_4 = \frac{\sum \alpha_i^m}{\sum \alpha_i^c} \qquad \text{(A1.7)}$$

Consider now the case of unweighted absolute differences (ie $w_i = 1$)

$$S = \sum_{i=1}^{n} (\alpha_i^m - f.\alpha_i^c)^2. \qquad (A1.8)$$

The least squares principle leads to the solution given by formula A1.4. If we take the case of unweighted relative differences (i.e. $p_i = 1$), we start with

$$S = \sum_{i=1}^{n} \frac{\left(\alpha_i^m - f.\alpha_i^c\right)^2}{\alpha_i^m} \qquad (A1.9)$$

The condition $\frac{dS}{df} = 0$ gives here as solution the formula A1.6.
The approach of relative differences with equal weights seems an attractive one, but it is not justified, since, implicitly, a special choice has been made for the statistical weights. And this choice is not justified at all. In the SAND II code the normalization is based on on the expression for f2. In the STAY'SL code one has two options for the normalization factor: the expressions for f1 and f3.
The best choice for the normalization factor f is that derived with the generalized least squares principle, in which the inverse of the full covariance matrix is introduced as weight matrix.
In principle however one should use as weighting factor

$$w_i = \frac{1}{s^2(\alpha_i)} = \frac{1}{s^2(\alpha_i^m) + f^2.s^2(\alpha_i^c)} \; . \qquad (A1.10)$$

This means that appropiate weighting requires the knowledge of the normalization constant to be determined. This implies that an iterative procedure is required for a good determination of the normalization constant. A further complicating point is that the quantity $s^2(\alpha_i^c)$ is related to variances and covariances in the input values for group fluence rates and group cross-sections. A better procedure might be to determine the best value of the normalization constant together with the other parameters in one generalized least-squares procedure.
The starting point is the minimization of the following expression

$$\boxed{S = \left[\underline{A}^m - f.\underline{A}^c\right]^T . \left[\underline{\underline{V}}(A)^c + \underline{\underline{V}}(A)^m\right]^{-1} . \left[\underline{A}^m - f.\underline{A}^c\right]} \qquad (A\ 1.11)$$

For convenience we write

$$\underline{\underline{W}} = \left[\underline{\underline{V}}(A)^c + \underline{\underline{V}}(A)^m\right]^{-1} \qquad (A\ 1.12)$$

The minimization condition leads to the solution

$$\boxed{f_o = \left[(\underline{A}^c)^T . \underline{\underline{W}} . \underline{A}^c\right]^{-1} . \left[(\underline{A}^c)^T . \underline{\underline{W}} . \underline{A}^m\right]} \qquad (A\ 1.13)$$

which is in fact a generalization of the following expression, obtained when all correlations are zero

$$f = \frac{\sum_{i=1}^{n} w_i . \alpha_i^m . \alpha_i^c}{\sum_{i=1}^{n} w_i . \alpha_i^c . \alpha_i^c} \qquad (A1.?)$$

The generalized least squares theory gives for the variance of f the following expression

$$\boxed{\text{var}\ (f) = \left[(\underline{A}^c)^T . \underline{\underline{W}} . \underline{A}^c\right]^{-1}} \qquad (A\ 1.14)$$

Appendix 2. Generalized least squares approach

We start with the set of activation equations in multigroup form

$$\alpha_i = \sum_{j=1}^{m} \sigma_{ij} \cdot \phi_j \quad (i=1...n) \qquad \text{(A2.1)}$$

where

α_i = reaction rate per target atom for i-th reaction;
ϕ_j = group fluence rate for group j;
σ_{ij} = cross-section for i-th reaction for neutrons in energy group j.

In matrix notation one can write

$$\underline{A} = \underline{\underline{S}} \cdot \underline{\phi} \qquad \text{(A2.2)}$$

where $\underline{A}$ is the vector of n reaction rates, $\underline{\underline{S}}$ is the matrix of (n x m) cross-section values, and $\underline{\phi}$ is the vector of m group fluence rates.
Let input values be available for $\underline{A}$, $\underline{\underline{S}}$ and $\underline{\phi}$.
We are now determining the best fitting vector $\underline{\phi}$, when input values variances and covariances for A, $\underline{\underline{S}}$ and $\underline{\phi}$ are given. Let the number of reaction rates, n, be smaller than the number of energy groups m.
From the system of equations (3.2), one can determine the best solution for $\underline{\phi}$, taking "best" in the least squares sense.
Let

$\underline{A}^m$ = vector of n measured reaction rates α_i^m;
$\underline{\phi}_o$ = vector of m input fluence rates ϕ_j;
$\underline{S}_o$ = vector of all group cross-section values σ_{ij} (library values), in series for all reactions involved;
$\underline{\underline{V}}(A^m)$ = covariance matrix for the n measured reaction rates;
$\underline{\underline{V}}(\phi_o)$ = covariance matrix for the m input values of the group fluence rates;
$\underline{\underline{V}}(S_c)$ = covariance matrix for the m.n input values of the group cross-sections.

Let further

$\underline{A}^c$ = vectors of n calculated reaction rates α_i^c, based on the input values $\underline{S}_o$ and $\underline{\Phi}_o$;

$\underline{\underline{V}}(A^c)$ = covariance matrix for $\underline{A}^c$, based on the input covariance matrices $\underline{\underline{V}}(\Phi_o)$ and $\underline{\underline{V}}(S_o)$.

For practical reasons it is asumed that reaction rates, cross-sections, and group fluence rates are random variables, and that their associated uncertainties are normally distributed.

The output values for the parameters, obtained with the least-squares principle, will be denoted with a $\hat{}$ symbol. We will follow here the approach as described by F.L. Perey ([9] and [24]). The generalized least squares principle implies that the best parameter vectors $\underline{\Phi}$ and $\underline{S}$ are obtained by minimizing the following quadratic expression (often called chi-square)

$$\begin{aligned} \chi^2(\underline{\Phi}, \underline{S}, \underline{A}) = & (\underline{\Phi}_o - \underline{\Phi})^T \cdot \underline{\underline{V}}(\Phi_o)^{-1} \cdot (\underline{\Phi}_o - \underline{\Phi}) \\ & + (\underline{S}_o - \underline{S})^T \cdot \underline{\underline{V}}(S_o)^{-1} \cdot (\underline{S}_o - \underline{S}) \\ & + (\underline{A}^m - \underline{A})^T \cdot \underline{\underline{V}}(A^m)^{-1} \cdot (\underline{A}^m - \underline{A}) \end{aligned} \qquad \text{(A2.3)}$$

Its minimum is $\chi^2 min = \chi^2(\hat{\underline{\Phi}}, \hat{\underline{S}}, \hat{\underline{A}})$; the matrix superscript T denotes the transpose of that matrix.

Here it is asumed that the three parameter vectors are independent. This generalized least squares expression can conveniently be written in matrix notation:

$$\chi^2 = \begin{bmatrix} \underline{\Phi}_o - \hat{\underline{\Phi}} \\ \underline{S}_o - \hat{\underline{S}} \\ \underline{A}^m - \hat{\underline{A}} \end{bmatrix}^T \cdot \begin{bmatrix} \underline{\underline{V}}(\Phi_o) & 0 & 0 \\ 0 & \underline{\underline{V}}(S_o) & 0 \\ 0 & 0 & \underline{\underline{V}}(A^m) \end{bmatrix}^{-1} \cdot \begin{bmatrix} \underline{\Phi}_o - \hat{\underline{\Phi}} \\ \underline{S}_o - \hat{\underline{S}} \\ \underline{A}^m - \hat{\underline{A}} \end{bmatrix} \qquad \text{(A2.4)}$$

The pattern of the matrix in the middle shows the assumption, that the three groups of input data ($\underline{\Phi}$, $\underline{S}$ and $\underline{A}^m$) are uncorrelated.

In this approach the input fluence rates and the input cross-sections are considered on equal footing.
The equations for χ^2 show that the solution of the minimization problem can be found by means of the inverse of the composite covariance matrix, which can be related to the combination of the inverses of the three covariance matrices $\underline{\underline{V}}(\Phi)$, $\underline{\underline{V}}(S)$ and $\underline{\underline{V}}(A^m)$. Let P now denote the following parameter vector

$$\underline{P} = \begin{bmatrix} \underline{\Phi} \\ \underline{S} \end{bmatrix} \tag{A2.5}$$

The covariance matrix for $\underline{P}$ has the form

$$\underline{\underline{V}}(P) = \begin{bmatrix} \underline{\underline{V}}(\Phi) & 0 \\ 0 & \underline{\underline{V}}(S) \end{bmatrix} \tag{A2.6}$$

The expression to be minimized can then be written as

$$\chi^2 = \begin{bmatrix} \underline{P}_o - \hat{\underline{P}} \\ \underline{Am} - \hat{\underline{A}} \end{bmatrix}^T \cdot \begin{bmatrix} \underline{\underline{V}}(P)_o & 0 \\ 0 & \underline{\underline{V}}(A^m) \end{bmatrix}^{-1} \cdot \begin{bmatrix} \underline{P}_o - \hat{\underline{P}} \\ \underline{A}^m - \hat{\underline{A}} \end{bmatrix} \tag{A2.7}$$

To write down the solution, one introduces the socalled sensitivity matrix $\underline{\underline{G}}$ as the matrix which transforms the changes in the parameter p_i, ie the vector

$$\Delta\underline{P} = \underline{P} - \underline{P}_o \tag{A2.8}$$

into changes of the calculated reaction rates α_i, the vector

$$\Delta\underline{A} = \underline{A} - \underline{A}^c. \tag{A2.9}$$

One has then

$$(\underline{A} - \underline{A}^c) = \underline{\underline{G}} \cdot (\underline{P} - \underline{P}_o) \tag{A2.10}$$

or

$$\Delta \underline{A} = \underline{\underline{G}} \cdot \Delta \underline{P} \cdot \qquad \text{(A2.11)}$$

Consider now the expression for the calculated reaction rates, based on input values for group cross-section and group fluence rates (for a normalized spectrum)

$$\alpha_i = \sum_{j=1}^{m} \sigma_{ij} \phi_j \qquad \text{(A2.12)}$$

or in matrix notation

$$\underline{A}^c = \underline{\underline{S}}_o \cdot \underline{\Phi}_o$$

The variances of the quantities α_i can be expressed in terms of variances and covariances of the quantities σ_j and ϕ_j, according to the law for the propagation of uncertainties.
With neglection of an extra cross product term, which occurs in this exact formula which applies in the case that a sum of products of zero or firstpower of independent variabeles (see appendix 4) one may write for the variance of $\underline{A}^c$

$$\underline{\underline{V}} (A^c) = \underline{\underline{G}}^T \cdot \underline{\underline{V}}(P_o) \cdot \underline{\underline{G}} \qquad \text{(A2.13)}$$

The sensitivity matrix contains in fact the partial derivatives of α_i to the parameters comprised in the vector $\underline{P}$.
Consider the i-th component of the reaction rate vector, ie α_i.

$$\frac{\partial \alpha_i}{\partial \phi_1} = \sigma_{i1} \; ; \; \frac{\partial \alpha_i}{\partial \phi_2} = \sigma_{i2} \cdots \frac{\partial \alpha_i}{\partial \phi_m} = \sigma_{im}. \qquad \text{(A2.14)}$$

This yields a horizontal vector $\underline{S}_i^T$.
Derivation of α_i to group cross-sections other than for reaction i are all zero.
Derivatives of α_i to group cross-section for reaction i are as follows:

$$\frac{\partial \alpha_i}{\partial \sigma_{i1}} = \phi_1 \; ; \; \frac{\partial \alpha_i}{\partial \sigma_{i2}} = \phi_2 \; ; \; \ldots\ldots \; \frac{\partial \alpha_i}{\partial \sigma_{im}} = \phi_m . \tag{A2.15}$$

This yields a horizontal vector $\underline{\Phi}$.

By considering all reaction rates one after the other, one can easily find that the sensitivity matrix $\underline{\underline{C}}$ (sometimes also called design matrix) is given by

$$\underline{\underline{C}} = \begin{pmatrix} \underline{S}_1^T & \underline{\Phi}^T & 0 & 0 & \cdot & \cdot & \cdot \\ \underline{S}_2^T & 0 & \underline{\Phi}^T & 0 & \cdot & \cdot & \cdot \\ \cdot & \cdot & \cdot & \cdot & \cdot & \cdot & \cdot \\ \cdot & \cdot & \cdot & \cdot & \cdot & \cdot & \cdot \end{pmatrix} \tag{A2.16}$$

This matrix has the dimensions n x (m+nm).

Since the covariance matrix $\underline{\underline{V}}(P_o)$ is diagonal in the space of $\underline{\Phi}$ and $\underline{S}$, the covariance matrix $\underline{\underline{V}}(A^c)$ is made up of two contributions: one related to $\underline{\underline{V}}(\Phi_o)$ and one related to $\underline{\underline{V}}(S_o)$.

$$\underline{\underline{V}}(A^c) = \underline{S}^T \cdot \underline{\underline{V}}(\Phi_o) \cdot \underline{S} + \underline{\Phi}^T \cdot \underline{\underline{V}}(S_o) \cdot \underline{\Phi} . \tag{A2.17}$$

We remark here that $\underline{A}^c$ and $\underline{\underline{V}}(A^c)$ are predictions based on a priori information on $\underline{\Phi}$ and $\underline{S}$ (ie the input vectors $\underline{\Phi}_o$ and $\underline{S}_o$) for the experimental reaction rates $\underline{A}^m$ and the experimental covariance matrix $\underline{\underline{V}}(A^m)$.

It can be shown, that the solution $\hat{\underline{P}}$ (ie the value of $\underline{P}$ which minimizes the χ^2-expression) is given by

$$\boxed{\hat{\underline{P}} - \underline{P}_o = \underline{\underline{V}}(P_o) \cdot \underline{\underline{C}}^T \cdot \left[(\underline{\underline{V}}(A^c) + \underline{\underline{V}}(A^m) \right]^{-1} \cdot (\underline{A}^m - \hat{\underline{A}})} \tag{A2.18}$$

The right hand side can be split up into two factors:

1) a matrix $\underline{\underline{C}}$, which comprises the sensitivity matrix and the covariance matrix for the parameter vector

$$\underline{\underline{C}} = \underline{\underline{V}}(P_o) \cdot \underline{\underline{G}}^T \cdot \qquad (A2.19)$$

This matrix has the dimensions (m+nm) x n.

2) a vector $\underline{X}$ which is dependent on the experimental reaction rates

$$\underline{X} = \left[\underline{\underline{V}}(A^c) + \underline{\underline{V}}(A^m)\right]^{-1} \cdot (\underline{A}^m - \underline{\hat{A}}). \qquad (A2.20)$$

This vector has the dimension n x 1.

Using these abbreviations, one can write

$$\underline{\hat{P}} - \underline{P}_o = \underline{\underline{C}} \cdot \underline{X} \cdot \qquad (A2.21)$$

The covariance matrix $\underline{\underline{V}}(\hat{P})$, corresponding to the output (adjusted) parameter vector $\underline{P}$, is given by the expression

$$\boxed{\underline{\underline{V}}(\hat{P}) - \underline{\underline{V}}(P_o) = -\underline{\underline{V}}(P_o) \cdot \underline{\underline{G}}^T \cdot \left[\underline{\underline{V}}(A^c) + \underline{\underline{V}}(A^m)\right]^{-1} \cdot \underline{\underline{G}} \cdot \underline{\underline{V}}(P_o)^T} \qquad (A2.22)$$

or

$$\underline{\underline{V}}(\hat{P}) - \underline{\underline{V}}(P_o) = -\underline{\underline{C}} \cdot \left[\underline{\underline{V}}(A^c) + \underline{\underline{V}}(A^m)\right]^{-1} \cdot \underline{\underline{C}}^T \cdot \qquad (A2.23)$$

The statistic χ^2 as defined above follows the well-known χ^2-distribution of Helmert-Pearson with n degrees of freedom (where n is the number of experimental reaction rates involved).

Furthermore it can be shown that the <u>minimum</u> value of χ^2 can be calculated with the expression

$$\boxed{\chi^2_{min} = (\underline{A}^m - \underline{\hat{A}})^T \cdot \left[\underline{\underline{V}}(A^c) + \underline{\underline{V}}(A^m)\right]^{-1} \cdot (\underline{A}^m - \underline{\hat{A}})} \qquad (A2.24)$$

It is important to note that the solution can easily be obtained since the expressions above imply simple matrix calculations, and contain the matrix, denoted by $\underline{\underline{W}}$

$$\underline{\underline{W}} = \left[\underline{\underline{V}}(A^c) + \underline{\underline{V}}(A^m)\right]^{-1} \cdot \qquad (A2.25)$$

Thus the matrix to be inverted has only the dimension n x m, where n is much smaller than (m x m), where m is the number of energy groups involved. The matrix $\underline{\underline{W}}$ defined above plays the role of a weight matrix. A solution can only be found if $\underline{\underline{W}}$ is a non-singular matrix. However, in practical cases this matrix is never singular; if a singular matrix is found, it is due to an oversight or a mistake.

Appendix 3. Structure of a correlation matrix

The correlation matrix for the m group values for the fluence rate, comprises m x m values, with unity values along the main diagonal. We wish to characterize the pattern of a correlation matrix with fewer parameters and to find a tool for the quantitative comparison of the structures of two or more (spectrum) correlation matrices. This approach requires a drastic reduction of data, and a means for data reduction of a correlation matrix is available in the factor analysis ([25], [26], [27]).

Factor analysis is a statistical technique which can be applied to deal with systematics and structures in multivariable data. The main aim of the factor analysis is to reduce the number of correlated variates to a smaller number of uncorrelated variates, but in such a way that the major part of the variances around a linear regression model can be described (or "explained").

We start our consideration with correlation matrix $\underline{\underline{R}}$. Such a matrix has the following properties:

1. it is a square matrix (with dimensions m x m);
2. it is a symmetric matrix;
3. the elements in the main diagonal are all equal to unity;
4. the other elements represent correlation coefficients for which the following relation holds $-1 \leq r_{ij} \leq 1$.

Characteristic parameters of the correlation matrix

A main characteristic of a matrix is its rank. The rank of a matrix can be defined as the highest value of the orders of the non-zero determinants of all possible square submatrices.

Expressed otherwise: A matrix is of rank r, if it contains at least one non-zero r x r minor, and no non-zero minor of dimensionality larger than r. Let $\underline{\underline{R}}$ has the rank r; then $r \leq m$.

A diagonal m x m correlation matrix (which has unit elements along the main diagonal and zero elements elsewhere) has a rank m.

A band matrix (which has elements approximately equal to unity in a band along the main diagonal, and elements approximately equal to zero

elsewhere) has a rank smaller than m.
The rank of such a matrix is decreasing when the width of the band matrix becomes wider.
For a unitary matrix (which contains unit values everywhere) the rank reaches a value 1.
A second characteristic is the average correlation coefficient, (denoted as $\bar{r}_{ij}$), where the averaging is performed over all m^2 elements of the correlation matrix

$$\overline{r_{ij}} = \sum\sum_{ij} r_{ij}/m^2 \quad . \tag{A3.1}$$

For a diagonal correlation matrix one has

$$\overline{r_{ij}} = 1/m \quad .$$

For a correlation matrix with unit elements one has

$$\overline{r_{ij}} = 1 \quad .$$

The value of $\overline{r_{ij}}$ does not give information on the magnitude of the compensation effect of positive and negative contributions outside the main diagonal.
To look at such an effect one needs eg to calculate $\sum|r_{ij}|$ or $\sum(r_{ij})^2$. A better approach may be to consider the variance of r_{ij}.
As third characteristic of a correlation matrix we consider the variance of all element values in the correlation matrix, ie the variance of the correlation coefficients. One has the general rule

$$\sigma^2(r_{ij}) = \langle r_{ij}^2 \rangle - \langle r_{ij} \rangle^2 \tag{A3.2}$$

where $\langle\ \rangle$ denote averaging over the corresponding probability density function. Or, for the finite population of m^2 elements:

$$s^2(r_{ij}) = \sum_{i=1}^{m}\sum_{j=1}^{m} r^2{}_{ij}/m^2 - \left(\sum_{i=1}^{m}\sum_{j=1}^{m} r_{ij}/m^2\right)^2 \tag{A3.3}$$

$$s(r_{ij}) = \sqrt{(\bar{r}^2{}_{ij}) - (\bar{r}_{ij})^2}. \tag{A3.4}$$

For a diagonal matrix one has

$$s(r_{ij}) = \sqrt{\frac{1}{m} - \frac{1}{m^2}} .$$

For a unitary matrix one has

$$s(r_{ij}) = 0.$$

Matrix algebra shows that any square matrix $\underline{\underline{A}}$ can be written in the following normal form:

$$\underline{\underline{A}} = \underline{\underline{T}}_1 \cdot \underline{\underline{D}} \cdot \underline{\underline{T}}_2 \qquad \text{(A3.5)}$$

where $\underline{\underline{T}}_1$ and $\underline{\underline{T}}_2$ denote left-side and right-side transformation matrices, constructed from the left-side and right-side eigenvectors, respectively, and $\underline{\underline{D}}$ denotes a diagonal matrix constructed from the eigenvalues of $\underline{\underline{A}}$. The number of eigenvalues is equal to the rank of the matrix $\underline{\underline{A}}$. Between the transformation matrices $\underline{\underline{T}}_1$ and $\underline{\underline{T}}_2$ there exists the following relation

$$\underline{\underline{T}}_1 = \underline{\underline{T}}_2^{-1} . \qquad \text{(A3.6)}$$

This relation means that $\underline{\underline{T}}_1$ (and also $\underline{\underline{T}}_2$) is an orthogonal matrix.
If the matrix $\underline{\underline{A}}$ is a symmetric matrix with real elements and a positive semi-definite character which is the case for correlation matrices), then the eigenvalues $\underline{\underline{\lambda}}$ are greater than zero, and the following relation holds:

$$\underline{\underline{T}}_1 = \underline{\underline{T}}_2^{T} \qquad \text{(A3.7)}$$

The matrix $\underline{\underline{T}}_1$ has the dimensions m x r

The usual technique to find the eigenvalues λ_i and the eigenvectors $\underline{\underline{a}}_i$ of $\underline{\underline{R}}$ is briefly indicated. By definition one has the relation

$$\underline{\underline{R}} \cdot \underline{a} = \lambda \cdot \underline{a} \quad \text{or} \quad (\underline{\underline{R}} - \lambda \underline{\underline{I}}) \cdot \underline{a} = 0 \qquad \text{(A3.8)}$$

The eigenvalues of $\underline{\underline{R}}$ are the roots of the polynomial expression in λ_D.

$$\det (\underline{\underline{R}} - \lambda . \underline{\underline{I}}) = o$$

The matrix $\underline{\underline{I}}$ denotes the identity matrix, i.e. a matrix with only unity values along the main diagonal, and only zero values elsewhere.
If r is the rank of the correlation matrix, then there are in principle r non-zero eigenvalues λ_i and r corresponding eigenvectors $\underline{a}_i$.
It is useful to arrange the eigenvalues λ_i in decreasing order. This means

$$\lambda_1 > \lambda_2 > \lambda_3 > \ldots\ldots \lambda_r > 0 \qquad \text{(A3.9)}$$

According to the theory the sum of the eigenvalues is equal to the trace of the correlation matrix.

$$\sum_{i=1}^{r} \lambda_i = \text{Tr } (\underline{\underline{R}}) = m \qquad \text{(A3.10)}$$

This relation leads to a practical way for determining the rank of large correlation matrices. The effective rank of a large correlation matrix is that number of ordered eigenvalues, which adds up to say 95 or 98 per cent of the trace of the matrix

We define a diagonal matrix for the eigenvalues: $\underline{\underline{D}}(\lambda_i)$

$$\underline{\underline{D}}(\lambda_i) = \begin{vmatrix} \lambda_1 & & 0 \\ & \lambda_2 & \\ & & \ddots \\ 0 & & \lambda_r \end{vmatrix} \qquad \text{(A3.11)}$$

The r eigenvectors are mutually orthogonal, ie they statisfy the following conditions

$$\underline{a}_i^T \cdot \underline{a}_j = \begin{cases} 0 \text{ for } i \neq j \\ 1 \text{ for } i = j \end{cases} \qquad \text{(A3.12)}$$

This leads directly to the following relation

$$\underline{\underline{R}}\ \underline{a}_i\ \underline{a}_j^T = \lambda\ \underline{a}_i\ \underline{a}_j^T \qquad \text{(A3.13)}$$

or

$$\underline{\underline{R}} = \begin{vmatrix} 1 & & r_{ij} \\ & 1 & \\ & & 1 \\ r_{ij} & & 1 \end{vmatrix} = (\underline{a}_1, \underline{a}_2 \cdots \underline{a}_r) \cdot \begin{vmatrix} \lambda_1 & & 0 \\ & \lambda_2 & \\ & & \ddots \\ 0 & & \lambda_r \end{vmatrix} \cdot \begin{vmatrix} \underline{a}_1^T \\ \underline{a}_2^T \\ \vdots \\ \underline{a}_r^T \end{vmatrix} \quad \text{(A3.14)}$$

matrix m x m — matrix m x r — matrix r x r — matrix r x m

The left side matrix contains in principle (due to its symmetry) $1/2\ m\ (m-1) + m = 1/2\ m\ (m+1)$ different values.
The right hand side expression contains $(r \times m) + r = r.(m+1)$ different values. Some further data reduction may be obtained by introducing vectors $\underline{l}_1$ which are proportional to the eigenvectors α_i (which have unit length).

$$\underline{l}_i = \sqrt{\lambda_i} \cdot \underline{a}_i \quad \text{(A3.15)}$$

In this way one has

$$\underline{\underline{R}} = (\underline{l}_1, \underline{l}_2 \cdots \underline{l}_r) \cdot \begin{vmatrix} \underline{l}_1^T \\ \underline{l}_2^T \\ \vdots \\ \underline{l}_r^T \end{vmatrix} \text{ or } \boxed{\underline{\underline{R}} = \underline{\underline{L}} \cdot \underline{\underline{L}}^T} \quad \text{(A3.16)}$$

The right hand side expression contains now in principle r x m different values.

A further data reduction is obtained by approximating matrix $\underline{\underline{R}}$ with dimensions(m x m) characterised by r vectors $\underline{l}_j$, by a symmetric square matrix $\underline{\underline{R}}$ with dimensions m x m.
This is done by taking instead of the whole set of r eigenvectors only the k most dominant ones.
The value of k is chosen in such a way that a major part of the sum of the eigenvalues (say 90 per cent) is taken into account. Another criterium may be to take only those eigenvectors for which the eigenvalues is larger than unity.

The choice for the first k eigenvectors determines then $\underline{\underline{R}}$ by the relation

$$\underset{\text{matrix } m \times m}{\underline{\underline{R}}} = \underset{\text{matrix } m \times k}{(\underline{l}_1, \underline{l}_2 \cdots \underline{l}_k)} \cdot \underset{\text{matrix } k \times m}{\begin{vmatrix} \underline{l}_1^T \\ \underline{l}_2^T \\ \cdot^T \\ \underline{l}_k^T \end{vmatrix}} = \underset{\text{matrix } k \times k}{\begin{vmatrix} h_1 & r_{ij} \\ & \cdot \\ & & \cdot \\ r_{ij} & & h_k \end{vmatrix}} \qquad \text{(A3.17)}$$

Since of $\underline{\underline{R}}$ some eigen vectors have been deleted, the elements along the main diagonal will not reach the value 1. Thus $h_i < 1$.

In factor analysis, the values along the main diagonal of $\underline{\underline{R}}$ are called communalities.

The communality h_i can be interpreted as the fraction of the total variance for variable i, which is taken into account by the description of only k eigen vectors.

In factor analysis the complements, $1 - h_i$, of the communalities are called specificities.

The specificity $1 - h_i$ can be interpreted as that fraction of the total variance of variable i, which is not taken into account by the restricted set of k eigen vectors.

We have not only that $h_i < 1$, but also $|\hat{r}_{ij}| < |r_{ij}|$. This means that the correlations in $\hat{\underline{\underline{R}}}$ are weaker than in $\underline{\underline{R}}$.

In analogy of the rule for matrix $\underline{\underline{R}}$

$$\sum_{i=1}^{r} \lambda_i = \mathrm{Tr}\,(\underline{\underline{R}}) \qquad \text{(A3.18)}$$

We have here for the matrix $\underline{\underline{R}}$

$$\sum_{i=1}^{k} h_i = \mathrm{Tr}\,(\underline{\underline{R}}) < m \qquad \text{(A3.19)}$$

or for the average communality

$$\bar{h} = \sum_{i=1}^{m} h_i/m < 1 \qquad \text{(A3.20)}$$

With respect to the magnitude of the components of the vectors $\underline{a}_i$ we have the following considerations.

Since the eigen vectors $\underline{a}_i$ have unit length ie $\left|a_i\right| = 1$, each of its components is smaller than unity.

We defined $\underline{l}_i = \underline{a}_i \cdot (\sqrt{\lambda}_i)$.

The maximum value for the components occur when λ has its highest value. The maximum value for the eigenvalue is m; this situation occurs when there is only 1 eigen vector, i.e. when the rank of the matrix is 1. Then the vector $\underline{a}_1$ has m components which are all equal to $1/\sqrt{m}$.

The maximum occurs for the situation

$$\underline{l}_1 \leq \begin{vmatrix} 1/\sqrt{m} \\ 1/\sqrt{m} \\ \\ 1/\sqrt{m} \end{vmatrix} \cdot \sqrt{m} = \begin{vmatrix} 1 \\ 1 \\ \\ 1 \end{vmatrix} \qquad \text{(A3.21)}$$

This yields

$$\left|\underline{l}_i\right| \leq 1 \qquad \text{(A3.22)}$$

and $-1 \leq l_{ij} \leq 1$ for all i and all j (A3.23)

In the theory of factor analysis, the vector $\underline{l}_i$ is called the i-th <u>factor loading</u>. The value l_{ij} is called <u>loading</u> of j-th factor to i-th variable. The components of all factor loadings have values between -1 an +1.

The matrix

$$\underline{\underline{L}} = (\underline{l}_1, \underline{l}_2, \ldots\ldots \underline{l}_k) \qquad \text{(A3.24)}$$

which is a m x k matrix, is then called <u>factor loading matrix</u>.

It can easily be shown that an orthogonal transformation of the loading matrix $\underline{\underline{L}}$ does not influence its ability to reproduce the correlation matrix $\underline{\underline{R}}$.

Let $\underline{\underline{T}}$ be an arbitrary k x k orthogonal matrix, which defines an orthogonal transformation (in fact a rotation in space). We

remember that we had $\underline{\underline{R}} = \underline{\underline{L}} \cdot \underline{\underline{L}}^T$. We postmultiply of $\underline{\underline{L}}$ with $\underline{\underline{T}}$, and substitute the result in the right hand side expression

$$(\underline{\underline{L}} \cdot \underline{\underline{T}}) \cdot (\underline{\underline{L}} \cdot \underline{\underline{T}})^T = (\underline{\underline{L}} \cdot \underline{\underline{T}}) \cdot \underline{\underline{T}}^T \cdot \underline{\underline{L}}^T = \underline{\underline{L}} \cdot \underline{\underline{L}}^T = \underline{\underline{R}} \qquad \text{(A3.25)}$$

This implies that a rotation of the matrix $\underline{\underline{R}}$ is permitted without loss of its characteristics (due to the fact that its geometrical representation in space is not influenced by an orthogonal transformation, ie a rotation).
It has some advantages to perform such a rotation, in order to arrive at a representation which allows an easier physical interpretation.

Factor rotation

We restrict ourselves to orthogonal rotation. The rotated $\underline{l}$ vectors are called rotated factor loadings. There are several procedures available in literature for the definition of a suitable rotation.
Thurstone has recommended to apply such a rotation, that a simple structure of the (rotated) factor loadings is obtained. This simple structure has ideally the following characteristic:

1. each row of the matrix should contain at least one zero;
2. each column of the matrix should contain at least k zero's;
3. every pair of columns should contain several responses whose loadings vanish in one column and not in the other;
4. if the number of factors k is four or more, every pair of columns of the matrix should contain a large number of responses with zero loadings in both columns;
5. conversely, for every pair of columns only a small number of responses should have non-zero loadings in both columns.

These criteria say that under a simple structure the responses fall into generally mutually exclusive groups whose loadings are high on single factors, perhaps moderate to low on a few factors, and of negligible size in the remaining dimensions.
The rotation widely used to obtain a simple structure is the varimax criterion by Kaiser (see eg [25], [26] or [27]). This criterium

maximizes an expression containing the sum of the variances of the squared loadings within each column of the loading matrix.
The maximand is

$$V = \text{var}\left[\frac{l_{ij}^2}{h_i^2}\right] = \frac{1}{m^2}\sum_{j=1}^{k} m \sum_{i=1}^{m}\left(\frac{l_{ij}^2}{h_i^2}\right)^2 - \left[\sum_{i=1}^{m}\frac{l_{ij}^2}{h_i^2}\right]^2 \qquad \text{(A3.26)}$$

where l_{ij} are the elements of the loading matrix and h_i are the communalities.

There exists some relation between the rank of a correlation matrix and the pattern of the rotated factor loading.
A correlation matrix with a high rank (eg matrices with a very small band along the main diagonal) indicates a system of a large number of independent linear equations.
In such a case there are only few constraints on the variables, in the sense of a few correlations, or in the sense of very weak correlations.
A high rank means also a high number of eigenvectors, and this implies small structure in the rotated factor loadings.
In the opposite case we have a correlation matrix with a low rank, eg obtained by many non-zero correlation coeeficients with very low values.
This implies many constraint conditions for the variables and less "degrees of freedom". Since there can only be a few important factor loadings, these can then have much structure. We have therefore the following scheme.

rank of matrix	correlation matrix	number of factors	factor loading
small	much structure; wide peak and valleys	small	oscillating
high	simple pattern; band structure	high	smooth structure

Appendix 4. Propagation of uncertainties

Consider a function $U = f(x, y, z)$, where we restrict for a moment the number of variables to 3.
Expansion in a Taylor series gives

$$U-U_o = \frac{\partial f}{\partial x} \cdot (x-x_o) + \frac{\partial f}{\partial y} \cdot (y-y_o) + \frac{\partial f}{\partial z} \cdot (z-z_o)$$
$$+ 1/2 \ \frac{\partial^2 f}{\partial x^2} \cdot (x-x_o)^2 + \frac{\partial^2 f}{\partial y^2} \cdot (y-y_o)^2 + \frac{\partial^2 f}{\partial z^2} \cdot (z-z_o)^2$$
$$+ 2 \left[\frac{\partial^2 f}{\partial x \partial y} \cdot (x-x_o) \cdot (y-y_o) + \frac{\partial^2 f}{\partial x \partial z} \cdot (x-x_o) \cdot (z-z_o) + \frac{\partial^2 f}{\partial y \partial z} \cdot (y-y_o) \cdot (z-z_o) \right]$$

+ terms with higher order deviatives (A4.1)

We form the square of this espression and take its expectation value

$$E\,(U-U_o)^2 = \left(\frac{\partial f}{\partial x}\right)^2 \cdot E\,(x-x_o)^2 + \left(\frac{\partial f}{\partial y}\right)^2 \cdot E\,(y-y_o)^2 + \left(\frac{\partial f}{\partial z}\right)^2 \cdot E\,(z-z_o)^2$$
$$+2 \ \left(\frac{\partial f}{\partial x}\right) \cdot \left(\frac{\partial f}{\partial y}\right) \cdot E\,(x-x_o) \cdot (y-y_o) + 2 \left(\frac{\partial f}{\partial x}\right) \cdot \left(\frac{\partial f}{\partial z}\right) \cdot E\,(x-x_o) \cdot (z-z_o)$$
$$+2 \ \left(\frac{\partial f}{\partial y}\right) \cdot \left(\frac{\partial f}{\partial z}\right) \cdot E\,(y-y_o) \cdot (z-z_o)$$

+ terms with higher order derivatives (A4.2)

Usually the higher order terms are being neglected. This leads to the well known formula for the propagation of uncertainties

$$\mathrm{var}(U) = \left(\frac{\partial f}{\partial x}\right)^2 \cdot \mathrm{var}(x) + \left(\frac{\partial f}{\partial y}\right)^2 \cdot \mathrm{var}(y) + \left(\frac{\partial f}{\partial z}\right)^2 \cdot \mathrm{var}(z)$$
$$+ 2 \left(\frac{\partial f}{\partial x}\right) \cdot \left(\frac{\partial f}{\partial y}\right) \cdot \mathrm{cov}(x,y) + 2 \left(\frac{\partial f}{\partial x}\right) \cdot \left(\frac{\partial f}{\partial z}\right) \cdot \mathrm{cov}(x,z) + 2 \left(\frac{\partial f}{\partial y}\right) \cdot \left(\frac{\partial f}{\partial z}\right) \mathrm{cov}(y,z)$$

(A4.3)

This law holds exactly for functions linear in the parameters (x,y,z), since the derivatives of second and higher order are zero.
The law gives a very practical approximation, if the function is non-linear in the variables. In the case of non-linear functions the quality of the approximation depends to some extent on the choice of the starting form (x_o, y_o, z_o).

Consider now a set of n functions $U_i = f(x_1, x_2 \ldots x_m)$ in which the m variables $x_1, \ldots x_m$ have known uncertainties and known correlations.
The expression for the propagation of uncertainties can be written as

follows:

$$\boxed{\text{var}\,(U_i) = \sum_{k=1}^{m} \sum_{l=1}^{m} \left(\frac{\partial f_i}{\partial x_k}\right) \cdot \text{cov}\,(x_k, x_l) \cdot \left(\frac{\partial f_i}{\partial x_l}\right)} \qquad \text{(A4.4)}$$

or in matrix nolation

$$\boxed{\underline{\underline{V}}\,(U) = \underline{\underline{G}}^T \cdot \underline{\underline{V}}\,(x) \cdot \underline{\underline{G}}} \qquad \text{(A4.5)}$$

where $\underline{\underline{V}}\,(x)$ denotes the covariance matrix of the variables $x_1 \ldots x_m$;

$\underline{\underline{G}}$ denotes the sensitivity matrix, ie the matrix of the partial derivatives $\left(\frac{\partial U_i}{\partial x_k}\right)$;

$\underline{\underline{G}}^T$ denotes the transport of matrix $\underline{\underline{G}}$;

$\underline{\underline{V}}\,(U)$ denotes the covariance matrix of the variables U_i.

If one considers now the sum of a set of adjacent group fluence rates

$$S = \sum_{j=1}^{m} \phi_j \qquad \text{(A4.6)}$$

then the law for the propagation of uncertainties leads to:

$$\text{var}\,(S) = \sum_{k=1}^{m} \sum_{l=1}^{m} \left(\frac{\partial S}{\partial \phi_k}\right) \cdot \text{cov}\,(\phi_k, \phi_l) \cdot \left(\frac{\partial S}{\partial \phi_l}\right) \qquad \text{(A4.7)}$$

or

$$\boxed{\text{var}\,(S) = \sum_{k=1}^{m} \sum_{l=1}^{m} \text{cov}\,(\phi_k, \phi_l).} \qquad \text{(A4.8)}$$

This relation holds exactly, since the punction S is linear in the

parameters.

These exists a special class of non-linear funtions for which one can obtain an exact expression for the propagation of uncertainties, by adding a restricted number of cross pr[illegible]rms to the usual expression.

This special class comprises functions which can be expressed as a sum of products of the first power of independent variables.

We will now demonstrate the application of this rule.

Consider a function of the type $U = x.y$. The covariance between variables x and y can be defined with aid of the general formula

$$cov(x,y) = E(x.y) - E(x) \cdot E(y). \qquad (A4.9)$$

or

$$E(x.y) = cov(x.y) + E(x) \cdot E(y).$$

Note that in the case where x and y are independent variables, one has

$$E(x.y) = E(x) \cdot E(y). \qquad (A4.10)$$

By virtue of definition one has

$$var(U) = E(U^2) - E(U) \cdot E(U). \qquad (A4.11)$$

This leads to

$$\begin{aligned} var(U) &= E[(xy) \cdot (xy)] - E(xy) \cdot E(xy) \\ &= E[(xx) \cdot (yy)] - E(xy) \cdot E(xy) \end{aligned} \qquad (A4.12)$$

Remembering that x and y are independent variables, we obtain

$$\begin{aligned} var(U) &= E(xx) \cdot E(yy) - E(xy) \cdot E(xy) \\ &= [cov(x,x) + E(x) \cdot E(x)] \cdot [cov(y,y) + E(y).E(y)] \\ &\quad - E(xy) \cdot E(xy) \end{aligned} \qquad (A4.13)$$

$$\begin{aligned} var(U) = {} & cov(x,x) \cdot cov(y,y) + E(x) \cdot cov(y,y) \cdot E(x) \\ & + E(y) \cdot cov(x,x)\, E(y) + E(x) \cdot E(x) \cdot E(y) \cdot E(y) \\ & - E(x) \cdot E(y) \cdot E(x) \cdot E(y) \end{aligned} \qquad (A4.14)$$

Then we obtain

$$\begin{aligned} var(U) = {} & E(y)\, var(x) \cdot E(y) + E(x) \cdot var(y) \cdot E(x) \\ & + var(x) \cdot var(x). \end{aligned} \qquad (A4.15)$$

If we had directly applied the law for the propagation of uncertainties, we would have obtained

$$var(U) = y^2 \cdot var(x) + x^2 \cdot var(y) \qquad (A4.16)$$

where we remind that this relation is not exactly valid here.
The exact relationship has an additional term in the form of a cross product term var (x), var (y).
In many practical this cross product sum can be neglected with respect to the other two contributions. The condition for neglection is

$$var(x) \ll E(x) \cdot E(x) \text{ and } var(y) \ll E(y) \cdot E(y). \qquad (A4.17)$$

The approximation loses its validity, if these conditions are not met.

We will now consider a sum of products, containing k terms, when the variables occur only in the zero or first power. We will apply it immediately to the case of a reaction rate, satisfying the relation

$$R = \sum_{j=1}^{m} \sigma_j \cdot \phi_j. \qquad (A4.18)$$

Note that the group cross-sections and group fluence rates are independent, when we consider a calculated input activation rate, or the calculated R_{Ni} and R_{dpa}.

In the case of calculated output activation rates, the σ_j and ϕ_j are not independent any longer.
We directly can write:

$$\mathrm{var}(R) = E(R^2) - E(R) \cdot E(R).$$

$$= E\Big[\Big(\sum_{j=1}^{m} \sigma_j \phi_j\Big).\Big(\sum_{k=1}^{m} \sigma_k \phi_k\Big)\Big] - E\Big(\sum_{j=1}^{m} \sigma_j \phi_j\Big).E\Big(\sum_{k=1}^{m} \sigma_k \phi_k\Big)$$

$$= E\Big[\Big(\sum_{j=1}^{m}\sum_{k=1}^{m} \sigma_j \phi_j \sigma_k \phi_k\Big)\Big] - E\Big(\sum_{j=1}^{m} \sigma_j \phi_j\Big).E\Big(\sum_{k=1}^{m} \sigma_k \phi_k\Big)$$

$$= E\Big[\sum_{j=1}^{m}\sum_{k=1}^{m} (\sigma_j \sigma_k).(\phi_j \phi_k)\Big] - \Big[\sum_{j=1}^{m} E(\sigma_j \phi_j)\Big].\Big[\sum_{k=1}^{m} E(\sigma_j \sigma_k)\Big]$$

$$= \sum_{j=1}^{m}\sum_{k=1}^{m} [\mathrm{cov}(\sigma_j,\sigma_k) + E(\sigma_j).E(\sigma_k)].[\mathrm{cov}(\phi_j,\phi_k)+E(\phi_j).E(\phi_l)]$$

$$- \sum_{j=1}^{m}\sum_{k=1}^{m} E(\sigma_j \phi_j).E(\sigma_k \phi_k)$$

$$= \sum_{j=1}^{m}\sum_{k=1}^{m} [\mathrm{cov}(\sigma_j, \sigma_k).\mathrm{cov}(\phi_j,\phi_k) + E(\sigma_j).\mathrm{cov}(\phi_j,\phi_k).E(\sigma_k)$$

$$+ E(\phi_j).\mathrm{cov}(\sigma_j,\sigma_k).E(\phi_k) + E(\sigma_j).E(\sigma_k).E(\phi_j).E(\phi_k)]$$

$$- \sum_{j=1}^{m}\sum_{k=1}^{m} E(\sigma_i).E(\phi_i).E(\sigma_k).E(\phi_k)$$

$$\mathrm{var}(R) = \sum_{j=1}^{m}\sum_{k=1}^{m} [\sigma_j.\mathrm{cov}(\phi_j,\phi_k).\sigma_k + \phi_j.\mathrm{cov}(\sigma_j,\sigma_k).\phi_k \qquad \text{(A4.19)}$$

$$+ \mathrm{cov}(\sigma_j,\sigma_k) \cdot \mathrm{cov}(\phi_j,\phi_k)]$$

Of special interest is the fact, that the contribution

$$\sum_{j=1}^{m} \sum_{k=1}^{m} \mathrm{cov}(\sigma_j,\sigma_k) \cdot \mathrm{cov}\,(\phi_j,\phi_k)$$

cannot any longer be neglected, if there are many covariance terms with a large value. It is not guaranteed that in adjustment situations like those considered in the REAL-80 exercise this neglection of the cross product terms is allowed.

The formalism mentioned above, which we applied to measurement uncertainties in the input data, can be applied also to the numerical precision of the computer representation of the values under consideration. This means that in cases when the numerical precision is insufficient, it might happen that computed variance values are unrealistically high or unrealistically low.

For more detailed consideration of the differences in mathematical modelling of the spectrum adjustment procedure, and the numerical treatment of the parameter estimations, we refer to a paper presented at the Visegrad Symposium, 27 September - 2 October 1982 [28].